

COOLABILITY OF DEGRADED CORE UNDER REFLOODING CONDITIONS IN NORDIC BOILING WATER REACTORS

I. Lindholm¹, L. Nilsson², E. Pekkarinen¹ & H. Sjövall³

¹VTT Energy
Espoo, Finland

²Studsvik EcoSafe AB
Nyköping, Sweden

³Teollisuuden Voima Oy
Olkiluoto, Finland

September 1995

ACKNOWLEDGEMENTS

The financial contributions by Swedish Nuclear Power Inspectorate (SKI) and by Finnish Ministry of Trade and Industry to the work are gratefully acknowledged.

The authors are gratefully to Dr. Wiktor Frid/ SKI, Mr. Juhani Hyvärinen/ STUK, Mr. Gunnar Jung/ Vattenfall AB, Mr. Erik Larsen/ Sydkraft Konsult AB and Mr. Yngve Waaranperä/ ABB Atom AB for technical support and constructive suggestions during the analyses.

CONTENTS

| | |
|--|----|
| EXECUTIVE SUMMARY..... | 1 |
| 1. INTRODUCTION..... | 4 |
| 2. PLANT DESCRIPTIONS..... | 6 |
| 2.1 TVO NUCLEAR POWER PLANT..... | 6 |
| 2.2 FORSMARK NUCLEAR POWER PLANT..... | 8 |
| 3. APPLIED CALCULATION TOOLS AND INPUT MODELS | 11 |
| 3.1 MELCOR 1.8.3 model for TVO..... | 11 |
| 3.2 MAAP4 model for TVO..... | 13 |
| 3.3 SCDAP/RELAP5..... | 14 |
| 3.3.1 TVO Model | 16 |
| 3.3.2 Forsmark 3 Model | 16 |
| 4. SCOPE OF CALCULATIONS | 18 |
| 4.1 TVO | 18 |
| 4.2 FORSMARK 3 | 19 |
| 5. TVO I/II RESULTS | 20 |
| 5.1 STATION BLACKOUT WITH SUCCESSFUL DEPRESSURIZATION OF RCS..... | 20 |
| 5.1.1 Cladding and Debris Temperatures | 24 |
| 5.1.2 Hydrogen Production | 28 |
| 5.1.3 Control Rods | 30 |
| 5.1.4 End State of Core | 32 |
| 5.2 STATION BLACKOUT WITH FAILURE TO DEPRESSURIZE RCS | 36 |
| 5.2.1 Cladding and Debris Temperatures | 40 |
| 5.2.2 Hydrogen Production | 43 |
| 5.2.3 Control Rods | 45 |
| 5.2.4 End State of Core | 47 |
| 6. FORSMARK 3 RESULTS | 52 |
| 6.1 BASE CASE CALCULATIONS WITHOUT REFLOODING | 53 |
| 6.1.1 Case 1L. Low Pressure Scenario with Normal ADS | 53 |
| 6.1.2 Case 1H. High Pressure Scenario with Failure to Initiate ADS | 54 |
| 6.2 REFLOODING WITH AUXILIARY FEED WATER AS TOP SPRAY | 56 |
| 6.2.1 Low Pressure Cases, Case 2,3 and 4 | 56 |
| 6.2.2 High Pressure Cases, Case 5 and 6 | 59 |
| 6.3 REFLOODING WITH HIGH FLOW RATES FROM THE ECCS | 61 |
| 7. DISCUSSION OF UNCERTAINTIES | 66 |
| 8. CONCLUSIONS | 70 |
| REFERENCES | 72 |

EXECUTIVE SUMMARY

Present work is part of the first phase of subproject RAK-2.1 of the new Nordic Co-operative Reactor Safety Program, NKS, which is planned for the four-year period, 1994 --97. The first phase comprises reflooding calculations for the boiling water reactors (BWRs) TVO I/II in Finland and Forsmark 3 in Sweden. The analysis is a continuation of earlier severe accident analyses which were made in the SIK-2 project of the preceding NKS research period.

The objective of the core reflooding studies is to evaluate when and how the core is still coolable with water and what are the probable consequences of water cooling. Furthermore, the results are intended to form a basis for the following phase of the RAK-2.1 project, in which recriticality studies will be performed. Conditions for recriticality might occur if control rods have melted away with the fuel rods intact in a shape that critical conditions can be created in reflooding with insufficiently borated water.

Core coolability was investigated for two reference plants, TVO I/II and Forsmark 3. The selected accident cases were anticipated station blackout with or without successful depressurization of reactor coolant system (RCS). The effects of the recovery of emergency core cooling (ECC) were studied by varying the starting time of core reflooding. The start of ECC systems were assigned to reaching a maximum cladding temperature: 1400 K, 1600 K, 1800 K and 2000 K in the core. Cases with coolant injection through the downcomer were studied for TVO I/II and both downcomer injection and core top spray were investigated for Forsmark 3.

At TVO the depressurization of RCS is manually initiated by operators at 1 h into the accident according to the present Emergency Operating Procedures, whereas in Forsmark the depressurization takes place automatically upon signal indicating low downcomer water level. Typically the opening of ADS valves takes place in 10-20 min after station blackout in Forsmark 3.

Calculations with three different computer codes: MAAP 4, MELCOR 1.8.3 and SCDAP/RELAP5/MOD 3.1 form the basis for the presented reflooding studies. These codes are extensively used worldwide and with critical evaluation of the calculated results, some insight to the reflooding phenomena can be achieved. This is carried out partially by comparing the results given by different codes and partially by evaluating the code models in general. Analyses for TVO were performed with all three computer codes in parallel, while the Forsmark calculations were performed solely with SCDAP/RELAP5.

In the performed calculations for TVO with core reflooding through downcomer injection MELCOR predicted fragmentation of the fuel and formation of a rubble bed with no fuel or cladding slumping into the lower head in the majority of the cases. Some of the code sensitivity parameters are anticipated to have effect on the results. MAAP4 in turn favored formation of a melt pool in the core, with no material relocations to the lower plenum, when core was reflooded. Also MAAP4 results are sensitive to user-input parameters. A SCDAP/RELAP5 calculation resulted in melt pool formation and rapid slumping of material into the lower head (in case, where the code was able to calculate far enough).

All codes predicted an increase in hydrogen production at the time the water level reached

the bottom of the active fuel. In the scenarios with failure to depressurize the reactor coolant system, all calculated cases with the three codes resulted in quenched end states of the core. In the cases with successful depressurization the core damages are larger than in the respective high pressure variations. This is partially explained with the used maximum temperature criteria for starting of reflooding, which does not necessarily reflect the actual wall clock time in the accident progression.

The final state of the core in TVO I/II according to MAAP4 calculations is the same if the reflooding is started at 1h 15 min independently whether the reactor is depressurized or not. The intact core geometry is lost and a melt pool has formed in the original core volume.

According to the Emergency Operating Procedures (EOP) for severe accidents at TVO, the reactor coolant system will be depressurized at latest 1 h into the accident. This seems to be close to optimum predicted by the calculations of this report. An earlier depressurization would lead to more rapid core degradation due to early loss of reactor coolant inventory. Delaying the depressurization beyond 1 h does not add much time to maintain intact fuel geometry after reflooding. By delaying the depressurization beyond 1 h there is a risk that debris relocates into the lower head at high reactor pressure and eventually causes high pressure melt ejection to the containment.

The SCDAP/RELAP5 results for Forsmark 3 show that the maximum temperature for which the core can be re-cooled might be slightly above 1800 K at normal, early ADS. Noticeably better cooling was obtained in the high pressure cases without ADS. Increased flow rates from the low pressure ECCS gave faster re-cooling than with the low flow rate from the auxiliary feed water system. Core spray seemed to be more efficient than downcomer injection. Pressure increase did, however, limit the mass flow rate from the low pressure ECCS. At start of re-cooling at 1800 K a substantial number of control rods had melted away, but other damages to the core were rather limited.

MAAP and MELCOR predicted a relatively small time window between the relocation of the control rods and the fuel in the core. According to MELCOR the time gap was only 1-2 min, MAAP predicted the time gap to vary between 3 min - 15 min and SCDAP/RELAP5 calculations did not result in major control rod slumping at all in cases with reflooding at 1400 K and 1600 K. In case with reflooding at 1800 K most of the absorber material had already melted and relocated prior to start of coolant injection in the low pressure case. In the respective high pressure case the control rods melted locally in the top and center part of the core. However, the rubble bed in MELCOR results consists of fuel and cladding particles with no absorber material present.

It seems that MELCOR is capable of predicting core melt progression under conditions without reflooding reasonably well. The results presented in this report reflect well the present understanding of severe accident progression. The general trends, like escalated hydrogen generation, are in accordance with the experimental observations. The validation of the code models for real plant applications is difficult, and even in the best of cases, will be based on experimental data obtained for single rod bundle. The present plant applications of MELCOR will bear some uncertainty which could be, to some extent, reduced by making sensitivity studies.

The accident progression in MAAP analyses follows generally the expected path by MAAP 4

models. Several user-input model parameters of MAAP 4 cause uncertainties that make sensitivity studies necessary.

SCDAP/RELAP5 analyses suggest similar trend in the core behaviour as the two other codes. The numerical performance of the code in cases, where extreme thermo-hydraulic conditions are reached quickly, is not good. However, the results from accident time periods, where the code seem to manage adequately, are relatively well in accordance with the predictions of other codes and with experimental data.

However, even if reflooding of an overheated reactor core is a key area when discussing severe accident management in the reactor coolant system, the understanding of the related phenomena is still rather poor. This is to large extent due to lack of specific experiments and good quality data. The present observations of fuel behaviour in reflooding situations have been more or less by-products from experiments that investigate core melt progression and the experiment has been terminated by water injection. Accident in TMI-2 is basically the only example of a plant scale reflooding scenario, where a severely damaged core was eventually quenched and RPV failure was avoided.

When discussing about reflooding of a severely damaged core, further information about the pertinent physical phenomena occurring during the quenching process is needed in order to evaluate the adequacy of the present calculational models for applications in the context of accident management.

Presently, an experimental programme on core reflooding phenomena has been started in Kernforschungszentrum Karlsruhe in QUENCH test facility. These QUENCH experiments are part of research programme funded by the European Union and the results should be available to member countries.

1. INTRODUCTION

Present work belongs to a first part of subproject RAK-2.1 of the Nordic Co-operative Reactor Safety Program, NKS, which is continuing for another four-year period, 1994 --97. The scope and objectives of RAK-2 is presented in Ref. 1. RAK-2.1 addresses the research area "Severe Accident Phenomenology", and is planned to comprise following five phases

- 1 Reflooding calculations
- 2 Analysis of recriticality
- 3 Late phase melt progression
- 4 Corium coolability
- 5 Containment behaviour, steam explosions

The reflooding calculations are performed for the boiling water reactors (BWRs) TVO I/II in Finland and Forsmark 3 in Sweden. This analysis is a continuation of earlier severe accident analyses which were made in the SIK-2 project of the preceding NKS research period [Ref. 2]. In SIK-2 calculations were made of station blackout (TB) scenarios without cooling recovery (SIK-2.2) and some tentative reflooding calculations for TB cases with cooling recovery (SIK-2.3). As calculation tools were used the codes MAAP, MELCOR and SCDAP/RELAP5.

Present phase 1 of RAK-2.1, comprises extended reflooding calculations for TVO-I/II with MAAP 4, MELCOR 1.8.3 and SCDAP/RELAP5/MOD3.1 and for Forsmark 3 with SCDAP/RELAP5.

The **objectives** of the reflooding studies were mainly the following:

- * To investigate if an overheated core can be recooled at recovery of the emergency core cooling after a severe accident and to evaluate the consequences of water injection into a hot core.
- * Determine the maximum core temperature at which recooling and rewetting of the core can be achieved for realistic scenarios with top spray and downcomer injection from the emergency core cooling systems.
- * Investigate the possibilities of obtaining a core in which early melt-down of control rods will leave a configuration of fuel bundles in which recriticality might occur at reflooding with unborated water.

The phenomena taking place in a severe accident are complicated and difficult to calculate, especially since the original geometry changes due to heat-up and melting of reactor components. Various materials can form eutectic mixtures which have lower melting temperatures than the base materials. In this respect the eutecticum formed between stainless steel and boron carbide in BWR control rods is of importance as this facilitates early melting of control rods. Refreezing of melts can form flow blockages. Oxidation, especially of zirconium, contributes to the heat-up power and generates hydrogen, the rate of reaction is depending on temperature, surface of the metal and availability of steam.

The modelling of severe accident phenomena in the codes is under continuous development and supported by validation of the codes against experiments in which separate effects are studied.

2. PLANT DESCRIPTIONS

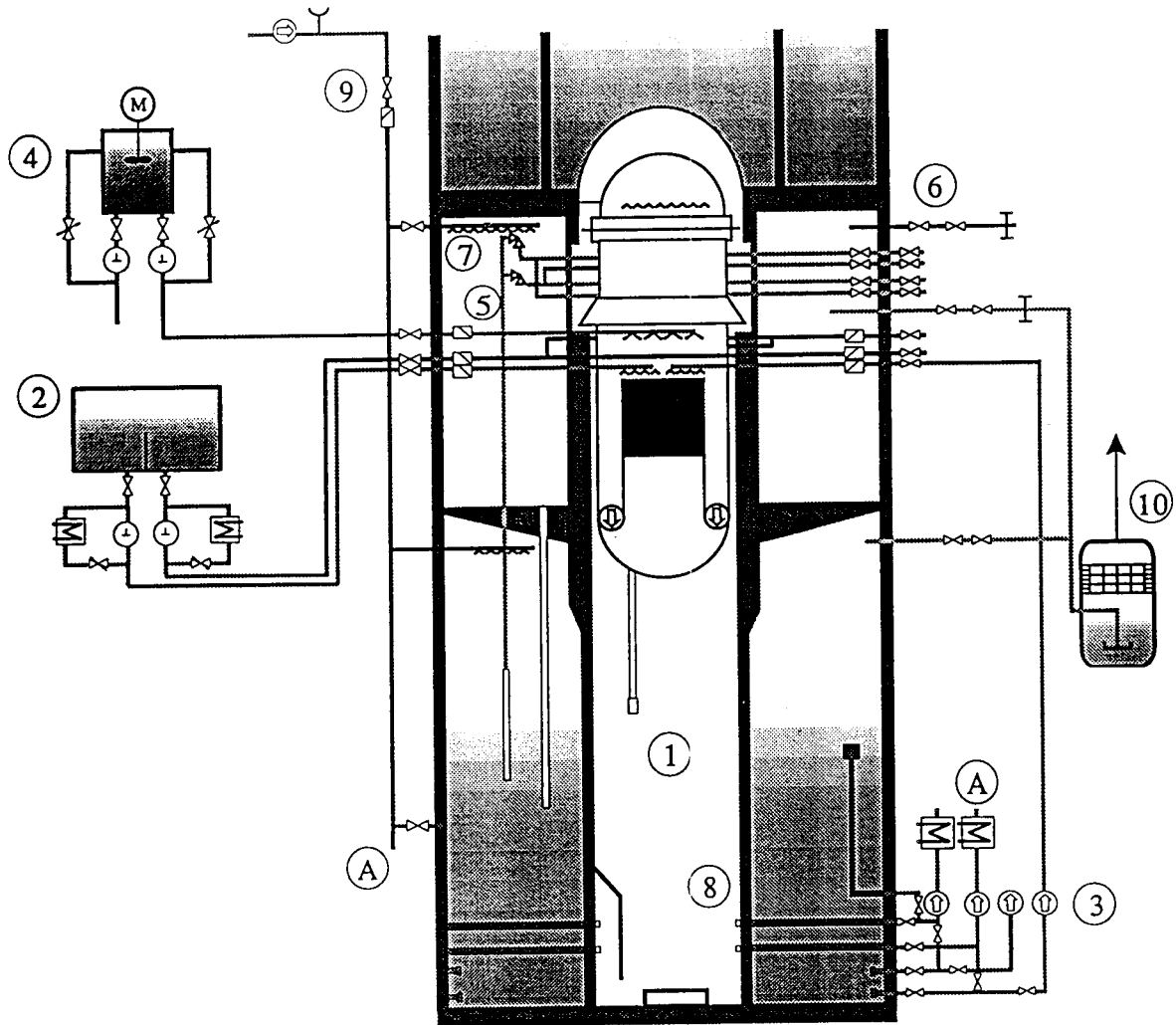
2.1 TVO NUCLEAR POWER PLANT

Teollisuuden Voima Oy (TVO Power Company) owns and operates the nuclear power plant units TVO I and II located on the west coast of Finland. The units have 2160 MW_{th} boiling water reactors designed by ABB Atom (formerly Asea-Atom) and the net electric output of the plant unit is 710 MW_e. The containment is of pressure suppression type and filled with nitrogen under operation.

The reactor operates at the pressure of 70 bar. The reactor pressure vessel is made of low-alloy carbon steel, with lining of stainless steel. The inner diameter of the vessel is 5.54 m and the inner height is 20.6 m with the weight totaling with the vessel cover to 631 metric tons. The coolant flow through the core is maintained with six internal circulation pumps, with the design based on the use of wet motors. Due to the internal pumps all major pipe nozzles are located above the top of the core, to ensure that the core is kept flooded in the event of a pipe rupture in the primary system. The core consists of 500 fuel assemblies of SVEA-64 type and the mass of UO₂ is 104 300 kg. The core equivalent diameter is 3.88 m and the core height is 3.68 m. The mass of zirconium in cladding and fuel channels is 35 850 kg. The number of cruciform control rods with boron carbide and hafnium as absorber material is 121.

The reactor containment is a prestressed concrete vessel of a basic design in all nuclear power plants built by ABB Atom. The containment is based on the principle of pressure suppression and consists of drywell, wetwell and pedestal. The condensation pool is enclosed in the annular space between containment vessel wall and an inner cylindrical wall, which also carries the biological shield. Vent pipes extend vertically from the drywell to the condensation pool. Steam emerging from possible ruptures and leaks in the primary system is condensed in the pool. Steam from reactor relief valves is blown into the pool through blow-down pipes from each valve. All 12 relief valves blow down to the suppression pool. A relief line with rupture disk activation is provided to exclude the possibility of a rapid containment failure in the case of pressure suppression bypass. A venturi scrubber unit is aligned to the containment gas cleanup for relieving the containment pressure following a severe accident. In a case of severe accident the pedestal is flooded before vessel melt through with water from the condensation pool in order to cool debris in the containment.

A schematic description of the alignment of the key engineering safety systems of TVO I/II NPP is shown in Figure 1.



- 1 Control rods
- 2 Auxiliary feedwater system (327)
- 3 Reactor core spray system (323)
- 4 Boron system
- 5 Automatic depressurization system (314)
- 6 Containment overpressure protection system
- 7 Containment spray system
- 8 Pedestal flooding system
- 9 Containment water filling system
- 10 Filtered containment venting system

Figure 1. Schematic description of the alignment of key engineering safety systems of TVO III

Emergency core cooling is provided by two different systems - the auxiliary feedwater system 327 and the core spray system 323.

The auxiliary feedwater system operates as high pressure coolant injection system. It has sufficient capacity to keep the core flooded following a rupture in any nozzle on the bottom of the reactor vessel.

The core spray system operates at low pressure. It feeds spray water into the reactor when the pressure drops either after the pressure blow-down or as a result of ruptures in pipes connected to the cylindrical part of the reactor vessel.

Both systems with associated auxiliary systems performing emergency cooling functions are divided up to four independent subsystems of which two are sufficient to manage a loss of coolant accident. This allows for convenient performance of testing and repair without limiting plant operation.

Each subsystem incorporates separate pumps, valves and power supply from correspondingly separated standby diesel generators. The auxiliary feedwater system takes its water from special storage tanks, one separated tank for each of the subsystems.

The core spray system draws water from the condensation pool inside the containment. The water of this pool is cooled by the containment vessel spray system, which in turn is cooled by the sea water system, via an intermediate fresh water system.

The condensation pool heat sink can accept decay heat for about eight hours after reactor shutdown without external containment cooling.

2.2 FORSMARK NUCLEAR POWER PLANT

The Forsmark 3 (F3) is a 3300 MW_{th} boiling light water reactor of ABB-Atom design. Its operating pressure is 7 MPa and the recirculation coolant flow is maintained by 8 internal recirculation pumps. The core has 700 fuel elements and in the modelling they are assumed to be all of the SVEA-64 type, each consisting of four 4x4 rod sub-bundles with an active core height of 3.71 m.

In the Forsmark reactors depressurization is automatically activated (ADS) after an accident upon a signal indicating low downcomer water level. In the analysed total blackout cases opening signal to the ADS valves was obtained after about 12 minutes. (In the Finnish TVO I/II reactors depressurization is manually activated after 1 hour into the accident)

The Emergency Core Cooling System (ECCS) in Forsmark 3 comprises four high-pressure auxiliary feed water loops (System 327) and four low-pressure loops (System 323). Each 327 feed water loop has a capacity of 22.5 kg/s that is injected through spray nozzles above the fuel bundle exits. The 323 ECCS loops are distributed so that two loops inject water above the core, like 327, and the two others feed into the downcomer. Water filled into the downcomer facilitates reflooding of the core from the bottom, if the core has been uncovered. The capacity of system 323 is depending on the back-pressure, i. e. the pressure difference between primary system and containment. It begins to inject water when the back pressure is below around 1.2 MPa and the flow rate increases to about 360 kg/s per loop as the back-pressure goes to zero. (The distribution of the 327 and 323 lines is the opposite in the Finnish TVO reactors)

Some salient data of Forsmark 3 and TVO I/II BWR used in the calculations are given in Table 1.

Table 1. *Forsmark 3 and TVO III main data used in the calculations.*

| Item/plant | Forsmark 3 | TVO I/II |
|---|----------------------|--------------------|
| Reactor vessel inside height and diameter | 20.8 m \ 6.4 m | 20.6 m \ 5.54 m |
| Moderator vessel I.D. | 5.094 m | 4.29 m |
| Total free volume in vessel incl. steam lines | 561.6 m ³ | 429 m ³ |
| Total mass of reactor vessel | 761 000 kg | 631 000 kg |
| Mass of UO ₂ fuel | 148 064 kg | 104 300 kg |
| Mass of Zr in fuel rod claddings (SVEA-64) | 31 329 kg | 22 200 kg |
| Mass of Zr in fuel boxes (SVEA-64) | 19 159 kg | 13 650 kg |
| Number of cruciform B ₄ C control rods | 169 | 121 |
| Mass of B ₄ C, total | 1673 kg | 1258 kg |
| Mass of liquid water at normal downcomer level | 234 800 kg | 182 000 kg |
| Mass of liquid water below active core | 100 100 kg | 74 300 kg |

A schematic of the reactor vessel with internals for a type reactor, ABB-Atom BWR-75 is shown in Figure 2.

It should be noted that there are some important differences in the features of the safety systems between the Forsmark and the TVO reactors, although they are all ABB Atom's internal pump BWRs. The simulation of realistic cases will consequently not be the same for F3 as for TVO I/II.

In the Forsmark reactors the depressurization is automatically activated (ADS) after an accident upon a signal indicating low downcomer water level. In the TB case of F3 the ADS valves open after about 10 minutes. In TVO I/II, however, depressurization is manually activated latest after 1 hour into the accident in station blackout.

Moreover, the distribution of the lines for emergency cooling water is different in the Forsmark and in the TVO reactors. The high pressure, low capacity auxiliary feedwater system 327 injects water as spray above the core with all four lines in F3. In TVO I/II only two lines feed the top spray, while two of the lines go into the top of the downcomer. The low pressure, high capacity system 323 also has four loops in both the Swedish and the

BWR 75 - REACTOR VESSEL AND INTERNALS

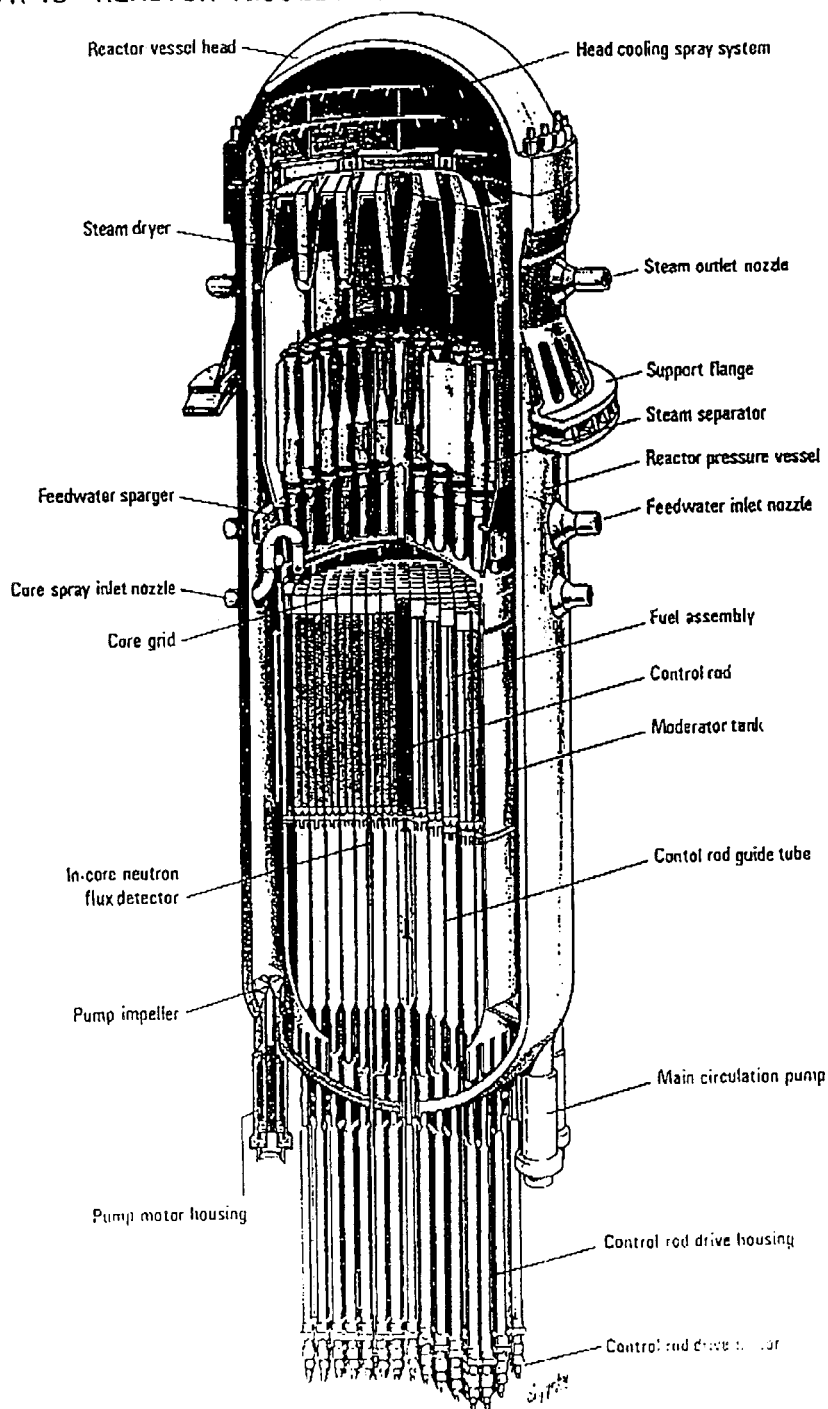


Figure 2. Reactor pressure vessel and internals in Forsmark 3 and TVO III NPPs.

Finnish reactors. In F3 two of the lines feed top spray nozzles above the core and two lines go into the downcomer. In TVO I/II all four 323-lines are directed to the spray nozzles above the core.

3. APPLIED CALCULATION TOOLS AND INPUT MODELS

3.1 MELCOR 1.8.3

MELCOR 1.8.3 is a fully integrated, engineering-level computer code developed by Sandia National Laboratories for the U. S. Nuclear Regulatory Commission (US-NRC), that models the progression of severe accidents in light water nuclear power plants [Ref. 14].

The reactor pressure vessel is modelled with 6 calculational control volumes: downcomer, lower head, core, bypass, upper plenum and steam dome. The core and lower plenum are subdivided into 5 radial rings and 14 axial levels. Four lowermost axial nodes reside in the lower head, the top one of which is the core support plate. The active core region is divided into 10 axial levels of equal height.

All radial rings have the same number of fuel bundles and flow area. Material masses in the TVO I/II core were modelled as given in Table 1.

The peaking factors for power calculation originate from measured plant data and are given in Table 2.

Table 2. Axial and radial power peaking factors used in calculations for TVO III.

| Axial node | Axial peaking factor | Radial node | Radial peaking factor |
|------------|----------------------|----------------|-----------------------|
| 10 (top) | 0.66548 | 1 (inner ring) | 1.22464 |
| 9 | 1.08560 | 2 | 1.2308 |
| 8 | 1.13468 | 3 | 1.17772 |
| 7 | 1.10816 | 4 | 0.91096 |
| 6 | 1.08564 | 5 | 0.45592 |
| 5 | 1.10634 | | |
| 4 | 1.11856 | | |
| 3 | 1.09248 | | |
| 2 | 0.97688 | | |
| 1 | 0.62632 | | |

The lower head model has 5 penetrations, one in each radial ring. The initial failure area of each penetration given in the input is calculated as a sum of cross-sectional areas of control rod guide tubes and neutron detection tubes residing in the respective radial ring. The initial failure area of each lower head penetration is 0.361 m².

The used core model takes into account the eutectic reactions of different materials in the core during the heatup. B4C and stainless steel react at 1520 K, fuel and cladding react forming U-O-Zr eutectic with melting point at 2800 K. Inconel grid spacers were not included in the core material input and thus reaction between Inconel and cladding at 1210 K is not activated. According to experimental observations (as is modelled also in MELCOR 1.8.3) cladding fails around 1200 K due to eutectic reaction between Inconel grid spacer and cladding. This results in release of fission product gases. However, the cladding failure and subsequent fission product release from the fuel is assumed to occur at user specified cladding temperature which was the code default value of 1173 K. Material relocations due to Inconel and cladding reactions would have been minor due to small initial mass of Inconel.

The used melting points of each core material are shown below in Table 3. The temperatures in Table 3 are the default values in MELCOR code, except for Zr. The melting temperature of Zr was changed from default value of 2098 K to the value of 2200 K used in MATPRO. The MATPRO value has been noticed to be superior in different validation tasks [Ref. 11], [Ref.12].

Table 3. Melting points of core materials used in MELCOR calculations.

| Material | Melting point [K] |
|------------------|-------------------|
| UO ₂ | 3113 |
| Zr | 2200 |
| ZrO ₂ | 2990 |
| Stainless steel | 1700 |
| Steel oxide | 1870 |
| B4C | 2750 |

The core support plate is assumed to fail when the material temperature reaches the user specified value, in these calculations the stainless steel melting temperature of 1700 K. Furthermore, the lower head model used in these calculations was the simpler old MELCOR model. The more detailed lower head description based on models developed in Oak Ridge National Laboratories, which are included in the MELCOR code and can be activated through user-input, were not applied in these studies.

MELCOR models the oxidation of Zircaloy by both steam and oxygen, and the oxidation of steel and B4C by oxygen. Zircaloy oxidation is calculated for cladding, canister components and control rod guide tubes. Steel oxidation is calculated for "other structure" components. Both Zircaloy and steel oxidation are calculated for particulate debris.

The term candling is used here to refer the downward flow of molten core materials and the subsequent refreezing of these materials as they transfer sensible and/or latent heat to cooler structures below. The candling model is based on fundamental thermo-hydraulic principles,

but uses user-specified refreezing heat transfer coefficients given in the input. The default value of $1000 \text{ W/m}^2\text{-K}$ was used in these studies. The material refrozen on a component is termed conglomerate debris.

The candling process can produce blockages, if the free volume becomes zero in a node. Molten material pool can accumulate on a blocked node. MELCOR models also the radial relocations of molten material and solid particulate debris. The liquid levels are balanced between the nodes if there are no intact BWR canister components between adjacent rings.

Particulate debris is formed whenever the unoxidized metal thickness of an intact component reaches a user-specified minimum value. This model is based on the assumption that oxide layers cannot provide any structural strength to a component and that metal of a certain thickness is sufficient to support an arbitrary mass above that point. Particulate debris is also formed by collapsing, i.e. intact fuel rods can fall to lower cells if the middle of the core melts away. The debris formation due to quench-induced shattering is not implemented in MELCOR 1.8.3.

Particulate debris is assumed to be of single-sized spherical particles. The default particle diameter of 5 mm was used in these calculations. The oxidizable fraction of the total surface area of the particulate debris is the fraction of total particulate debris volume that is of Zircaloy and ZrO_2 . The particle diameter is an important parameter for oxidation calculation.

3.2 MAAP4 Model for TVO

The Modular Accident Analysis Program (MAAP) Version 4 is a computer code that can simulate the response of light water reactor power plants during severe accident sequences, including actions taken as part of accident management. Models are included to represent the actions that could stop the accident progression by in-vessel cooling.

The active core region is divided into radial rings and axial levels in the same way as in the MELCOR input, but the whole lower plenum is modelled as a single node.

Each MAAP4 core node may contain six components: fuel, cladding, fuel can, control blade, control/water rod, and coolant. These calculations do not contain control/water rods because of the SVEA-64 type fuel. Since the uranium can dissolve into the clad to form U-O-Zr mixture, decay heat can also be generated in the cladding directly.

Heat transfer by radiation and axial radial convection and conduction is modelled in each core node between the fuel, cladding, fuel can, control blade and coolant. MAAP4 models oxidation of Zr and stainless steel, the fuel-clad interaction, and the fuel can/control blade interaction. Cladding ballooning is evaluated based on the fuel-cladding gap pressure against the primary system pressure. If there exists fuel cans which effectively prevent any radial flow in the core, distinct boiled-up water levels are determined per channel. If the fuel can fails, its water level is adjusted to account for any potential communication with the rest of the core depending upon the location of the failure.

As the core temperature rises beyond 2000 K, UO_2 will be dissolved by Zr into U-O-Zr mixture. In BWRs the Zr fuel canister will chemically interact with the SS control blade at

around 1500 K. When the temperature at any location in the core reaches the material mixture melting point, the materials melt and refreeze as they flow down the outer cladding surface. Consequently subchannels may become partially and fully blocked. The steam and H₂ mixture flowing below a blockage would then be redistributed among the other channels according to the flow resistances.

In the covered part of the core steam can be formed by boiling and also by flashing if the RPV pressure changes with time. In the case, where the core is recovered from below after an extensive period of uncovering, the heat transfer rate from the hot fuel rods into the pool is limited by two-phase hydrodynamic stability considerations. A maximum gas superficial velocity exists beyond which liquid droplets would be entrained in the gas stream and kept from getting in contact with core material.

Inter-node heat transfer models are activated only for uncovered nodes or for hot degraded covered nodes. The applied radial power profile shows a significant reduction in the power generation in the outer core ring fuel assemblies. The central core assemblies may be at high temperature, while the temperatures of the outer core assemblies may be much lower. This represents a large potential driving force for radial heat transfer in the core.

MAAP4 models five types of fuel geometry to account for the damage state of fuel: (1) intact fuel pin configuration, (2) collapsed fuel pin configuration, (3) thickened fuel pin configuration due to candling, (4) node filled to a user-specified porosity due to downward relocation and no longer considered fuel pin configuration or penetratable and (5) fully molten node. The degradation types are irreversible.

When one or more nodes reach a molten state, the energy and mass transfer between these nodes enhances due to the pool natural circulation and a crust can form around a molten pool. MAAP4 considers bottom, top and side crusts. The crust prevents the coolant flow from interacting with molten nodes. Due to the continuous generation of decay heat in the pool the crust will eventually break and molten debris will be poured into the lower plenum or lower core region. Once the material satisfies the criteria for core geometry type (4), the only way for molten material to proceed downward is the failure of the crust at the bottom of the node. The crust failure criteria can be controlled by the user through input in MAAP4.

The calculation of Zircaloy oxidation rate has two options:

1) Application of Baker-Just model above 1875 K and the Cathcart model below 1850 K. An interpolated rate is used between these two temperatures

or

2) the oxidation rate is taken from the EG&G material properties library MATPRO.

3.3 SCDAP/RELAP5

SCDAP/RELAP5 has been developed to be a best estimate, transient simulation code for analysis of in-vessel thermal hydraulics, as well as of severe accident phenomena like core-melt progression, oxidation of metallic components with hydrogen generation and release and

transport of fission products in light water reactors. The code is the result of merging the well-established thermal-hydraulics RELAP5 code and the severe accident code SCDAP. By means of the COUPLE subroutine it is also possible to calculate the core debris interaction in the lower plenum and the lower head failure. Fission product inventory in the fuel can be derived from PARAGRASS and fission product transport and deposition behaviour are calculated based on models from TRAP-MELT. The latter may be replaced in later versions by a data link to the more detailed fission product code VICTORIA. Thermal properties of reactor materials, not specified by the user, are obtained from MATPRO subroutine.

The specific features of SCDAP/RELAP5/MOD3.1 are described in five volume set of manuals covering theory, and use of the code for severe accident applications [Ref. 4].

The reactor system can be nodalized in an arbitrary number of one-dimensional volumes and heat structures, and volumes can be connected by 1D to 3D connections (flow junctions). There are also a number of special component models for e.g. pumps, steam separators and core components. Thermal-hydraulic transport phenomena are based on nonhomogeneous, non-equilibrium, six equation and two-fluid model solved by a partial implicit numerical scheme.

Core components are individually modelled in the SCDAP part of the code with detailed specification for fuel rods, channel boxes and control rods. A special BWR control rod-blade box model developed in Oak Ridge National Laboratory has been implemented in current MOD3.1 version. The blade/box model was unfortunately not operable in the code version used for the calculations on TVO I/II. Since the Forsmark 3 calculations were made later, another code release C was available with these models functioning.

Models for core heat transfer include radiation on assembly level, i.e. rod surface-to-surface with absorption by fluid. Cladding oxidation is calculated by models with three various rates for different temperature levels, taking into account steam starvation, vapor diffusion and possible double-sided oxidation. Eutectic reactions, which can result in early melting, are accounted for between Inconel grid spacers and Zr cladding and between boron carbide and stainless steel with the ORNL blade/box model. Ballooning of fuel cladding with reduction of the channel flow area is calculated with respect to hoop stress compared to the failure stress as function of temperature and oxide thickness. Meltdown, relocation and refreezing (candling) is based on the LIQSOL model.

Model improvements in the latest code version of interest are the local and global oxide shattering models for reflooding. Other new models are for calculation of radial and axial spreading of molten material into surrounding porous debris and intact assemblies, and for removal of blockages due to melting and slumping. The underprediction of hydrogen generation in the late phase of accident progression should be solved in the next version by an improved model for debris thermal-hydraulics to treat post shattering and reflooding of debris beds.

Some of the important models for the TVO calculations are described briefly in the following section.

3.3.1 TVO Model

The control volume nodal model is basically the same as in earlier TVO applications .

Unfortunately the BWR specific B₄C control blade and channel box component model could not be used in the calculations. Therefore the older B₄C control rod and shroud models were used instead. This resulted in the same problems as recognized in earlier calculations with older code versions (for example too high temperature differences between control rods and shroud). The fuel rod ballooning was taken into account (ballooning model was on) which was a new feature in comparison to the earlier calculations.

In general the RELAP-part of the input was changed to correspond with MELCOR-input data (volumes etc.). Also the core part was divided into five core channels (and five bypass channels) . The SCDAP-part of the core model consists of five different fuel components, shroud components and control rod components. Each channel has 10 axial nodes. The model presumes conversion of the cruciform geometry into a cylindrical shape.

The control rod model is designed to calculate the melting of cylindrical rod filled with boron carbide. In the former calculations the data for German type of control rods were used. In these calculations data for the control rod of ABB-type is used.

A tentative COUPLE - model is used to calculate the heatup of debris and/or surrounding structures. The COUPLE code is a two-dimensional, finite element, steady state and transient heat conduction code . The code was developed to solve both plane and axisymmetric type heat transfer problems with anisotropic thermal properties. This model takes into account the decay heat and internal energy of newly formed or fallen debris and calculates the transport by conduction of the heat in the radial and axial directions to the wall structures and water surrounding the debris. In the TVO calculations the penetrations through the pressure vessel wall are not taken into account. Also the material properties used have to be checked and changed if more detailed model is required.

3.3.2 Forsmark 3 Model

The input model for Forsmark 3 is mainly the same as the one used in the previous SIK-2.3 calculations [Ref. 7]. Only the reactor vessel and internals and the steam lines limited by the inner isolation valves are modelled, since SCDAP/RELAP5 treats only in-vessel phenomena. The reactor core model comprises five parallel core channels, each with a number of fuel bundles and a bypass channel and a corresponding fraction of control rod blades. The active height of the core is divided into ten axial subcells. The new Oak Ridge BWR fuel model, recently implemented into the code, is now utilized instead of the earlier, simplified model.

Table 2 gives figures of the division of the core cross section inside the moderator vessel. Core zone 1 is in the centre, and zone 5 comprises the outermost bundles with the large bypass area inside the moderator vessel :

Table 4. Data for the five core zone model in SCDAP.

| Zone No. | 1 | 2 | 3 | 4 | 5 | Total |
|------------------------|--------|--------|--------|--------|--------|----------------------|
| No. of fuel bundles | 176 | 176 | 176 | 80 | 92 | 700 |
| Flow area of bundles | 1.891 | 1.891 | 1.891 | 0.859 | 0.988 | 7.520 m ² |
| Radial power factor | 1.24 | 1.18 | 1.12 | 0.59 | 0.33 | (1.00) |
| Power fraction | 0.3117 | 0.2962 | 0.2817 | 0.0675 | 0.0429 | 1.000 |
| Inlet flow restriction | 60 | 60 | 60 | 100 | 140 | - |
| No of control rods | 44 | 44 | 44 | 20 | 17 | 169 |
| Bypass flow area | 0.629 | 0.629 | 0.629 | 0.286 | 3.827 | 6.000 m ² |

The fuel bundles and bypass channels are modelled as RELAP5 "pipe" components. "Branch" components are used for the bypass inlet in order to facilitate transversal distribution of the inlet flow in the bypass. The RELAP5 model comprises 150 volumes and 163 flow junctions. Structures in the vessel and the vessel itself are modelled as RELAP5 heat structures, while all structures in the core are modelled as SCDAP components. The SVEA fuel geometry was converted into the ORNL Blade/box model and three components were employed in each core zone: the fuel, the blade/box and the shroud component, the latter was used to model the SVEA water cross.

The power distribution was modified compared to that used in SIK-2.3. It is based on POLCA-4 calculations for a core with a burn-up of 24 000 MWD/TU, which gave individual bundle power factors at 25 axial levels [Ref. 9]. The power factors input to SCDAP/RELAP5 were derived by averaging, using the same axial heat flux distribution with ten steps and a peak power factor of 1.13 for all five core channels.

Also the power decay curve after scram was modified. It is now based on a new ANSI-85 standard (ISO/DIS 10645), which gives a slightly lower power level (faster decay) than the ANSI-79 curve used in previous SIK-2 calculations. The power decay during the first 10 s after loss of AC-power, during pump coast-down and before scram is a function of void feedback and still based on a separate RELAP5 reactor kinetics calculation.

To facilitate simulation of radial spreading of a possible core melt and its interaction with the lower head of the vessel, the structures below the core are modeled as COUPLE components. A rather coarse nodalization is used here for the reflooding calculations. (The COUPLE model has probably to be refined for the analysis of late phase melt progression and lower head interaction, which is planned to be done during stage 3 of RAK-2.1 projects).

4. SCOPE OF CALCULATIONS

4.1 TVO

Two base case scenarios were chosen for the study on the basis of PSA level 1 for TVO I/II: Initial loss of power followed by depressurization of reactor coolant system through ADS (system 314) leading to low pressure scenario and initial loss of power with failure to depressurize RCS leading to high pressure scenario. The ADS valves are assumed to be opened at 1 h into the accident in the low pressure scenario.

Table 5. shows the key specifications of the calculated 10 base scenarios. Some parameter sensitivity runs were carried out with MAAP4 and MELCOR 1.8.3 to see the effect of key model parameters.

Table 5. Accident Scenario specifications for TVO III .

| Case | Depressurization of RCS | Cooling recovery | Mass flow rate (kg/s) | Starting temperature (PCT)* (K) |
|------|-------------------------|-------------------|-----------------------|---------------------------------|
| 1 | 1 h | No | 0 | - |
| 2 | 1 h | 327, DC injection | 45 | 1400 |
| 3 | 1 h | " | 45 | 1600 |
| 4 | 1 h | " | 45 | 1800 |
| 5 | 1 h | " | 45 | 2000 |
| 6 | No | No | 0 | - |
| 7 | No | 327, DC injection | 45 | 1400 |
| 8 | No | " | 45 | 1600 |
| 9 | No | " | 45 | 1800 |
| 10 | No | " | 45 | 2000 |
| 11** | No | " | 45 | 2300 |
| 12** | No | " | 45 | 2730 |

* The temperature when water reaches the active core

** Only calculated with MAAP4

The timing of recovery of power was varied in both base cases in a way that reflooding water reached the bottom of the active fuel, at the time, when maximum cladding temperature reached values: 1400 K, 1600 K, 1800 K and 2000 K.

The core was reflooded via operation of system 327 with capacity of 45 kg/s (two pump lines) injecting to the downcomer in all variations. The cases, where the system 327 would inject water on top of core through core spray spargers, were not studied. If the core

temperatures are high at the recovery of power, the core spray spargers residing close above the core may already be damaged at the time of power recovery.

4.2 FORSMARK 3

A total of nine cases was chosen for the calculations including two base cases with different primary system pressure levels. In the low pressure group an early, automatic start of depressurization (ADS) was simulated, initiating on low downcomer water level. The vessel pressure was then relieved to equal the containment pressure, which was set to 5 bar. In the other group of calculations it was assumed that the ADS failed, so the pressure stayed at 70 bar all through the time of the analysis.

The scenario in the selected base cases for Forsmark 3 was station blackout (TB) with no recovery of AC power, i.e. without reflooding of the core. The reflooding cases include simulation of recovery of either the high pressure auxiliary feedwater system (327) or of the low pressure Emergency Core Cooling System (ECCS, 323), both with half the nominal capacity. Injection from the ECCS is possible only in the low pressure cases. The difference between the reflooding cases is the time, or rather the peak cladding temperature (PCT) at which cooling water was introduced to the core, as shown in Table 6.

Table 6. Calculation matrix for Forsmark 3.

6a. Low pressure scenarios (with ADS).

| Case No. | Cooling recovery | Mass flow rate (kg/s) | Starting temperature (PCT)** (K) |
|----------|-------------------|-----------------------|----------------------------------|
| 1L | No | 0 | - |
| 2 | 327, core spray | 45 | 1400 |
| 3 | " | 45 | 1600 |
| 4 | " | 45 | 1800 |
| 7 | 323, core spray | 580* | 1800 |
| 8 | 323, DC injection | 580* | 1800 |

* Corresponds to the flow rate of two loops at a back pressure of 4 bar

6b. High pressure scenarios (without ADS)

| Case No. | Cooling recovery | Mass flow rate (kg/s) | Starting temperature (PCT)** (K) |
|----------|------------------|-----------------------|----------------------------------|
| 1H | No | 0 | - |
| 5 | 327, core spray | 45 | 1600 |
| 6 | " | 45 | 1800 |

** The temperature when the water reaches the active core

5. TVO I/II RESULTS

5.1 STATION BLACKOUT WITH SUCCESSFUL DEPRESSURIZATION OF RCS

The key figures of merit from the calculated low pressure scenarios with MELCOR 1.8.3 are gathered into Table 7. The respective MAAP4 results are shown in Tables 8a and 8b and the key figures of merit from low pressure scenarios with SCDAP/RELAP5 in Table 9.

Table 7. Key results from reflooding sequences in TVO I/II plant calculated with MELCOR 1.8.3. Initial station blackout with depressurization of RCS through system 314 at 1 h into the accident. Reflooding with system 327 to downcomer with capacity of 45 kg/s.

| Case | ME1 No reflooding | ME2 Reflooding at 1431 K | ME3 Reflooding at 1603 K | ME4 Reflooding at 1757 K | ME5 Reflooding at 1850 K | ME6 Reflooding at 1985 K | ME7 Reflooding at 2076 K |
|--|-------------------------|--------------------------------|--------------------------------|--------------------------------|--------------------------------|--------------------------------|--------------------------------|
| Top of fuel uncovered | 2100 s | 2100 s | 2100 s | 2100 s | 2100 s | 2100 s | 2100 s |
| ADS valve open | 3600 s | 3600 s | 3600 s | 3600 s | 3600 s | 3600 s | 3600 s |
| Total fuel uncovery | 4160 s | 4160 s | 4160 s | 4160 s | 4160 s | 4160 s | 4160 s |
| H ₂ prod. begins | 4910 s | 4190 s | 4190 s | 4190 s | 4190 s | 4190 s | 4190 |
| 327starts: time, max clad temp | - | 4991 s 1150 K | 5345 s 1350 K | 5823 s 1500 K | 5992 s 1600 K | 6402 s 1750 K | 6588 s 1800 K |
| Reflowd enters core: time,max clad temp | - | 5631 s 1431 K | 5990 s 1603 K | 6443 s 1757 K | 6570 s 1850 K | 6959 s 1985 K | 7140 s 2076 K |
| Total core recovery | - | 8670 s | 9000 s | 9330 s | 9570 s | - | - |
| Core plate failure | 7566 s | - | - | - | - | 7506 s | 7566 s |
| RPV failure | 7658 s | - | - | - | - | 7763 s | 7755 s |
| In-vessel H ₂ prod. | 424 kg (*) | 373 kg | 445 kg | 413 kg | 489 kg | 500 kg (*) | 475 kg (*) |
| Zr oxid. fraction | 24.2 % (*) | 21.9 % | 25 % | 23.7 % | 28.5 % | 29.7 % (*) | 28.4 % (*) |
| Max core support plate temp | 1700 K (**) | 850 K | 1241 K | 1550 K | 1560 K | 1700 K (**) | 1700 K (**) |

(* at core support plate failure

(** failure temperature of core support plate

Table 8a. Key results from reflooding sequences at TVO III BWR plant calculated with MAAP 4.00a. Reflooding with auxiliary feed water system 327, injection capacity 45 kg/s to downcomer. Manual depressurization of RCS at 1 h. Calculation time is 10000 s.

| Case | MA1 | MA2 | MA3 | MA4 | MA5 | MA6 |
|--|--------------------|----------------------|------------------------|------------------------|------------------------|------------------------|
| | No reflooding | Reflooding at 1260 K | Reflooding at 1400 K | Reflooding at 1600 K | Reflooding at 1800 K | Reflooding at 2000 K |
| Top of fuel uncovered | 1800 s | 1800 s | 1800 s | 1800 s | 1800 s | 1800 s |
| Hydrogen production starts | 2700 s | 2700 s | 2700 s | 2700 s | 2700 s | 2700 s |
| Depressurization, manual ADS | 3600 s | 3600 s | 3600 s | 3600 s | 3600 s | 3600 s |
| Total core uncover | 3700 s | 3700 s | 3700 s | 3700 s | 3700 s | 3700 s |
| Control rod melting begins | 5000 s | 5000 s | 5000 s | 5000 s | 5000 s | 5000 s |
| Core fuel melting begins | 6100 s | 6100 s | 6100 s | 6100 s | 6100 s | 6100 s |
| Start of water injection, max core temperature | - | 4270 s 1090 K | 4460 s 1190 K | 4860 s 1430 K | 5040 s 1530 K | 5500 s 1790 K |
| Reflood enters the core, max core temperature | - | 4560 s 1260 K | 4800 s 1400 K | 5220 s 1600 K | 5400 s 1800 K | 5810 s 2000 K |
| Mass of melt in core when reflood enters core | - | - | - | 80 kg | 400 kg | 2800 kg |
| Core collapse | 7700 s | - | 5900 s | 5360 s | 5600 s | 5970 s |
| Core recovered | - | 6300 s | 6850 s | 7200 s | 7340 s | 7700 s |
| Core plate failure | 8600 s | - | - | - | - | - |
| Vessel failure | 8800 s | - | - | - | - | - |
| In-vessel H ₂ generation | 110 kg | 81 kg | 240 kg | 450 kg | 410 kg | 490 kg |
| Oxidation fraction of cladding | 9 % | 5 % | 15 % | 30 % | 28 % | 38 % |
| Oxidation fraction of channels | 1 % | 3 % | 8 % | 17 % | 13 % | 8 % |
| Max core node temperature, time | 4520 K 8790 s | 2790 K 5200 s | 2910 K 5290 s | 3120 K at the end | 3110 K at the end | 3040 K at the end |
| Max amount of melt in core, time | 50900 kg 8400 s | 1400 kg 5230 s | 23180 kg at the end | 24950 kg at the end | 36000 kg at the end | 64550 kg at the end |

Table 8b. Sensitivity studies. Reflooding sequences at TVO III BWR plant calculated with MAAP 4.00 a. Reflooding with auxiliary feedwater system 327, injection capacity 45 kg/s to downcomer. Manual depressurization of RCS. Calculation time is 20000 s.

| Case | MA7 | MA8 | MA9 |
|---|---|---|---|
| | No reflooding. Enhanced debris coolability in lower head and late vessel failure. | Reflooding at 1400 K. Modified Larson-Miller parameters. Crust failure. | Reflooding at 2000 K. Modified Larson-Miller parameters as in MA8. Crust failure. |
| Top of fuel uncovered | 1800 s | 1800 s | 1800 s |
| H ₂ production starts | 2700 s | 2700 s | 2700 s |
| Depressurization, manual ADS | 3600 s | 3600 s | 3600 s |
| Total core uncover | 3700 s | 3700 s | 3700 s |
| Control rod melting begins | 5000 s | 5000 s | 5000 s |
| Core fuel melting begins | 6100 s | 5250 s | 5850 s |
| Start of reflooding, max core temperature | - | 4460 s 1190 K | 5500 s 1800 K |
| Reflood enters core, max core temperature | - | 4800 s 1400 K | 5810 s 2000 K |
| Mass of melt when reflood enters core | - | - | 2800 kg |
| Core collapse | 7700 s | 5900 s | 6000 s |
| Core recovered | - | 6850 s | 7700 s |
| Core plate failure | 8600 s | - | - |
| Vessel failure | 16000 s | - | - |
| In-vessel H ₂ production | 200 kg | 340 kg | 520 kg |
| Oxidation fraction of cladding | 16 % | 24 % | 40 % |
| Oxidation fraction of channels | 2 % | 8 % | 8 %e |
| Max core node temperature, time | 3110 K 10870 s | 2910 s at the end | 3120 K 18640 s |
| Max amount of melt in core, time | 50910 kg 8400 s | 56060 kg at the end | 63490 kg at the end |

Table 9. Key results from reflooding sequences in TVO III nuclear power plant calculated with SCDAP/RELAP5/MOD 3.1. Initial station blackout with depressurization of RCS through system 314 at 1 h into the accident. Reflooding with system 327 to downcomer with capacity of 45 kg/s.

| Case | SC1 No reflooding | SC2 Reflooding at 1420 K | SC3 Reflooding at 1592 K | SC4 Reflooding at 1824 K | SC5 Reflooding at 1857 K |
|--|-----------------------|---|---|--|--|
| Top of fuel uncovered | 1450 s | 1450 s | 1450 s | 1450 s | 1450 s |
| ADS activated | 3600 s | 3600 s | 3600 s | 3600 s | 3600 s |
| Total fuel uncover (active fuel) | 3625 s | 3625 s | 3625 s | 3625 s | 3625 s |
| H ₂ prod. begins | 3360 s | 3360 s | 3360 s | 3360 s | 3360 s |
| Cladding overstrain failure | 4691 s | 4531 s | 4570 s | 4695 s | 4699 s |
| 327 starts: time, max clad temp | - | 4025 s 921 K | 4200 s 1006 K | 4616 s 1198 K | 4642 s 1209 K |
| Water enters core: time, max clad temp | - | 4825 s 1420 K | 4900 s 1592 K | 5380 s 1824 K | 5420 s 1857 K |
| Grid spacers and cladding start to slump | 4997 s | 4943 s | 4844 s | 5035 s | 5025 s |
| Molten pool formation and slumping to lower head | | 5173 s | | | |
| In-vessel H ₂ production | 100 kg (at 5343 s) | 162 kg (at 5178 s, still continuing) | 188 kg (at 5201 s, still continuing) | 82 kg (at 5420 s, still continuing) | 166 kg (at 5527 kg, still continuing) |

Calculated accident scenarios were initiated with total loss of power. The pressure in the reactor coolant system (RCS) started to rise and was controlled by safety relief valves (SRV) around 70 bar. The coolant level in the core decreased due to loss of steam through SRVs and fuel temperatures started to rise in the core. Depressurization of RCS through ADS was initiated at 1 h into the accident. Two thirds of the core height was uncovered at the opening of ADS valves. Opening of ADS valves caused a large steam flow through the core to the suppression pool cooling temporarily the fuel and the control rods. After the closure of the ADS valves at RCS pressure of 3 bar, the core started to heatup again. According to MELCOR and SCDAP/RELAP5 the water level in the vessel had sunk to about 1.5 m below active core during the blowdown, according to MAAP4 the water level remained slightly

higher. The temperature of the hottest core node had reached 1100 K prior to opening of the ADS valves according to MAAP4 and SCDAP/RELAP5 and during the depressurization the peak core temperature decreased to 860 K due to steam flow through core. The respective core temperatures were predicted to be about 200 K lower by MELCOR. After the depressurization of the RCS, the core was totally uncovered and the core temperature started to increase again. The average heatup rate was 0.4 K/s.

Two lines of the system 327 started to inject 45 kg/s of water into the downcomer when the defined maximum cladding temperature was reached. The injected water run down and mixed with the water pool in the lower head filling up the vessel from the bottom upwards. About 6-10 min after the initiation of system 327 the water penetrated to the active fuel.

5.1.1 Cladding and Debris Temperatures

MELCOR predicted melting and relocations of cladding and fuel in all low pressure cases. The hottest core node was the second highest from top of core, the temperature decreased when moving downwards in the core. However, the temperature differences between the axial levels were rather small in all low pressure cases prior to beginning of reflooding.

Material relocations started in MELCOR calculations, when cladding temperature reached the zirconium melting temperature of 2200 K. The fission product release from the fuel rods occurred by rupture of cladding at the temperature of 1173 K, which is determined by user input. When metallic zirconium on the inner surface of the cladding reached its melting temperature the non-oxidized cladding started to candle down. MELCOR calculations show that the melt refroze on the lower parts of the core. As the amount of metallic cladding became small enough in a node by candling, the cladding oxide layer and the fuel pellets collapsed and formed particulate debris. Particulate debris was supported from below, if intact components existed in the node below or the node was blocked.

The particulate debris bed was not fully quenched by the end of the calculation (at 10000 s). In fact, the temperature of the inner parts of the rubble bed was still high (above 2000 K). MELCOR calculates the melting point of rubble bed as a mixture melting temperature of its different material components. The main component of particulate debris by weight fraction was UO_2 and thus the rubble bed had a high melting temperature ~ 3100 K. The particle diameter of the rubble bed was assumed to be 5 mm. This can be an important parameter, when considering the oxidation of particles and the coolability of a particle bed. In the calculated cases coolant was not able to penetrate to packed inner parts of the particle bed to guarantee fast quenching.

In all MELCOR calculations (as well as in MAAP 4 and SCDAP/RELAP5 calculations, too) the cladding temperature prior to opening of the ADS valves was below 1200 K.

In the non-reflooded base case MAAP4 predicted the core fuel melting to commence at 1 h 40 min into the accident, when the average core temperature was 1608 K. The maximum fuel temperature was at the time 2131 K. The zirconium in the cladding started to melt and dissolve UO_2 and ZrO_2 . The core collapsed at 2 h 10 min into the accident, when the amount of melt in core was 36 metric tons consisting mainly of molten control rods. The fuel melting and relocations were minor at this time. The melt blocked the upper part of the core, but fuel

geometry was still intact. The upper part in the central nodes collapsed into particles, that relocated onto deformed fuel in the lower part of the core. The fuel geometry in outer channels was intact except for the lowest nodes.

MAAP4 predicted the core plate failed at 2 h 25 min, when the temperature of the core plate exceeded 1370 K. The temperature of debris on core plate varied between 2200 K and 2700 K. The vessel failed 3 minutes after fuel had relocated to the lower plenum due to ejection of instrument tubes. At the time of vessel failure 104 tons of melt had accumulated in the lower head with the average temperature of 2013 K, 195 K above the melting point.

In the case MA2 the water injection was started 11 minutes after depressurization, when the maximum core temperature reached 1090 K. The two-phase level in the core had dropped below the active core region during the blowdown and it took 5 minutes before the water level reached the bottom of the active fuel. At the time water entered the core region the maximum cladding temperature was 1260 K (the average core temperature was 1016 K). The reflooding from bottom upwards caused a rapid temperature increase due to cladding oxidation. The maximum core temperature (2790 K) was reached 11 min after the water level reached the bottom of active fuel in the uppermost node in the centre of the core. This node contained no fuel.

The core was quenched completely in 29 min from start of auxiliary feedwater system and the cladding temperature had dropped to the saturation temperature in all core nodes. The quenching took place already before the core was fully recovered by two-phase mixture. During reflooding there existed large temperature differences in the core. The lower part was in saturation temperature, below 500 K, while the temperature of the upper part was well beyond 2000 K.

In the cases MA3-MA6 the reflooding was started later. The maximum core temperature, when reflooding entered the core, varied between 1400 K and 2000 K. All the cases showed a similar behaviour: When water enters the core from below, the upward steam flow accelerates cladding oxidation resulting in rapid temperature escalation.

In the case MA3 reflooding entered the core 20 min after activation of ADS, when the maximum core temperature had reached 1400 K. For 8 minutes the core temperatures increased until they started to sink again when the reactor water level had risen high enough. The temperature decrease is, however, only temporary. The whole core upper half collapses at 1h 38 min. A particle bed is formed on deformed fuel. Just before the collapse the fuel geometry was still intact, but the upper part was blocked. The highest core temperatures were then 2000-2100 K. The two-phase level had risen halfway to the active core. After the collapse the temperatures increased again and core materials began to melt. When the calculation was terminated at 2 h 50 min the amount of melt in the core was 23 tons and the average temperature of core was 1700 K.

In the other sequences the core collapsed within 3 min after reflooding had entered the core. At the time of collapse the highest core temperatures were about 2800-2900 K.

In all SCDAP/RELAP5 calculations of low pressure scenarios the cladding temperature histories were identical before the depressurization of the primary system. The temperatures started to rise after about 2000 s. The cooling during the depressurization was quite rapid and the temperatures started to decrease before the end of calculation in all cases. In general,

the lower the temperature level was during the water entry, the better the code version managed to calculate the thermal-hydraulic behaviour of the core.

SCDAP/RELAP5 predicted that the core damage began with overstrain failures of fuel cladding in several locations. Also the channel flow areas reduced. The grid spacers started to melt and slump first in the upper half of the core in the center channels. Also the melting of the cladding started as well as the relocation and slumping of the metallic melt into lower nodes. These phenomena occurred in all cases. The clogging of material stopped the local oxidation and formed blockages.

In the case SC2 (1400 K) the calculations could be continued up to the point, when formation of cohesive debris started at the axial node 8 in the core channel 2. Debris formation was caused by zirconium oxide melting. Heatup of the debris caused a local melt pool formation with additional new material slumping into the pool from the nodes above.

The input parameters were chosen so, that the melt slumped into the lower head, whenever the material at the outer boundary of the core became molten. This provided an estimate of the earliest possible time of melt pool slumping. The thickness of the substrate supporting melt pool prior its slumping (5173 s) was about 2 cm. There were about 232 kg of uranium dioxide and 68 kg of zirconium dioxide in the lower head at the end of the calculation.

In general the code version did not manage to calculate properly the more extreme reflooding conditions in cases where the core temperature level was higher than 1400 K. In cases SC3...SC5 the code predicted local melt pool formation in central channels at earlier times. In these situations the core was quenched but some rubble formation occurred due to fragmentation of the embrittled fuel rods.

The cladding temperatures in the top axial level, in the center of the core are shown in Figures 3, 4, 5 and 6 for different low pressure reflooding cases calculated with SCDAP/R5, MELCOR and MAAP 4. In the early phase of the accident, the temperature of the top centre node represents also the maximum cladding temperature, but when the core heatup proceeds further, the maximum cladding temperature was reached in other nodes. This is the reason, why the points indicating start of reflooding do not necessarily coincide with the maximum cladding temperature of the recovery criterion. Particularly in MAAP4 and SCDAP/RELAP5 calculations the hottest core node is located in a lower axial elevation than in MELCOR calculations.

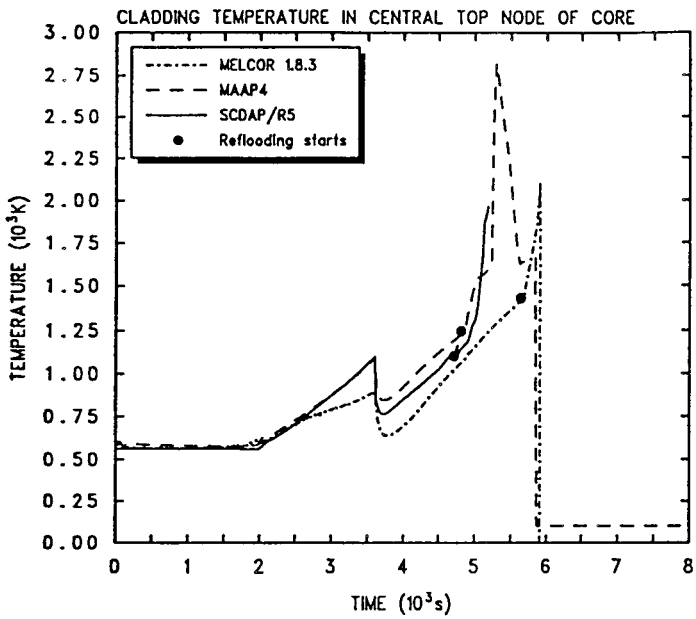


Figure 3. Cladding temperature in top center core node. Reflooding started 1400 K. Low pressure case.

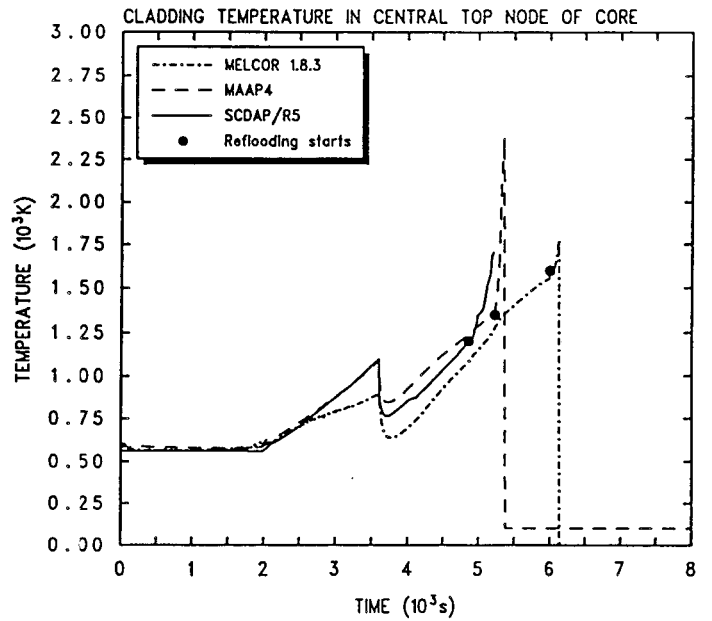


Figure 4. Cladding temperature in top center core node. Reflooding started at 1600 K. Low pressure case.

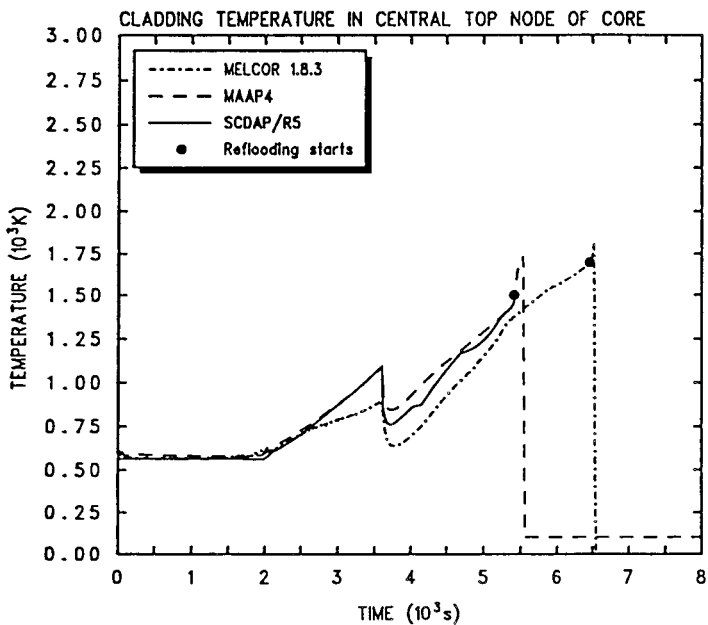


Figure 5. Cladding temperature in top center core node. Reflooding started 1800 K. Low pressure case.

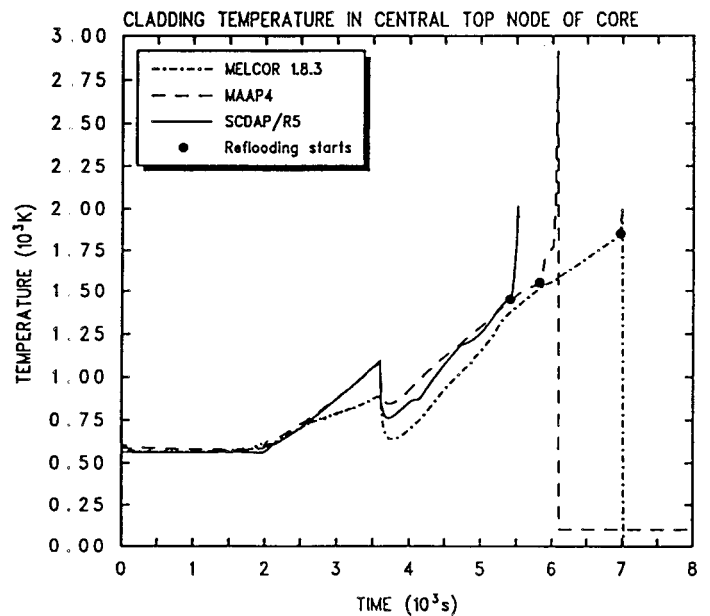


Figure 6. Cladding temperature in top center core node. Reflooding started at 2000 K. Low pressure case.

5.1.2 Hydrogen Production

MELCOR predicted the rapid oxidation to start when water level reached the bottom of the active fuel. Cladding oxidation was most efficient in the upper third of the core. MELCOR predicted highest oxidation fractions for cladding, but also fuel cans were oxidized. Some minor steel oxidation took place in the control blades. The overall (cladding + cans) oxidation fraction varied from 22 % to 29 %. In the case ME2 (1400 K) MELCOR predicted higher hydrogen generation than MAAP, but in all other low pressure scenarios with reflooding MAAP 4.0 and MELCOR 1.8.3 prediction agreed remarkably well.

In the MAAP4 base case without reflooding, the hydrogen generation in the core was very low, only 1.1 kg, before debris slumped in the lower plenum. When debris slumped into the lower plenum pool producing a lot of steam, the hydrogen production accelerated. MAAP 4 does not calculate gradual relocation of metallic melt into the lower head before core plate failure. This would lead to enhanced steam production and cladding oxidation, and would thus accelerate core degradation. The debris was not cooled in the lower plenum and an early vessel melt through resulted. The total hydrogen generation was 110 kg. The cladding oxidation fraction was 9 % and the respective fuel can oxidation fraction was 1 %. The MELCOR prediction for in-vessel H₂ production was much higher, 424 kg, in the respective base case ME1.

In a sensitivity run (MA7), where debris cooling in the lower plenum was enhanced, the vessel failure was delayed. Compared to the previous case hydrogen generation almost doubled to 200 kg.

The effect of the timing of depressurization was studied with assumed delaying of manual activation of ADS. When the depressurization was delayed with 20 min, the amount of hydrogen generated in the core roughly doubled to the base case. Delaying the depressurization further, with 30 min, resulted in total H₂ generation of 340 kg. In both cases the hydrogen generation accelerated the core degradation and nearly all hydrogen was released prior to corium slumped into the lower head.

In case MA2 core reflooding with auxiliary feedwater took place at low enough temperature that the core quenching was successful. Consequently hydrogen generation was only 81 kg. The hydrogen was generated during the time interval of 20 min after the start of reflooding.

In all cases MA3...MA6 the trend of hydrogen generation was very similar. The amount of hydrogen generated increased, if the core temperature at the start of reflooding was higher. However, the hydrogen release was not finished when the core was recovered with water, but continued at a lower rate. The total amount of hydrogen generated was 240 ...490 kg.

The amounts of hydrogen produced up to the of the calculation in low pressure cases varied from 82 kg to 166 kg in SCDAP/RELAP results (Table 8.). When the primary system was depressurized, the total mass of produced hydrogen increased very quickly after the water entered the core. The experimental results support this observation. The energy addition (due exothermic oxidation of the cladding) to some nodes was so rapid, that it caused numerical problems in code execution.

Figures 7...10 show the calculated in-vessel hydrogen production in different low pressure cases.

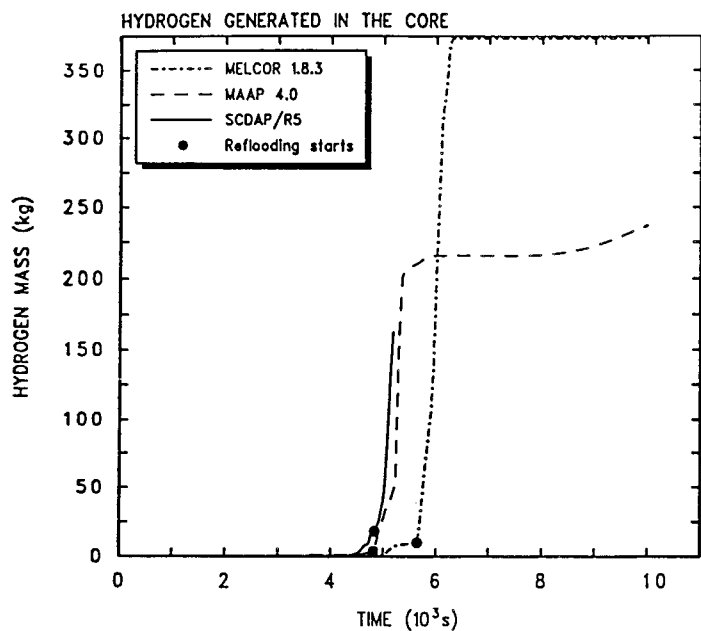


Figure 7. In-vessel hydrogen generation in TB case with ADS and reflooding at max cladding temperature of 1400 K in TVO IIII.

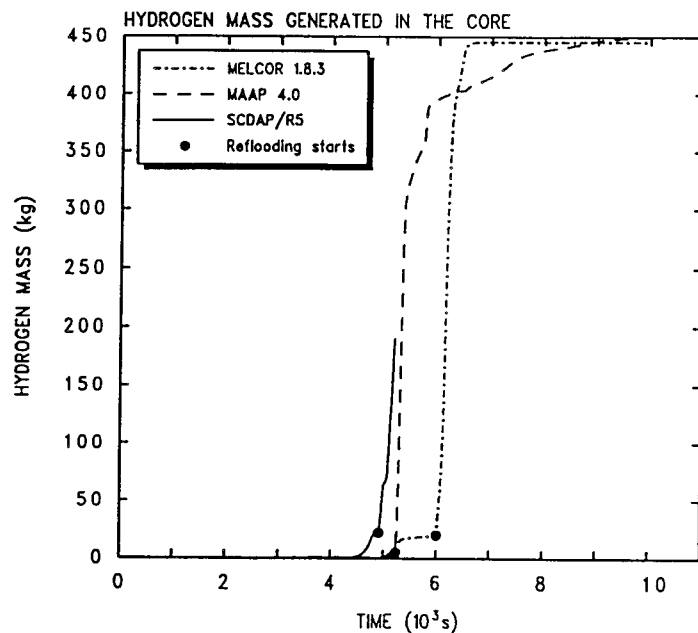


Figure 8. In-vessel hydrogen generation in TB case with ADS and reflooding at max cladding temperature of 1600 K in TVO IIII.

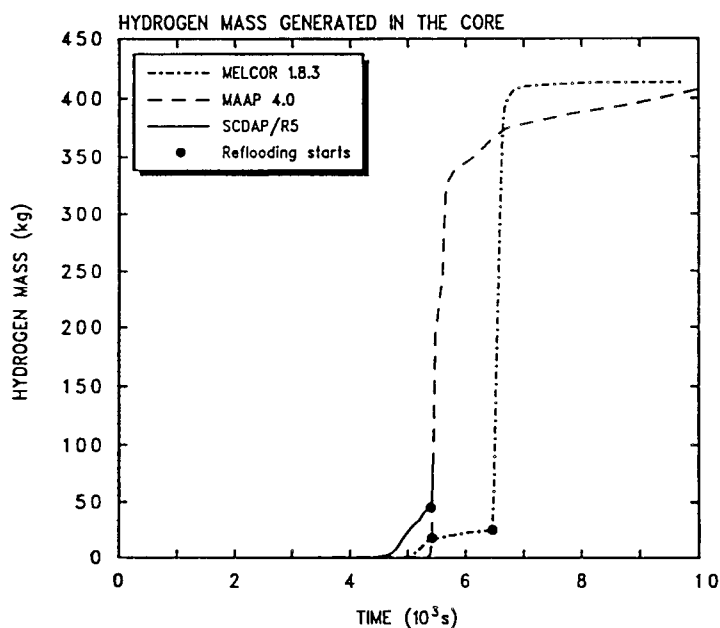


Figure 9. In-vessel hydrogen generation in TB case with ADS and reflooding at max cladding temperature of 1800 K in TVO IIII.

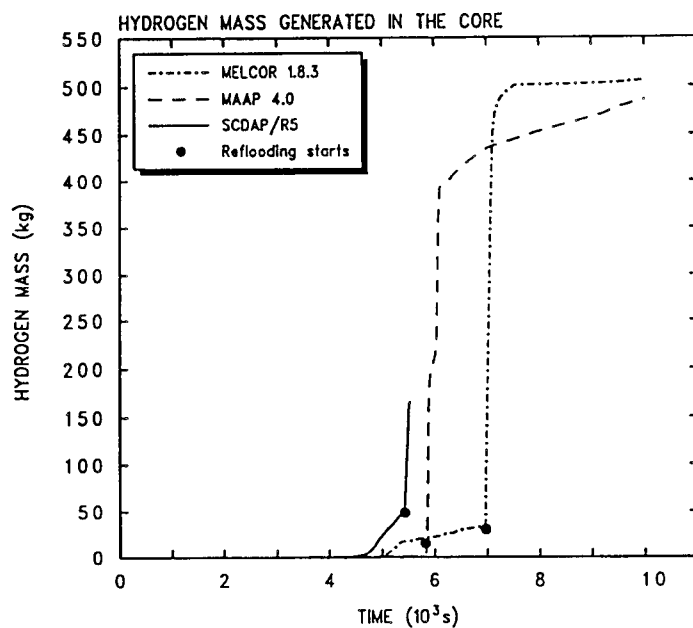


Figure 10. In-vessel hydrogen generation in TB case with ADS and reflooding at max cladding temperature of 2000 K in TVO IIII.

5.1.3 Control Rods

In the MELCOR model the control rods are assumed to slump down when reaching the melting temperature of stainless steel, 1700 K. Boroncarbide and steel will react on the inner surface of the control blades and form eutectic mixture with melting temperature of 1520 K. The melt inside a control blade is held in its place until the melting temperature of the outer surface is reached. MELCOR predicts much smaller temperature difference between the control rods and the fuel than SCDAP/RELAP5, which is due to the fact that SCDAP/RELAP5 resulted in unrealistically low control rod temperatures. The slumping of the control rods occurred about 1 min earlier than relocations of fuel in the respective node in the MELCOR results. This time gap was small because the control rods were heated up to their melting point rapidly after breakoff oxidation started in the cladding.

In the MAAP calculations the control rods started to melt and relocate at a lower temperature than cladding and fuel. A eutectic of stainless steel and B_4C was formed at circa 1500 K. The fact that core absorbing material can relocate while fuel geometry is still intact makes recriticality during and after reflooding a possible risk.

In the case MA2, where the core was quenched after reflooding the two uppermost axial rows in the inner radial channels had significant relocation of absorbing material. That means that circa 0.7 m (20 % of total height) from the top of the core and 60 % of the core area is practically without control rods.

In the case MA3 half of the core height in the inner radial channels was free of absorbing material before the core collapsed and lost its geometry. At that time the core water level was also at half of the core height. Due to the high void fraction and high temperature in the absorbing material recriticality in the absorber free part of the core is not likely or the power level caused by recriticality is expected to be very low. The narrow time window for possible recriticality before core collapses makes its impact on the progression of accident small. The core collapses about 15 min after reflooding enters the core.

In the cases where core was reflooded at 1600 K- 2000 K the core was practically free of absorbing material except for the one or two outermost radial rings before core collapse according to MAAP4 predictions. The core collapse, however, took place rapidly after the start of reflooding, within circa 3 minutes. The time window for possible recriticality is again very narrow. At the time of core collapse the water level was 30 - 40 cm above the core bottom. The high void fraction and high temperature in the core makes the anticipated power level of recriticality very low or prevent recriticality totally.

The SCDAP/RELAP5 model for TVO did not contain BWR specific blade/box model, which makes the control rod temperature predictions unreliable. The control rod temperatures were too low in SCDAP/RELAP5 results. The insufficiency of the TVO model for SCDAP/RELAP5 can be clearly seen when comparing the control rod temperature predictions calculated for Forsmark 3 plant with the newer code version having proper blade/box model. However, the general trend in control rod temperature behaviour can be considered valid and was similar to that of the fuel rods. When the ADS was initiated, the control rod temperatures decreased due to steam cooling. The water coming from the lower plenum cooled down the lowest axial nodes except in case SC3 (1600 K). In all SCDAP/RELAP5 calculations the probable control rod melting temperature was reached and some local deformations were to be expected.

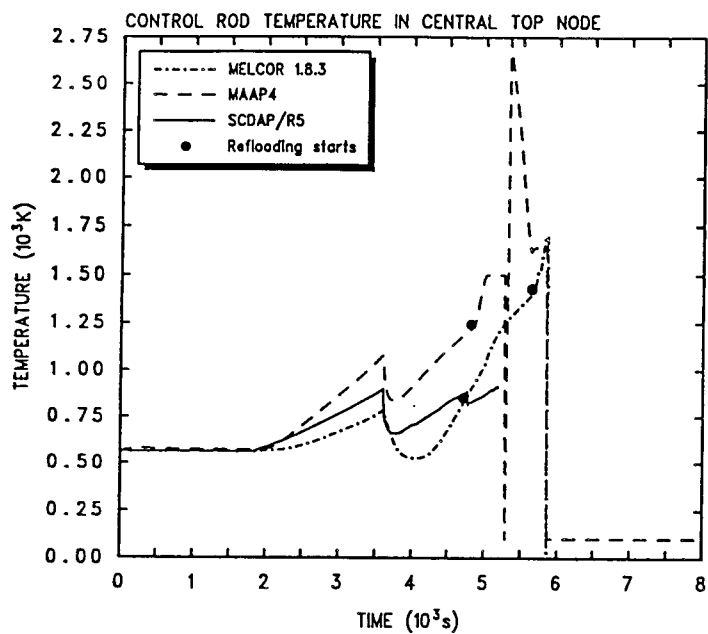


Figure 11. Control rod temperature in top center core node. Reflooding started at 1400 K. Low pressure case.

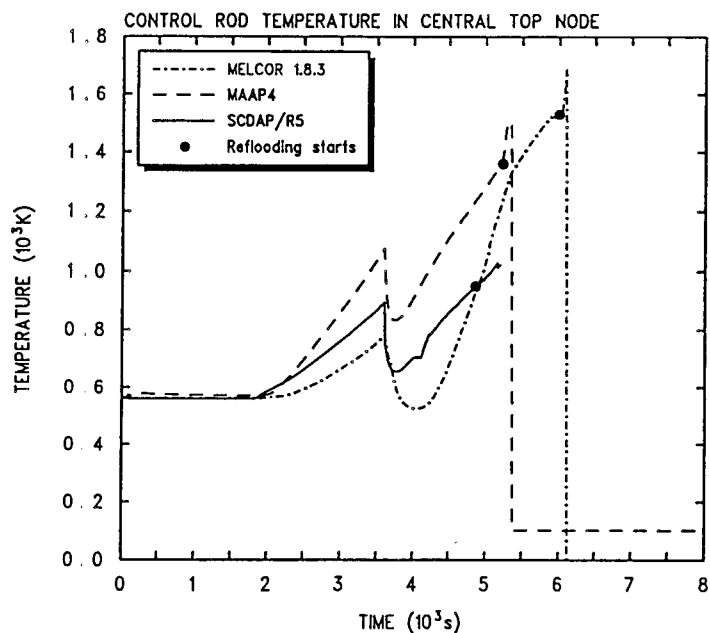


Figure 12. Control rod temperature in top center core node. Reflooding started at 1600 K. Low pressure case.

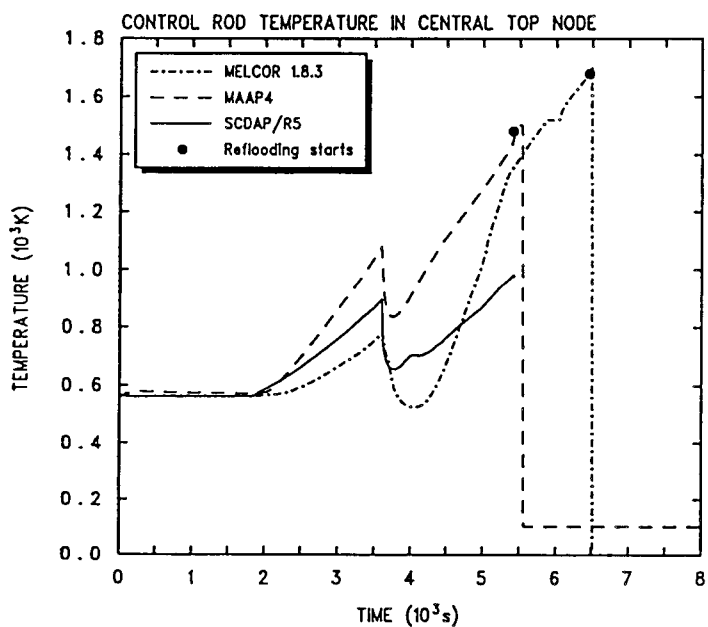


Figure 13. Control rod temperature in top center core node. Reflooding started at 1800 K. Low pressure case.

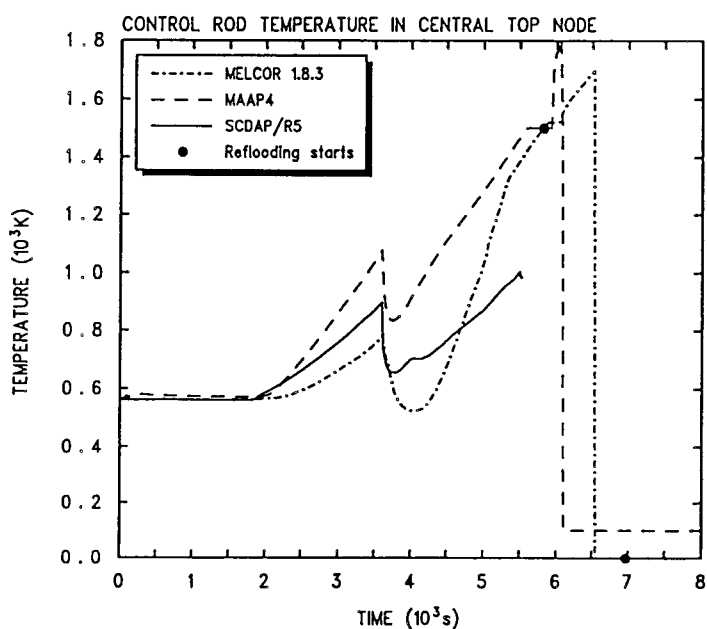


Figure 14. Control rod temperature in top center core node. Reflooding started at 2000 K. Low pressure case.

5.1.4 End State of Core

The MELCOR predictions of the end states of the TVO core in different reflooding variations of the low pressure scenario are shown in figures 15...18.

All MELCOR calculations resulted in severe core damages. Typical for MELCOR prediction is, that the end state of the core comprises a void in the upper third or upper half of the core, below which is a particulate rubble bed. Particulate debris bed is supported by blockages of molten and refrozen material on the intact components formed by candling of material from the upper parts. Conglomerate debris and the intact parts in the lower end of the core are quenched, but the particulate debris bed has parts where temperatures are still very high at the end of calculation (~ 3000 K). The highest temperature is in the axial node just above the beginning of the conglomerate debris area. At the end of the calculation the top rubble bed node was cooling down. Some particulate debris was also found on the core support plate.

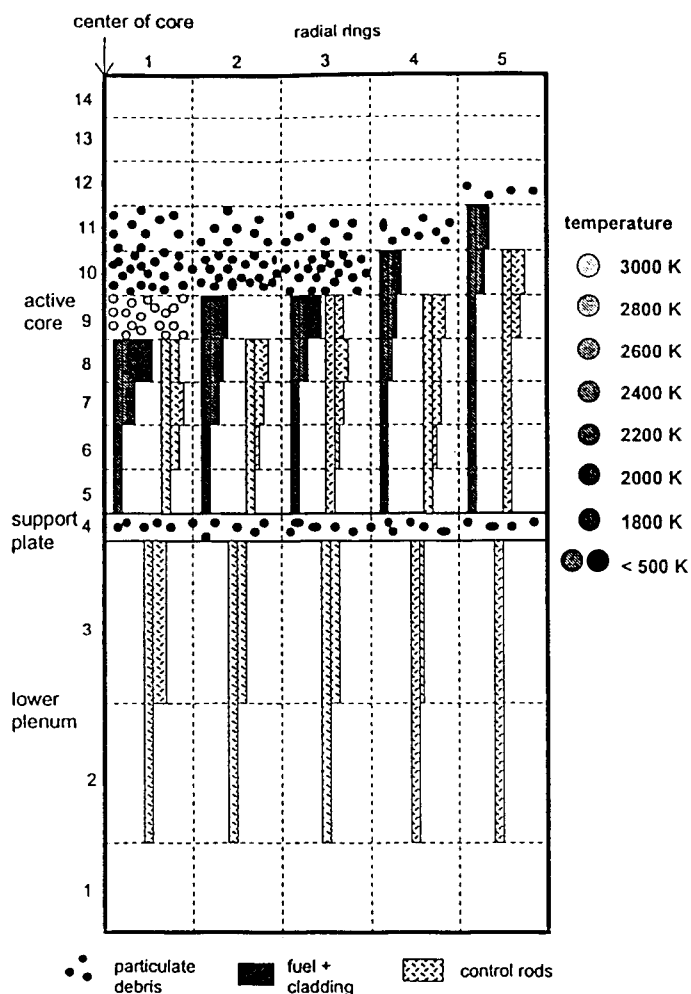


Figure 15. Schematic end state of core in low pressure case with reflooding at 1400 K. MELCOR run.

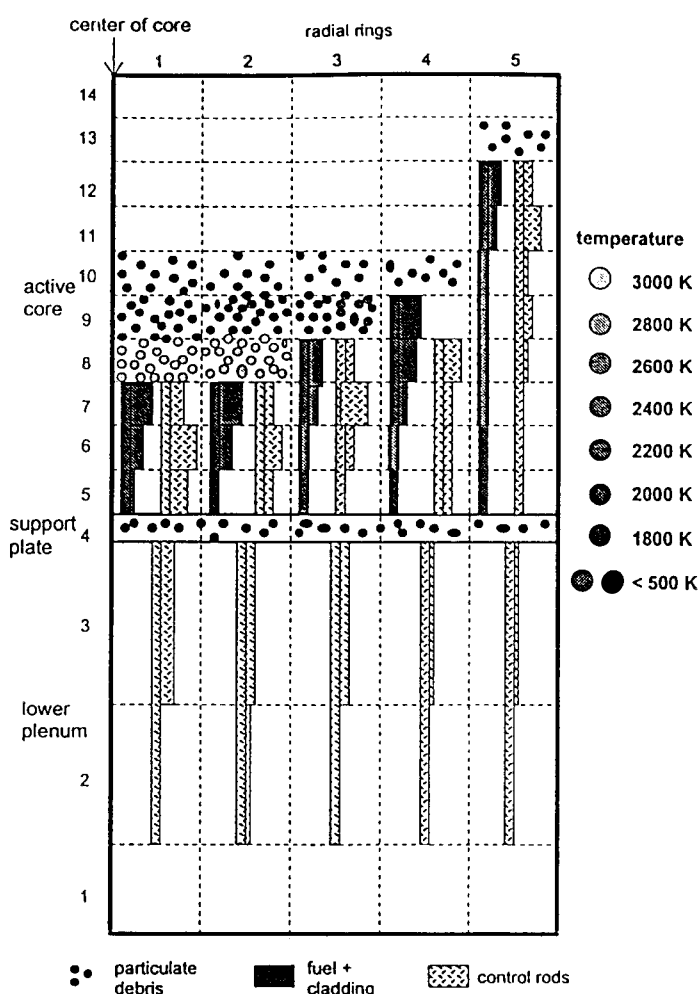


Figure 16. Schematic end state of core in low pressure case with reflooding at 1600 K. MELCOR run.

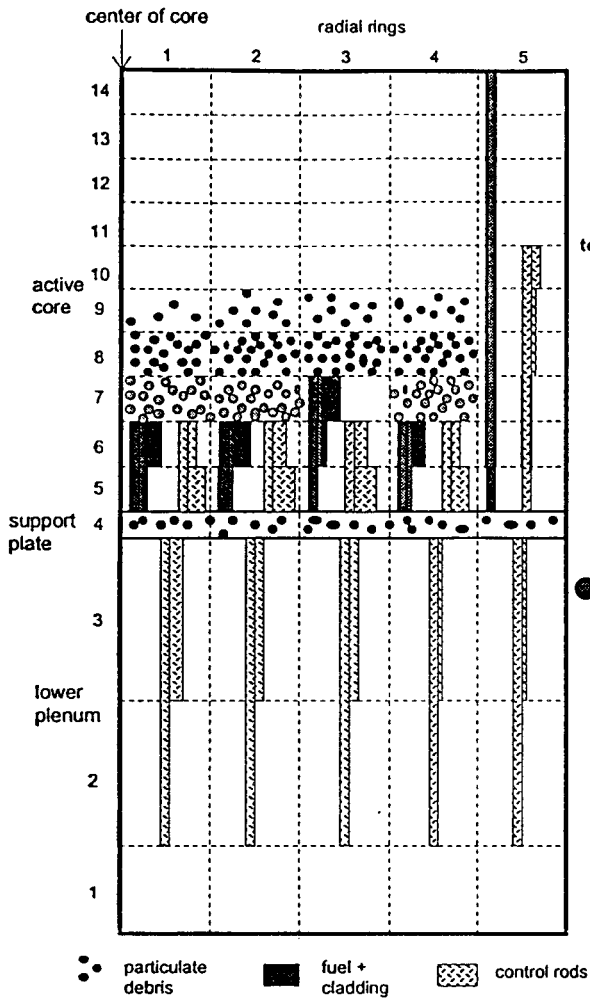


Figure 17. Schematic end state of core in low pressure case with reflooding at 1800 K. MELCOR run.

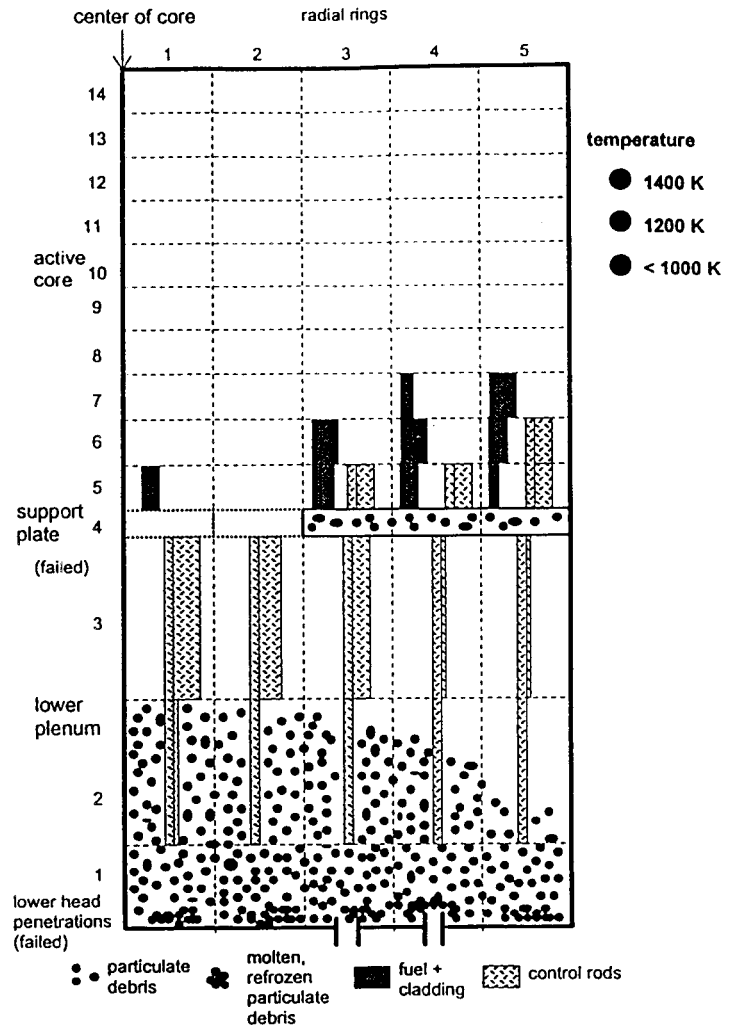


Figure 18. Schematic end state of core in low pressure case with reflooding at 2000 K. MELCOR run.

The core outer ring suffered least of geometrical deformations. In case ME4, the cladding in the outer ring was oxidized, but otherwise there were no geometrical deformations. Particulate debris bed contained large amounts of UO_2 , but no absorber material. Also in some radial rings in the lower part of the core the fuel rod stubs with refrozen material were without control rods.

The core support plate failure was avoided if the reflooding entered the core at max cladding temperature of 1850 K or lower. The cases, where reflooding entered the core at max core temperature of 1985 K or higher, resulted in core plate failure and subsequent failure of lower head penetrations.

In the MAAP calculation the case without reflooding the reactor vessel failed at about 2 h 30 min, if early vessel failure by instrument tube ejection was assumed. If the debris was initially quenched in the lower plenum, a global creep rupture took place at 4 h 30 min.

The schematic descriptions of the end states in reflooding cases with default Larson Miller parameters are shown in Figures 19...22.

When the auxiliary feedwater system was started 11 minutes after depressurization (MA2), the core was quenched according to MAAP. The core maximum temperature was 1260 K when water entered the core 5 min after start of system 327. No fuel relocation took place but fuel was dissolved by molten zirconium in the upper part of the core. The fuel geometry remained intact. Absorbing material relocated in the core upper part to minor extent.

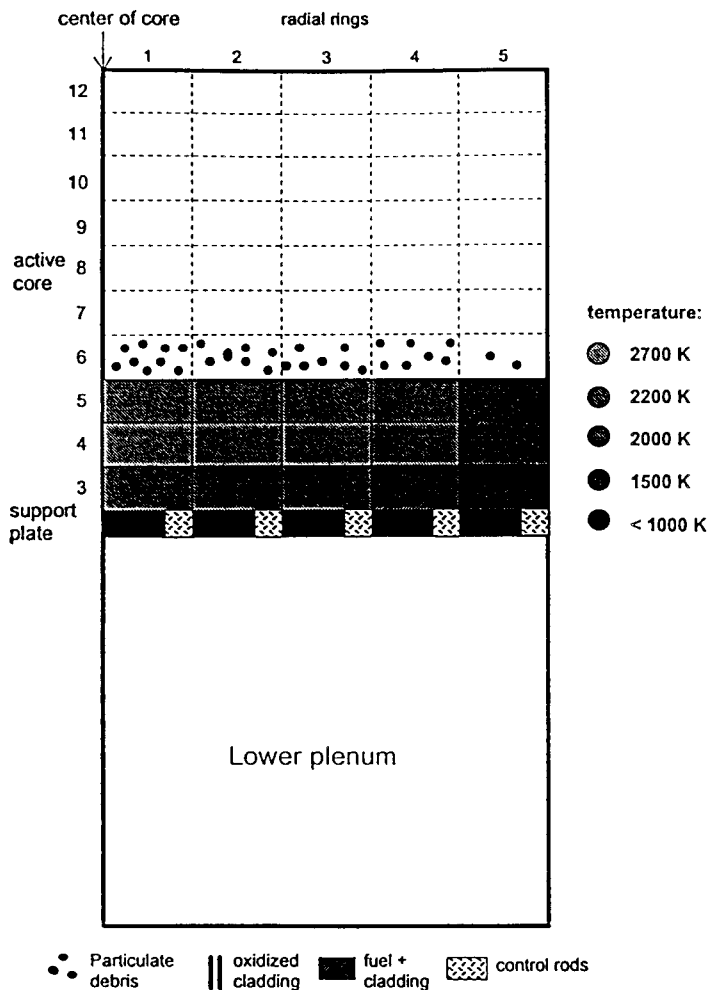


Figure 19. Schematic end state of core in low pressure case with reflooding at 1400 K. MAAP4 run.

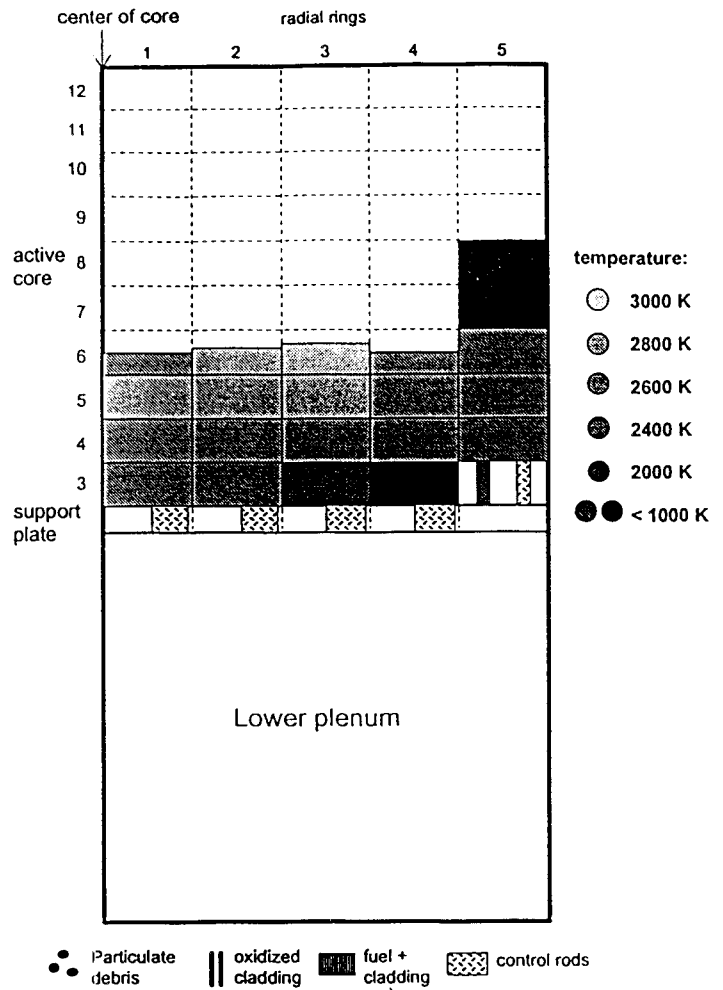


Figure 20. Schematic end state of core in low pressure case with reflooding at 1600 K. MAAP4 run.

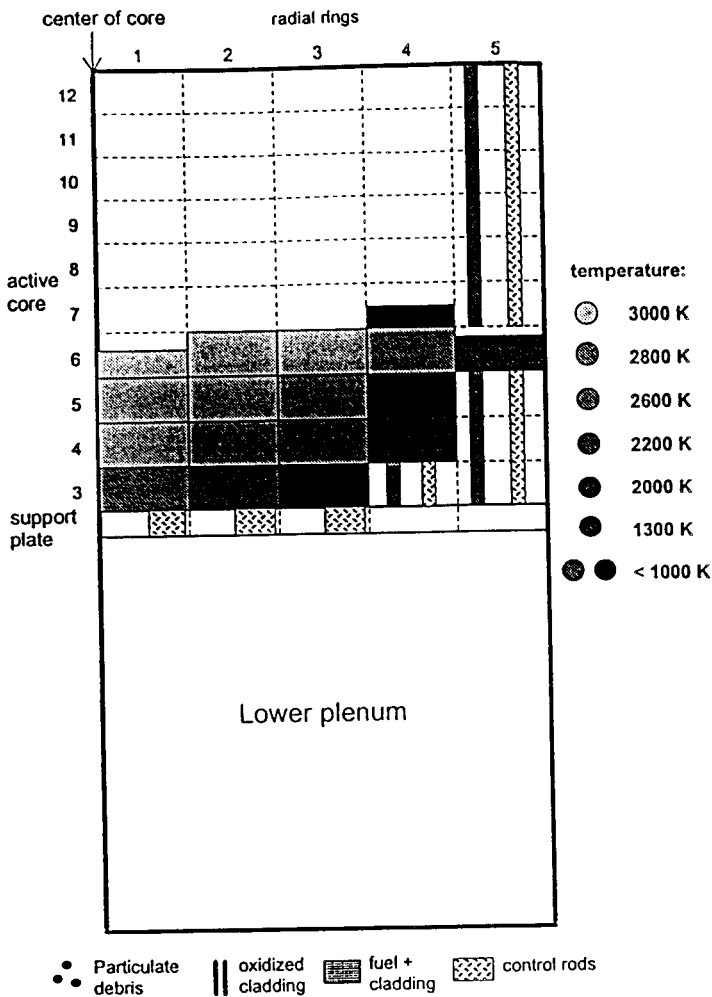


Figure 21. Schematic end state of core in low pressure case with reflooding at 1800 K. MAAP4 run.

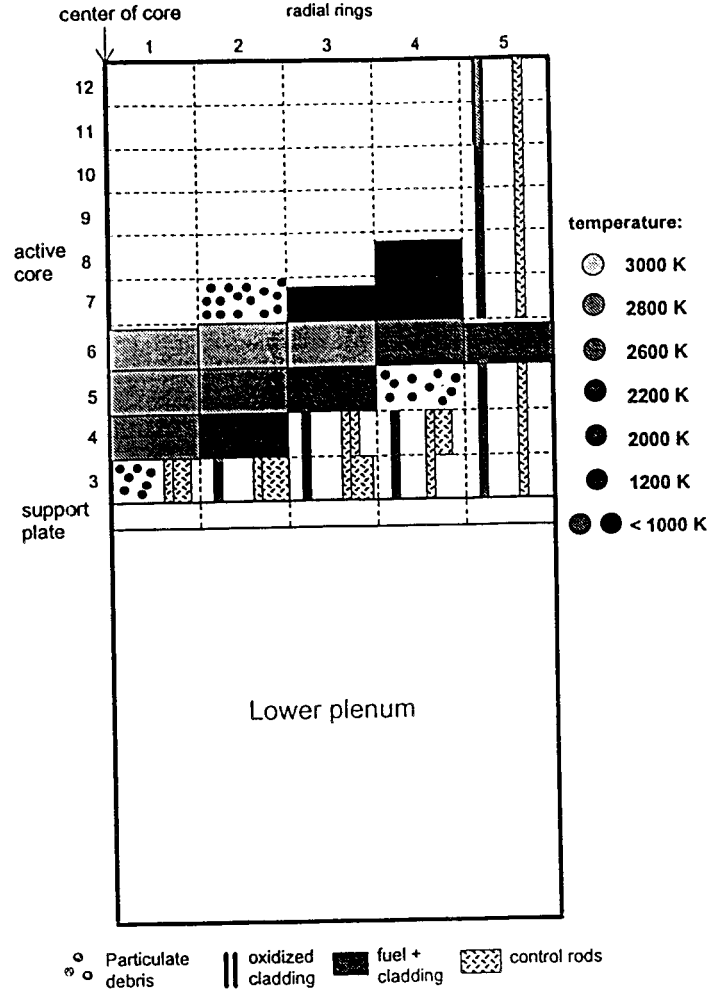


Figure 22. Schematic end state of core in low pressure case with reflooding at 2000 K. MAAP4 run.

According to MAAP the core was totally degraded when auxiliary feedwater system started at 1 h 14 min (MA3). When water entered the active core, the highest core temperature had already reached 1400 K, but there was no melt in the core. When the calculation was terminated at 2 h 50 min, no core material was left in the core upper half. The total amount of melt in the core was 23 metric tons. Fragmented fuel was collected on top of partially molten debris. The melting continued and the temperatures were rising. In the base case the debris was held in the original core volume.

When the Larson-Miller parameters which control the strength of debris crust were modified, (case MA8), the side crust failed at 4 h 50 min and melt relocated to the lower plenum. When this calculation was terminated at 5 h 30 min, the amount of debris in the lower plenum was 20 tons. The debris was quenched with average temperature of 820 K at the end of the calculation. The vessel failure was prevented. At the same time the amount of melt in the core was 56 tons with average temperature of 2200 K.

When reflooding was started later, at higher temperatures of 1600 K - 2000 K, most of the core was totally destroyed. In all cases the outermost radial ring was almost intact at the end of calculation at 2 h 50 min. This is different from the case MA3, where the whole upper part of the core collapsed. This is likely due to blockage formation by melt in the upper part of the core. These blockages prevent a global collapse. With default Larson-Miller parameter values, the debris was contained in the original core volume. With modified parameter values the side crust failed at 1 h 41 min and melt relocated into the lower plenum. At the end of the calculation the amount of melt in the core totalled 64 tons with average temperature of 2500 K. The lower plenum had accumulated 21 tons of melt. The debris was quenched to average temperature of 580 K, which again prevented the vessel failure.

Because none of the SCDAP/RELAP5 calculations could be calculated to the target end time, the end state is taken as the latest still reasonably reliable phase of calculation (numerical stability is still acceptable). Major relocation occurred in case SC2, where the reflood water entered to the core at core max temperature of 1400 K. Fuel was liquefied at axial node 8 in the second channel. The molten material slumped immediately to the lower plenum (input assumption). In all cases fuel rods ruptured in several locations due to ballooning. In the cases SC3...SC5 some local debris formation took place during the quenching due to fragmentation of the embrittled fuel cladding.

5.2 STATION BLACKOUT WITH FAILURE TO DEPRESSURIZE RCS

The initiation of the accident was the same as in the low pressure scenario, but the ADS valves failed to open. The pressure in the RCS remained high due to slow boiloff of coolant from the core. The safety relief valves (SRV) were able to keep the pressure around 70 bar. The water level was still in the active core region, at least 0.7 m above the bottom of the active fuel, when the system 327 started water injection in all calculated variations. The injection of cold water into the core decreased the pressure in the RCS. After total core recovery the pressure started to rise again.

Key figures of merit from the high pressure scenarios are shown in Tables 10 (MELCOR), 11a and 11b (MAAP4) and 12 (SCDAP/RELAP5).

Table 10. Key results from high pressure reflooding sequences in TVO III calculated with MELCOR 1.8.3. Initial station blackout with failure of ADS. Reflooding of core with system 327 to downcomer with the capacity of 45 kg/s.

| Case | ME8 No reflooding | ME9 Reflooding at 1400 K | ME10 Reflooding at 1600 K | ME11 Reflooding at 1800 K | ME12 Reflooding at 2000 K |
|--|-------------------------|--------------------------------|---------------------------------|---------------------------------|---------------------------------|
| Top of fuel uncovered | 2100 s | 2100 s | 2100 s | 2100 s | 2100 s |
| ADS valves open | - | - | - | - | - |
| Total fuel uncover | 6950 s | - lowest level 0.8 m | - lowest level 0.75m | - lowest level 0.73 m | - lowest level 0.73 m |
| H ₂ production begins | 3600 s | 3600 s | 3600 s | 3600 s | 3600 s |
| 327 starts: time max clad temp | - | 4268 s 1400 K | 4504 s 1600 K | 4590 s 1800 K | 4600 s 2000 K |
| Reflooding enters core: time max clad temp | - | 4268 s 1400 K | 4504 s 1600 K | 4590 s 1800 K | 4600 s 2000 K |
| Total core recovery | - | 6200 s | 6250 s | 6300 s | 6350 s |
| Core plate failure | 10409 s | - | - | - | - |
| RPV failure | 10503 s | - | - | - | - |
| In-vessel H ₂ production | 730 kg (*) | 32 kg | 90 kg | 90 kg | 90 kg |
| Zr oxidation fraction | 41 % (*) | 1.8 % | 4.4 % | 4.4 % | 4.4 % |
| Max core support plate temp | 1700 K | 560 K | 560 K | 560 K | 560 K |

(* at core support plate failure)

Table 11a. High pressure reflooding sequences at TVO III BWR plant calculated with MAAP 4.00a. No depressurization of RCS, reflooding through downcomer 45 kg/s. Calculation time is 10000 s.

| Case | MA10 No reflooding | MA11 Reflooding at 1400 K | MA12 Reflooding at 1600 K | MA13 Reflooding at 1800 K | MA14 Reflooding at 2000 K | MA15 Reflooding at 2300 K | MA16 Reflooding at 2730 K |
|---|--------------------------|---------------------------------|---------------------------------|---------------------------------|---------------------------------|---------------------------------|---------------------------------|
| Top of fuel uncovered | 1800 s | 1800 s | 1800 s | 1800 s | 1800 s | 1800 s | 1800 s |
| Hydrogen production starts | 2700 s | 2700 s | 2700 s | 2700 s | 2700 s | 2700 s | 2700 s |
| Depressurization, manual ADS | - | - | - | - | - | - | - |
| Total core uncover | 9980 s | - (min 0.97 m)* | - (min 0.95 m)* | - (min 0.91 m) | - (min 0.91 m)* | - (min 0.88 m)* | - (min 0.67 m)* |
| Control rod melting begins | 4340 s | 4400 s | 4340 s |
| Core fuel melting begins | 4470 s | 4760 s | 4460 s |
| Start of reflooding, max core temperature | - | 4250 s 1400 K | 4390 s 1600 K | 4420 s 1800 K | 4440 s 2000 K | 4530 s 2300 K | 5260 s 2730 K |
| Reflood enters core, max core temperature | - | 4250 s 1400 K | 4390 s 1600 K | 4420 s 1800 K | 4440 s 2000 K | 4530 s 2300 K | 5260 s 2730 K |
| Mass of melt in core when reflooded | - | - | 10 kg | 50 kg | 200 kg | 2700 kg | 7300 kg |
| Core collapse | 5300 s | - | - | - | - | 4700 s | 5300 s |
| Core recovered | - | 5600 s | 5900 s | 5900 s | 5900 s | 5900 s | 7000 s |
| Core plate failure | 9980 s | - | - | - | - | - | - |
| Vessel failure | 9980 s | - | - | - | - | - | - |
| In-vessel H ₂ production | 500 kg | 63 kg | 150 kg | 140 kg | 140 kg | 240 kg | 380 kg |
| Oxidation fraction of cladding | 38 % | 4 % | 10 % | 8 % | 9 % | 17 % | 28 % |
| Oxidation fraction of channels | 12 % | 2 % | 5 % | 4 % | 4 % | 5 % | 9 % |
| Max core temperature, time | 3030 K 8190 s | 2740 K 4620 s | 2790 K 4560 s | 2760 K 4560 s | 2890 K 4590 s | 2760 K 8140 s | 3090 K at the end |
| Max amount of melt in core, time | 73440 kg, 9960 s | 1800 kg, 4680 s | 4920 kg, 4530 s | 5070 kg, 4560 s | 5830 kg, 4560 s | 60500 kg, at the end | 19230 kg, at the end |

* From bottom of core

Table 11b. Sensitivity studies of high pressure reflooding sequences at TVO III BWR plant calculated with MAAP 4.00a. Reflooding with auxiliary feedwater system 327, injection capacity 45 kg/s to downcomer. No depressurization of RCS. Calculation time is 10000 s

| Case | MA17 | MA18 |
|--|---|---|
| | Reflooding at 2300 K. Modified Larson-Miller parametres. Crust failure. | Reflooding at 2730 K. Modified Larson-Miller parametres as in MA17, but no crust failure. |
| Top of fuel uncovered | 1800 s | 1800 s |
| H ₂ production begins | 2700 s | 2700 s |
| Depressurization, manual ADS | - | - |
| Total core uncover | - (min 0.88 m above bottom of core) | - (min 0.67 m above bottom of core) |
| Control rod melting begins | 4340 s | 4340 s |
| Core fuel melting begins | 4460 s | 4460 s |
| Start of reflooding, max core temperature | 4530 s, 2300 K | 5260 s, 2700 K |
| Reflood enters core, max core temperature | 4530 s, 2300 K | 5260 s, 2700 K |
| Mass of melt in core, when reflood enters core | 2700 kg | 7300 kg |
| Core collapse | 4700 s | 5300 s |
| Core recovered | 5900 s | 7000 s |
| Core plate failure | 9970 s | - |
| Vessel failure | 9970 s | - |
| In-vessel H ₂ production | 250 kg | 380 kg |
| Oxidation fraction of cladding | 17 % | 28 % |
| Oxidation fraction of channels | 5 % | 9 % |
| Max core node temperature | 2746 K, 8030 s | 3110 K, 10700 s |
| Max amount of melt in core | 59150 kg, 9900 s | 21450 kg, at the end |

Table 12. Key results of reflooding sequences in TVO III nuclear power plant calculated with SCDAP/RELAP5/MOD3.1. Initial station blackout, no depressurization of RCS. Reflooding with system 327 to downcomer with capacity of 45 kg/s.

| Case | SC6 No reflooding | SC7 Reflooding at 1394 K (max core temp.) | SC8 Reflooding at 1588 K | SC9 Reflooding at 1801 K | SC10 - Reflooding at 2000 K |
|--|-----------------------|--|--------------------------------|--------------------------------|--------------------------------------|
| Top of active fuel uncovered | 1450 s | 1450 s | 1450 s | 1450 s | 1450 s |
| Lowest water level (above the bottom of active fuel) | 0.47 m (at 5970 s) | 0.84 m | 0.69 m | 0.69 m | 0.68 m |
| H ₂ production begins | 3360 s | 3360 s | 3360 s | 3360 s | 3360 s |
| 327 starts: time max clad temp | - - | 4210 s 1394 K | 4500 s 1588 K | 4685 s 1801 K | 4737 s 2000 K |
| Grid spacers and cladding starts to slump | 4430 s | - | - | 4844 s | 4813 s |
| Embrittled cladding quenched and fragmented | | | | | 5519 s |
| In-vessel H ₂ production | 333 kg (at 5970 s) | 11 kg (at 5181 s) | 27 kg (at 5210 s) | 77 kg (at 5400 kg) | 100 kg (at 5527 kg) |

5.2.1 Cladding and Debris Temperatures

MELCOR predicted that the collapsed water level remained in the active core region and the core was never totally uncovered in the cases ME9... ME12. In the early phase of the accident MELCOR predicted higher core temperatures and earlier start of core heatup than MAAP4 and SCDAP/RELAP5 in the high pressure cases, which is opposite to the results in low pressure cases. The flow junction data between the RCS control volumes was updated and modified before running the high pressure cases with MELCOR. The different flow areas in the input caused the temperature differences in the early phase of the heatup. However, when the core temperatures reached 1000 K, the core temperature predictions with the three codes agreed well till the start of reflooding.

MELCOR predicted larger temperature differences in the core in axial direction in high pressure scenarios than in low pressure cases due to slower boiloff of water in the core. Vaporized water oxidizes cladding in the uncovered upper parts of the core increasing further

the temperature of the upper parts. Actually, the breakoff oxidation temperature is reached in the top nodes of the core, while the two lowest axial levels are still covered and cooled with water. This is also the reason, why varying the value of maximum cladding temperature as criteria for starting of reflooding resulted in minor differences in hydrogen production and core end states. The maximum cladding temperature was always reached in the top node of the core. In case ME9 the whole core was quenched and the original core geometry was maintained. In all other variations the top node reached 2200 K, the melting point of Zr, causing candling of the top axial level downwards. However, the whole core was quenched at the end of calculation in all investigated high pressure variations.

In the MAAP4 calculation with no reflooding (case MA10) the PSA level 1 fuel failure limit 1477 K is reached at 1h 12 min. The zirconium oxidation is strongly accelerated, which increases significantly the fuel heat-up rate. Core fuel melting commenced at 1h 15 min into the accident, when the average core temperature was only 980 K. Large temperature differences existed in the core. The water level was 0.9 m above bottom of the core and the core material below water level was in saturation temperature. The core collapsed at 1h 28 min into the accident. At the time the amount of melt in the core was 9 metric tons consisting mainly of molten control rods. The upper part in the central nodes collapsed into particles, that relocated on deformed fuel in the lower part of the core. The fuel geometry in outer channels was intact.

In the non-reflooding case the core plate failed at 2 h 50 min, when the temperature of the core plate exceeded 1370 K. Mass of melt in the core had reached 73 tons. The vessel failed by instrument tube ejection within one minute after fuel had relocated to the lower plenum. At the time of vessel failure 190 tons of melt had collected into the lower plenum. The average temperature of the melt was 2090 K, which is 240 K above the melting point.

In the case MA11 the reflooding took place at 1h 11 minutes, when the maximum core temperature reached 1400 K. The two-phase level in the core had dropped to the level 0.97 m above the bottom of the active fuel. The maximum core temperature of 2740 K was reached at 1h 17 min in the uppermost node in the centre of the core. The core was quenched completely at 1 h 31 min.

The cases MA12-MA14 show a similar trend as MA11. The reflooding was started later, at 1600 K, 1800 K and 2000 K. The core was not totally uncovered before reflooding and there was a rapid temperature increase due Zr oxidation in the uncovered upper part of the core after start of reflooding. Some melt was formed in the core, that refroze. The core was totally quenched within 30 minutes.

When the reflooding was started at 2300 K the results were different. The whole upper part of the core collapsed in 3 minutes after the start of reflooding. Prior to the collapse the fuel geometry was still intact, but the upper part of the core was blocked in the three innermost channels. The amount of melt in the core was 4 tons at the time of collapse. The highest core temperatures were circa 2000 K. When the calculation was terminated at 2 h 50 min, the amount of melt was 60 tons and the average temperature of the core was 2060 K.

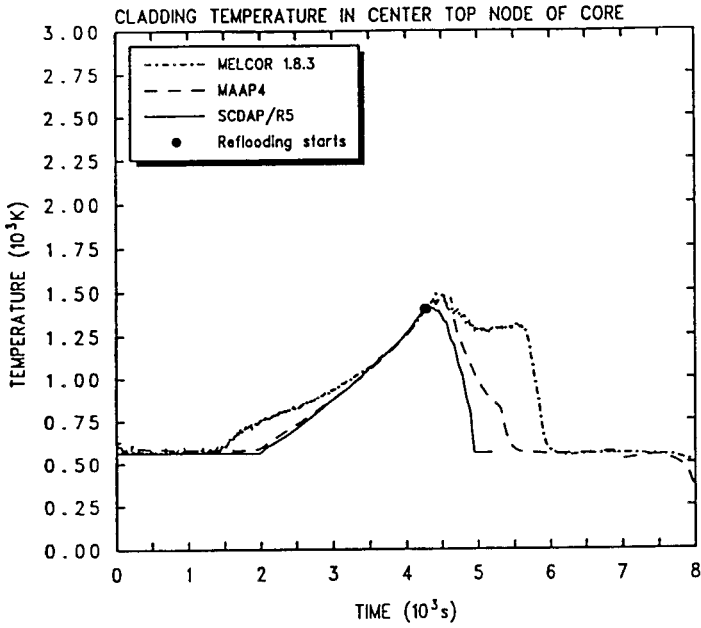


Figure 23. Cladding temperature in TB case with no ADS and reflooding at max clad temperature of 1400 K.

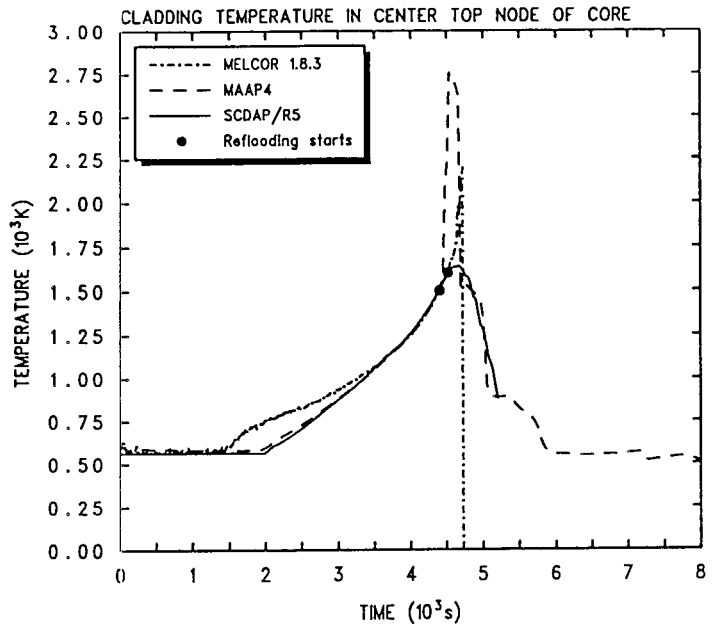


Figure 24. Cladding temperature in TB case with no ADS and reflooding at max clad temperature of 1600 K.

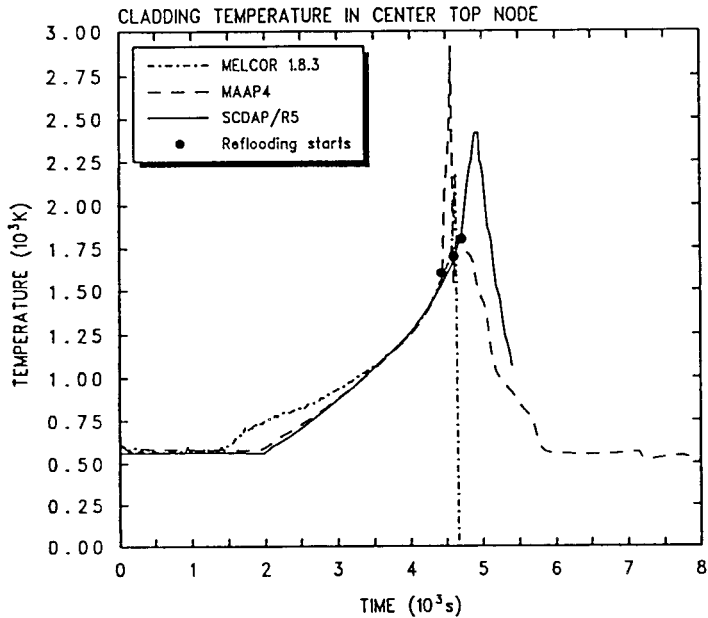


Figure 25. Cladding temperature in TB case with no ADS and reflooding at max clad temperature of 1800 K.

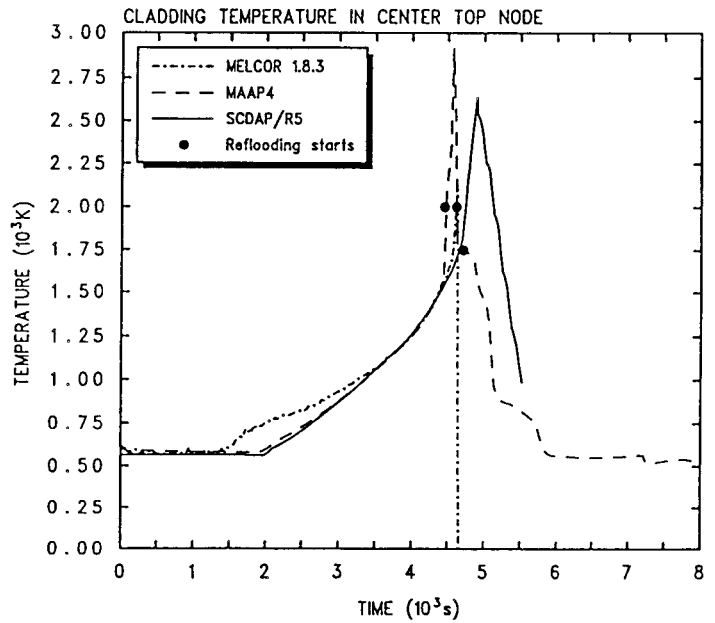


Figure 26. Cladding temperature in TB case with no ADS and reflooding at max clad temperature of 2000 K.

When the core was reflooded at 2730 K, the the core behaviour changed again. When the reflood water entered the core some nodes in the core were already empty and the upper part was blocked in the three innermost radial rings. The upper part of the core collapsed almost simultaneously with the start of water injection, except for the outermost radial ring. The maximum core temperatures were reached at the end of calculation, which means that the core was not quenched.

SCDAP/RELAP5 predicted cladding failures due to interaction with grid spacers in cases SC8 and SC10. The candling also stopped the local oxidation in some nodes. In the case SC10 the embrittled cladding quenched and fragmented in the middle channel at axial node 9. Case SC10 was the only calculated high pressure case, where rubble bed existed at the end of the calculation.

5.2.2 Hydrogen Production

Hydrogen production was much lower in the high pressure scenarios with reflooding than in respective low pressure scenarios.

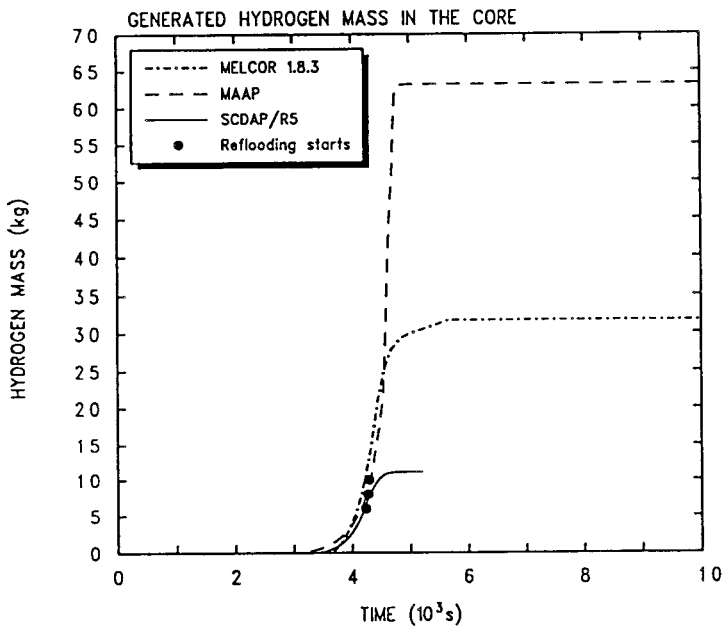


Figure 27. In-vessel H_2 production in TB case with no ADS, reflooding at max cladding temperature of 1400 K.

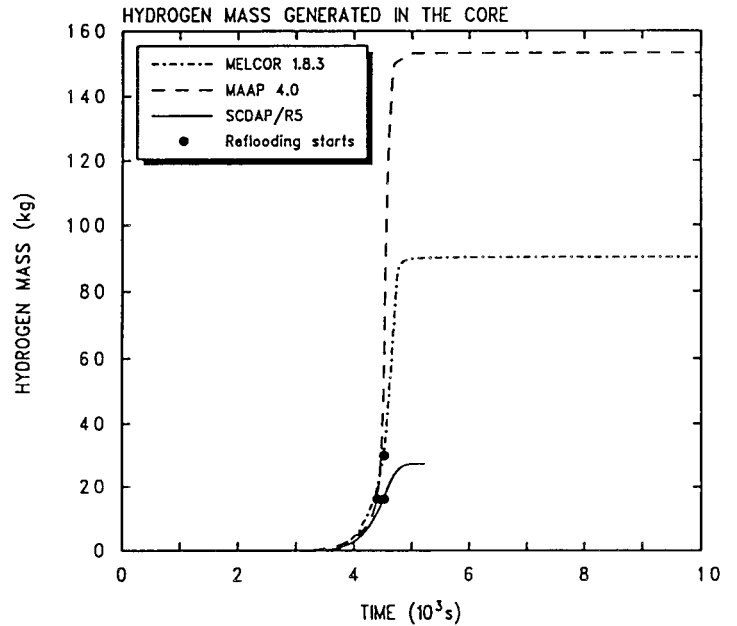


Figure 28. In-vessel H_2 production in TB case with no ADS, reflooding at max cladding temperature of 1600 K.

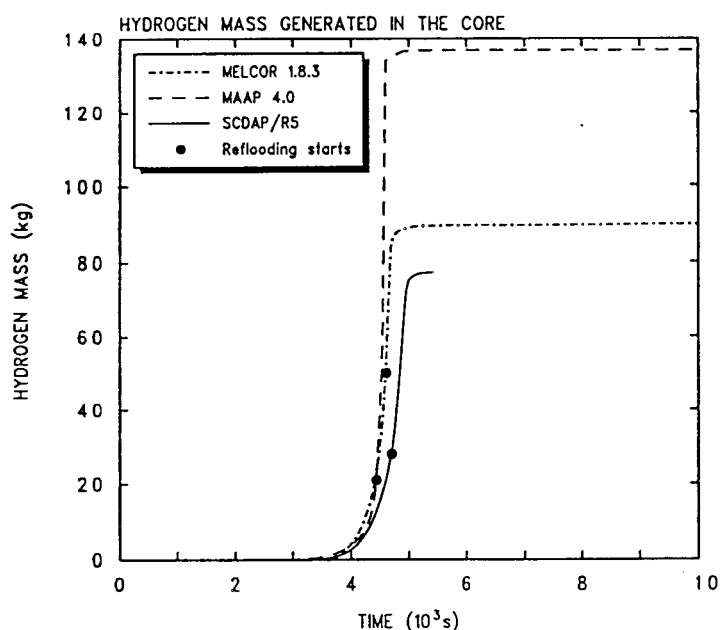


Figure 29. In-vessel H_2 production in TB case with no ADS, reflooding at max cladding temperature of 1800 K.

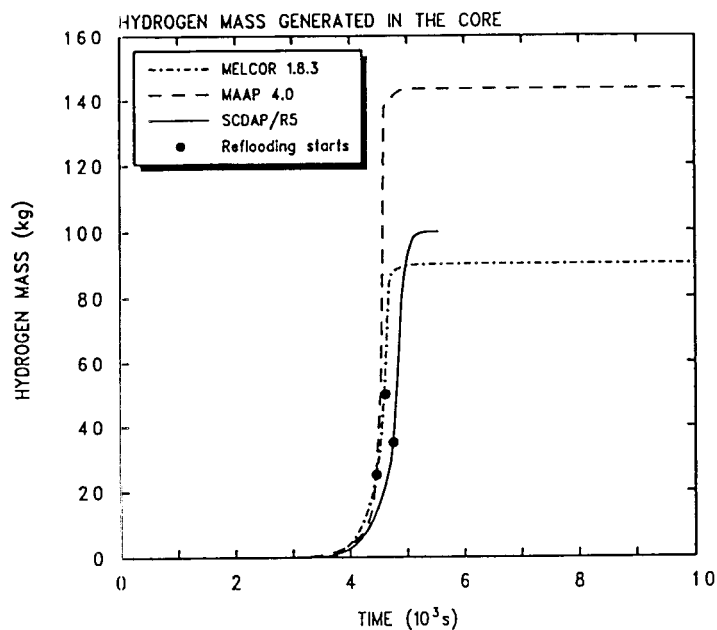


Figure 30. In-vessel H_2 production in TB case with no ADS, reflooding at max cladding temperature of 2000 K.

MELCOR predicted low H_2 generation varying from 32 kg to 90 kg. There was practically no difference in the H_2 generation in MELCOR predictions if reflooding was started at 1600 K, 1800 K or 2000 K. This is due to the fact, that very rapid oxidation takes place in the top nodes of the core forming a local hot spot. The material melts on top and moves downward and refreezes. Hydrogen generation ceases.

In all reflooding variations MAAP 4 gave the highest amount of hydrogen varying from 63 kg to 153 kg. In MAAP4 calculations, where reflooding was started at higher maximum cladding temperatures than 2000 K, the hydrogen production was larger. In case with reflooding at 2300 K about half of the total 240 kg of H_2 was produced before reflooding. The fraction becomes larger as the starting temperature of reflooding grows.

SCDAP/RELAP5 gave in general lower values for in-vessel H_2 production than MAAP 4 or MELCOR 1.8.3. The hydrogen production stopped or slowed down to a low level in all calculated high pressure cases.

However, if core was not reflooded, MAAP 4 and MELCOR both predicted high in-vessel H_2 generation in later phases of core heatup, when molten material slumped into the bottom head. MELCOR 1.8.3 calculation resulted in total in-vessel H_2 production of 730 kg at the core support plate failure and the respective value for MAAP 4 was 500 kg. This suggests that if reflooding of core was started at a later phase than studied in this report, much higher

in-vessel hydrogen generation rates would result. Similar trend could perhaps be seen also in cases, where the depressurization through ADS valves would be performed, when core temperatures are high.

5.2.3 Control Rods

In the MELCOR calculations the control rods remained in intact geometry in case ME9. The peak temperature of control rods was 1500 K. In other cases the control rod temperature reached the melting point of stainless steel causing slumping of control rods in two or three topmost axial nodes. In all cases at least the control rods in lower half of the core remained completely intact.

In the MAAP4 calculation, where the core was reflooded at 1400 K only two nodes were free of absorbing material after quenching. In other cases, where the core was quenched, half of the core height in the three inner radial channels was free of absorbing material.

If the core was reflooded at 2300 K and at 2730 K, MAAP4 predicted that the absorbing material relocated in the center of the upper half of the core. The core collapsed, however, soon after the start of reflooding, within about 3 minutes. The time window for possible recriticality is very narrow. At the time of core collapse the water level was circa 1 m above the bottom of the core. The high temperature, high void fraction and deformed geometry in the core make the power level of recriticality low and makes recriticality unlikely.

In the SCDAP/R5 results the temperatures of the control rods were highest in the upper parts of the core (axial nodes 9 and 10). The temperatures reached the stainless steel melting point in cases where the water pumping was started at maximum core temperatures of 1600 K and 2000 K. In several experiments the melting of the control rods has been observed to start at much lower temperatures (about 1500 K). The maximum temperatures in the upper part of the core were at about 1500 K or just below in cases where the water pumping started at 1400 K and 1800 K. In conclusion some control rod melting is to be expected also in high pressure cases where the collapsed liquid level never reached the core bottom.

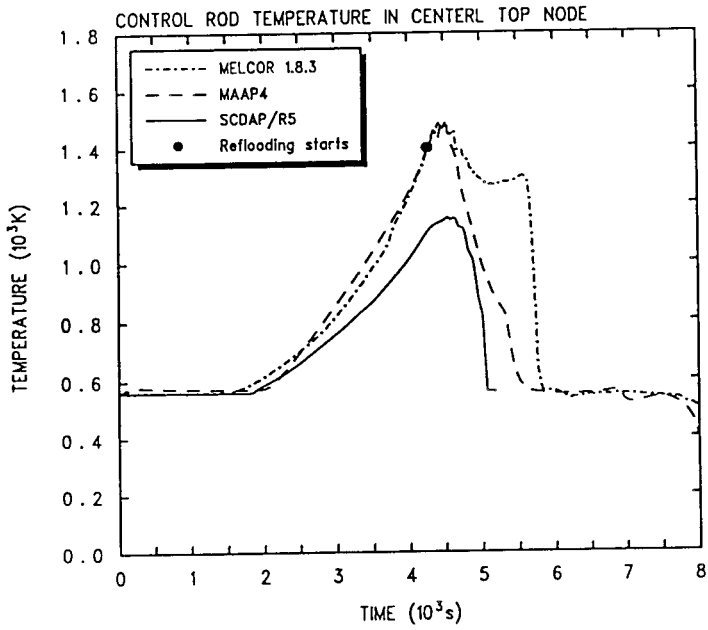


Figure 31. Control rod temperature in TB case with no ADS, reflooding at max cladding temperature of 1400 K.

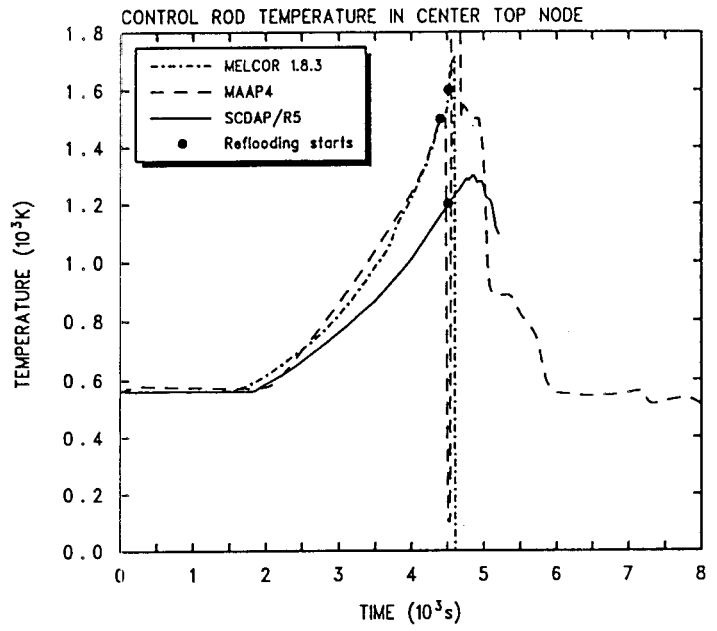


Figure 32. Control rod temperature in TB case with no ADS, reflooding at max cladding temperature of 1600 K.

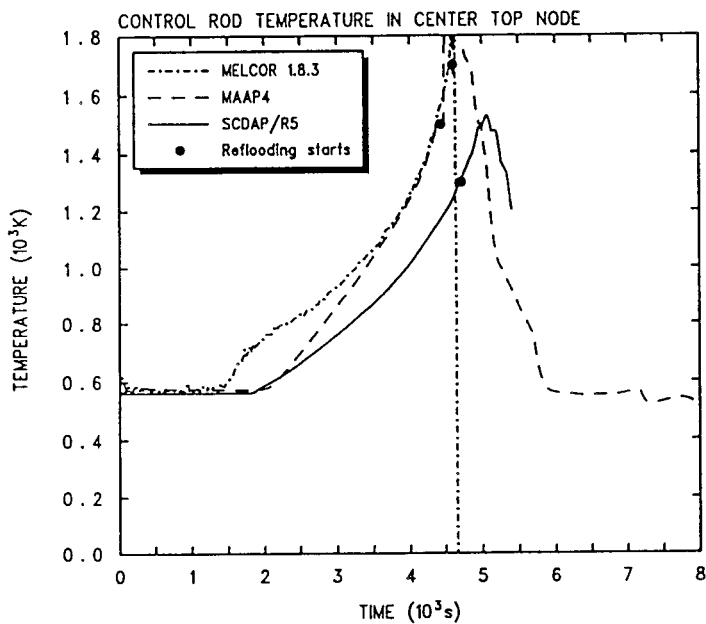


Figure 33. Control rod temperature in TB case with no ADS, reflooding at max cladding temperature of 1800 K.

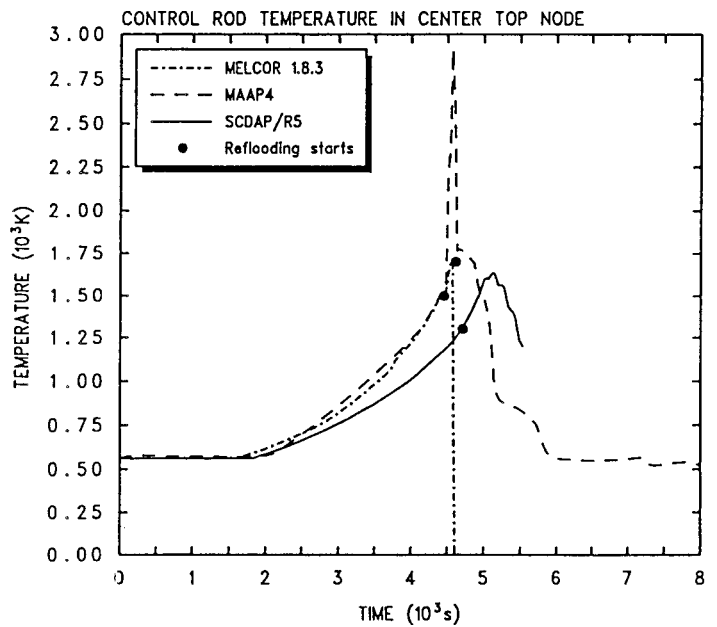


Figure 34. Control rod temperature in TB case with no ADS, reflooding at max cladding temperature of 2000 K.

5.2.4 End State of Core

MELCOR predicted that the core was quenched in all calculated reflooding cases. In case with lowest system 327 starting temperature, 1400 K, the three topmost axial levels were oxidized but the core remained in its original geometry and no material deformations or relocations took place. Control rods maintained their original positions and thus there is no possibility of recriticality of core (Fig. 35).

The case ME10 resulted in material melting and relocations in three upmost axial levels in four radial rings (Fig. 36). The outer radial ring remained geometrically intact. Cladding and control rods melted and slumped downwards from the top axial level in radial rings 1 and 2. The candled material was refrozen on two axial levels below. Molten top node of radial ring 3 relocated sideways, leaving the flow channel unchoked by blockages, but the cladding is strongly oxidized in the upper half of the core. The same applies to the radial ring 4, too, but without any fuel and cladding relocations.

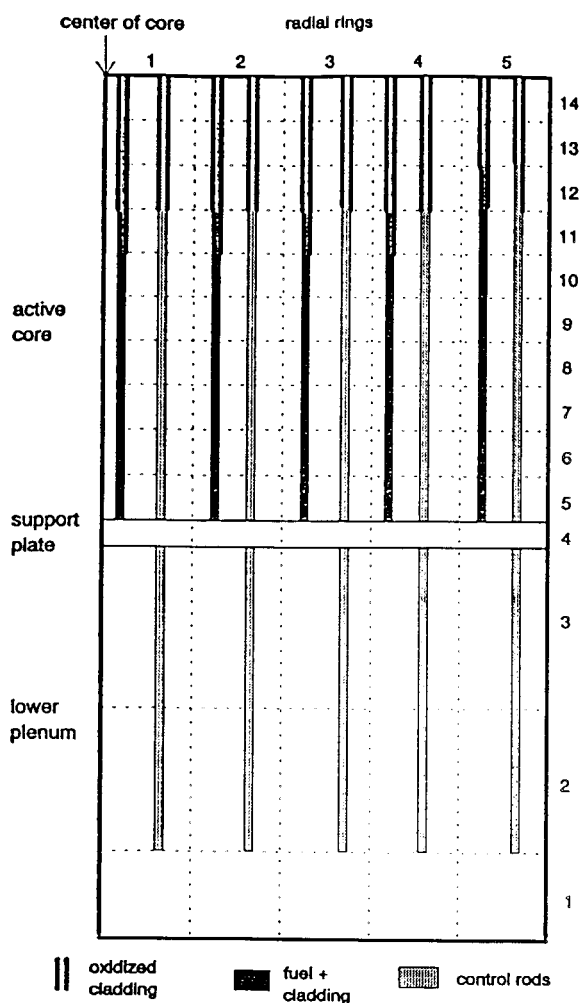


Figure 35. The end state of the TVO core in TB case with no ADS and reflooding at max cladding temperature of 1400 K. MELCOR 1.8.3 prediction.

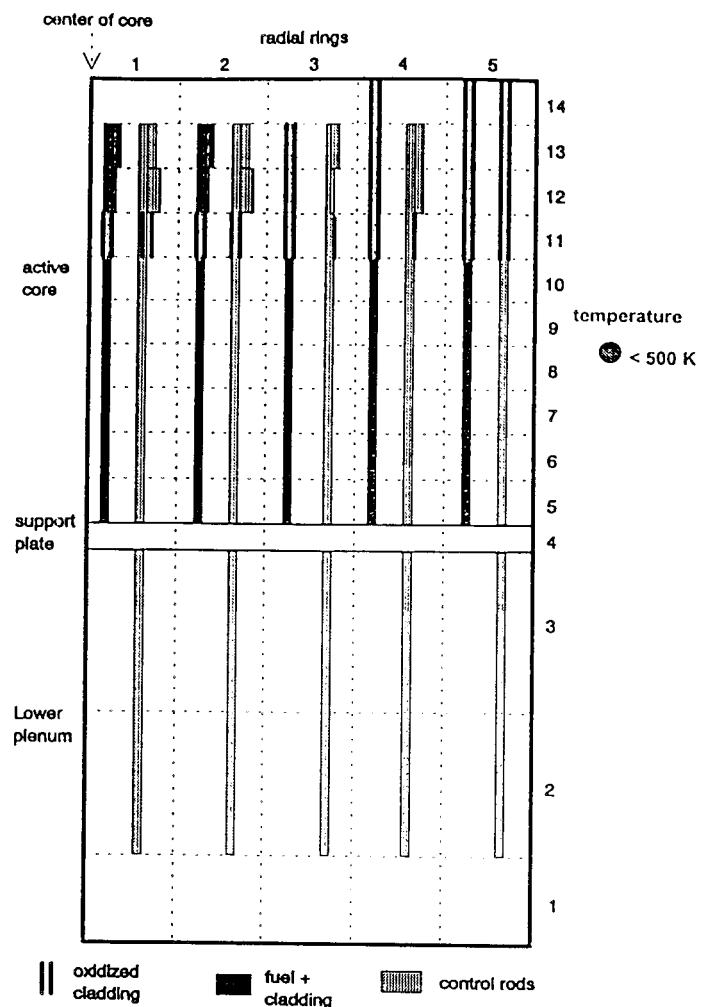


Figure 36. The end state of the TVO core in TB case with no ADS and reflooding at max cladding temperature of 1600 K. MELCOR 1.8.3 prediction.

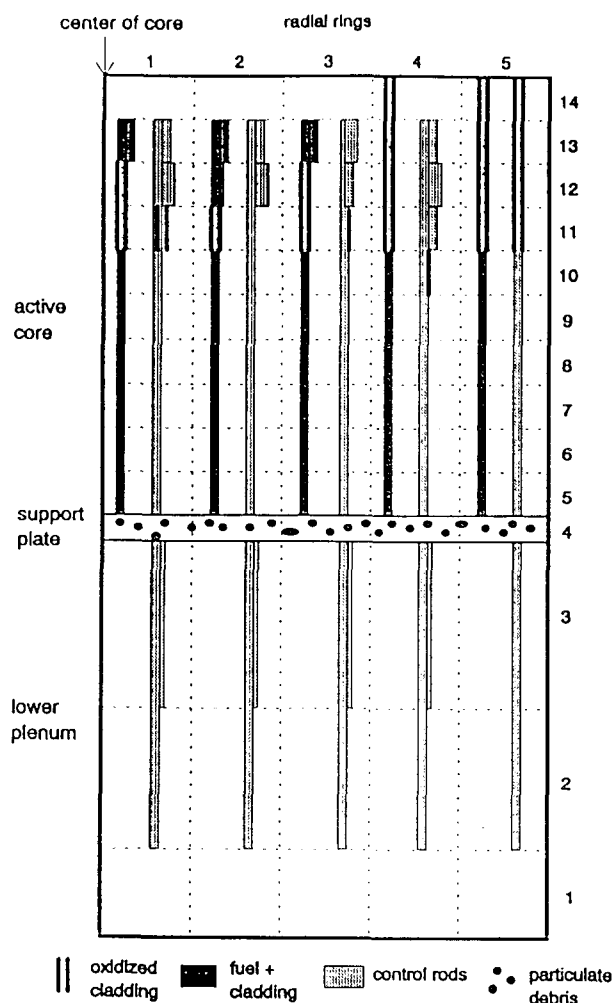


Figure 37. The end state of the TVO core in TB case with no ADS and reflooding at max cladding temperature of 1800 K. MELCOR 1.8.3 prediction.

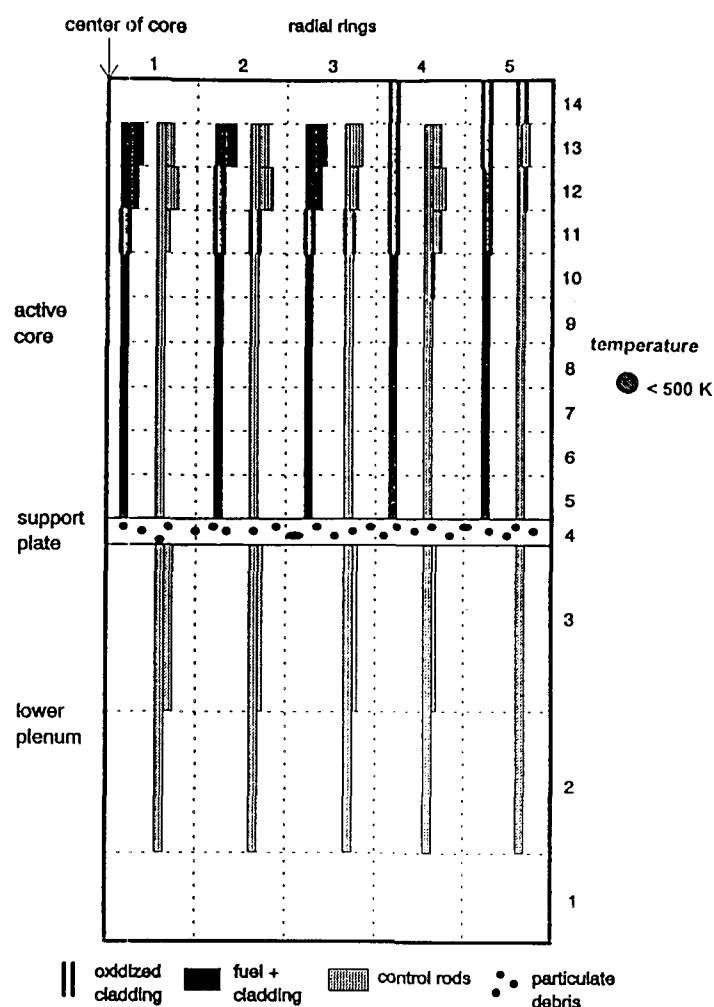


Figure 38. The end state of the TVO core in TB case with no ADS and reflooding at max cladding temperature of 2000 K. MELCOR 1.8.3 prediction.

The control rods have melted and canded downwards from the top of core in radial ring 4. The cladding in the outermost radial ring of the core is oxidized but otherwise intact. The top axial node in radial ring 4 is without absorber material, but contains fuel in intact geometry.

The case ME11 has only minor differences to the previous case. The amounts of molten and refrozen material are slightly larger causing more blockage of the flow channels in axial levels 12 and 13. Small amounts of particulate debris has been formed due to more complete oxidation in upper part of the core. Particulate debris consists of UO_2 , Zr and ZrO_2 and has slumped to the core support plate. The top node of the radial ring 4 has fuel rods in intact geometry, but no absorber material (Fig. 37)

The last case with reflooding when maximum cladding temperature reached 2000 K follows the trends of case ME11. The difference is that now some control rod melting and deformations start also in the outermost ring. The fuel and cladding, however, are still in intact geometry in the radial ring 5. The fuel in top axial level of radial ring 4 is without absorber material (Fig. 38).

In the MAAP4 case without reflooding the core plate failed and debris relocated to the lower plenum. The reactor vessel failed at about 2 h 50 min, when early vessel failure due to instrument tube ejection was assumed.

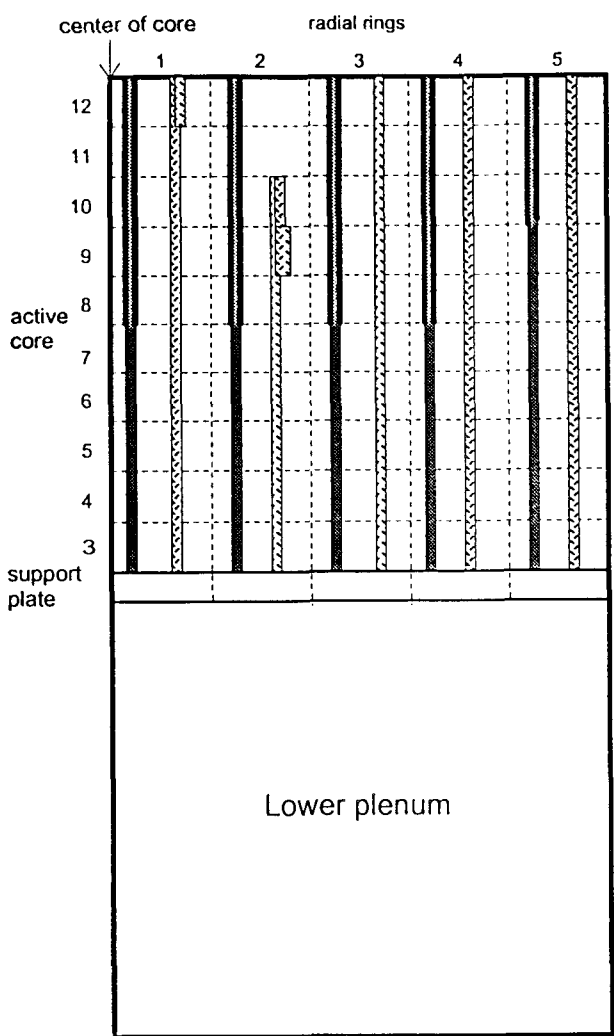


Figure 39. The end state of the TVO core in TB case with no ADS and reflooding at max cladding temperature of 1400 K. MAAP4 prediction.

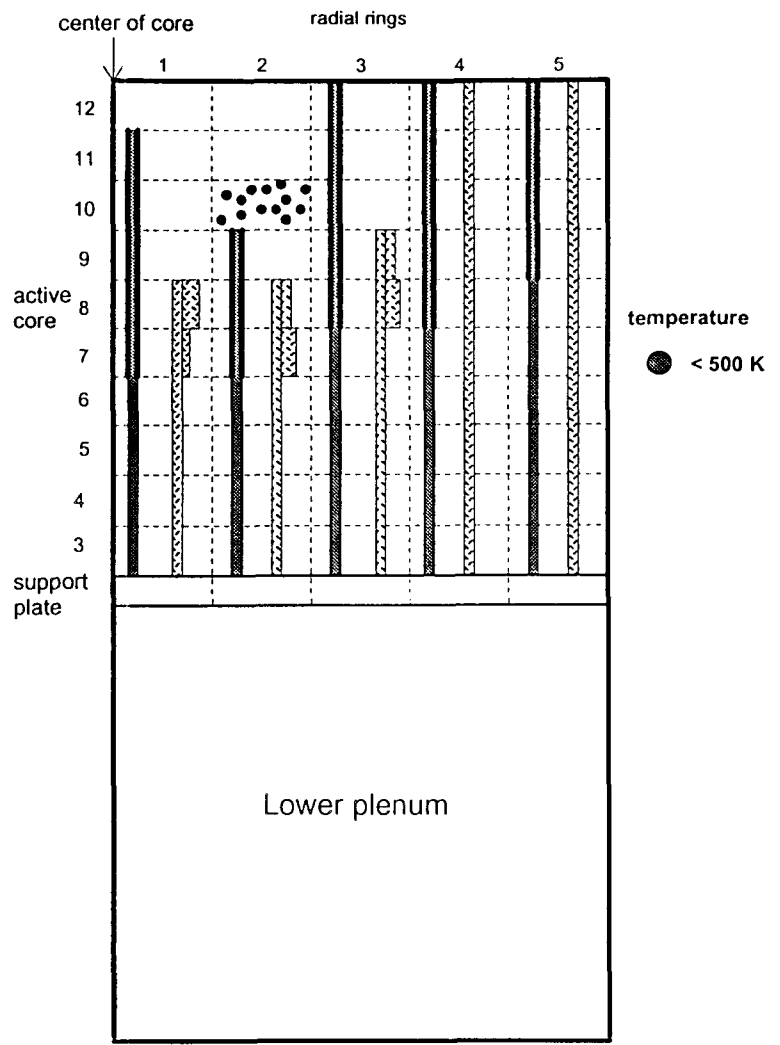


Figure 40. The end state of the TVO core in TB case with no ADS and reflooding at max cladding temperature of 1600 K. MAAP4 prediction.

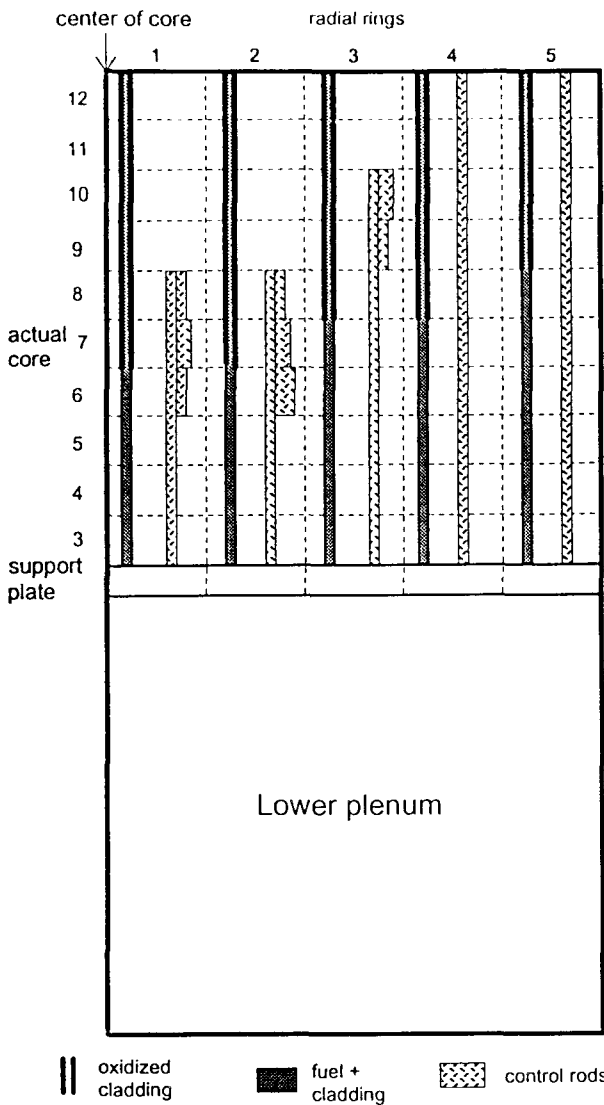


Figure 41. The end state of the TVO core in TB case with no ADS and reflooding at max cladding temperature of 1800 K. MAAP4 prediction.

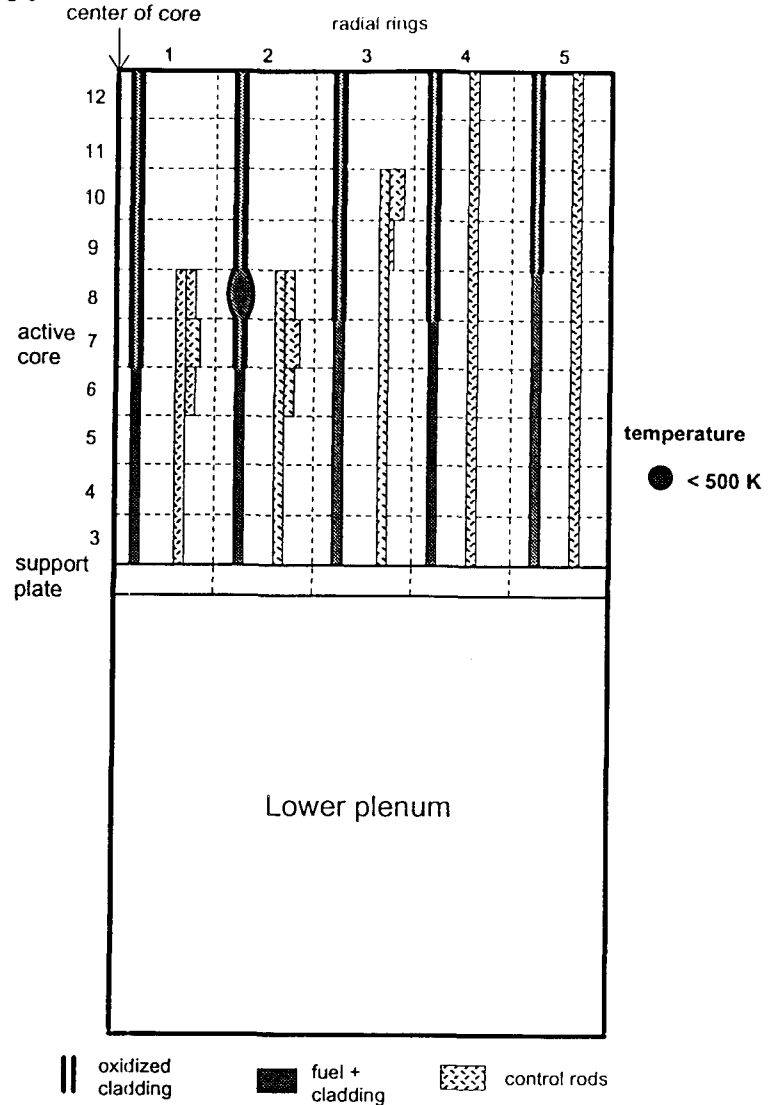


Figure 42. The end state of the TVO core in TB case with no ADS and reflooding at max cladding temperature of 2000 K. MAAP4 prediction.

When the reflooding was started at latest 1 h 14 min (case MA14) the core was quenched according to MAAP4. The highest temperature at the start of reflooding was 2000 K. Some fuel relocation and dissolution by molten zirconium takes place in the upper part of the core. The fuel geometry remains intact. Absorbing material relocates from the upper part of the core to some extent. At most one fifth of the core total height is free of absorber material. Recriticality may be possible and raise the core power level. Core damages are more extensive if the reflooding is started later.

The core upper part was totally degraded when reflooding was started at 1 h 15 min, when the highest core temperature had reached 2300 K. When the calculation was terminated, the upper half of the core was completely void. The total amount of melt in the core was 60 metric tons. Fragmented fuel was collected on top of debris. The melting continued and the

temperatures were rising. In the base case the debris was contained in the original core volume. When Larson-Miller parameters were modified the bottom crust failed at 2 h 50 min and melt relocated into the lower plenum. Vessel failure resulted at high reactor pressure by instrument tube melt-through.

If the reflooding was started later than 1 h 28 min, the core was destroyed, but the outermost radial ring and the bottom nodes remained geometrically intact. This differs from the previous case, where the whole core upper part collapsed. This is likely due to melt relocation in the core upper nodes before reflooding. Also, already 2/3 of the total hydrogen mass was released before reflooding. These facts were likely to prevent a global collapse. Material which could collapse had already relocated and H₂ production was not significantly accelerated. Due to the intact geometry at the core boundaries, modification of default Larson-Miller parameters did not fail the crust.

All temperatures were decreasing in the SCDAP/RELAP5 results at the end of the calculations. However, in the 1800 K and 2000 K cases some melting and fragmentation took place. Fuel cladding failed due to interaction with the grid spacers. The cladding and grid spacer materials slumped into lower nodes causing termination of local oxidation. In the case SC10, embrittled cladding was quenched but fragmented in axial node 9 in the center channel.

6. FORSMARK 3 RESULTS

All runs were started from the steady-state run and performed until a simulated time of 2 hours for the low flow rate injection cases and up to 1 hr, 20 min for the high flow rate cases. The transients were initiated by setting the trip for loss of power to the RCP pumps after an initial, extended steady state period of 10 seconds. Loss of power (TB, Total Blackout) also initiated closure of the feed water lines. Isolation signal (SI) was set after another 10 s which also initiated scram. A table function is used in the calculations to specify power as a function of time, where the initial decay for the first 10s is given by the void feed-back due to RC pump coast down.

The SI signal initiated closure of the valves in the steam lines which led to increase in pressure and opening of safety valves to maintain the dome pressure at 7 MPa. The loss of water mass through steam relief decreased the water level in the reactor vessel. When the DC level had sunk to low level, L4, about 0.5 m above core exit, signal to initiate automatic depressurisation, ADS was obtained. This took place 12.5 minutes after loss of power and up to this point the results are identical for the low and high pressure cases. ADS was not initiated in the high pressure cases. The steam generated by the decay power (and the exothermic power from oxidation) was there blown off through the safety valves at full, 70 bar, pressure.

The decrease in downcomer water level for the low and high pressure base cases are compared in Figure 43.

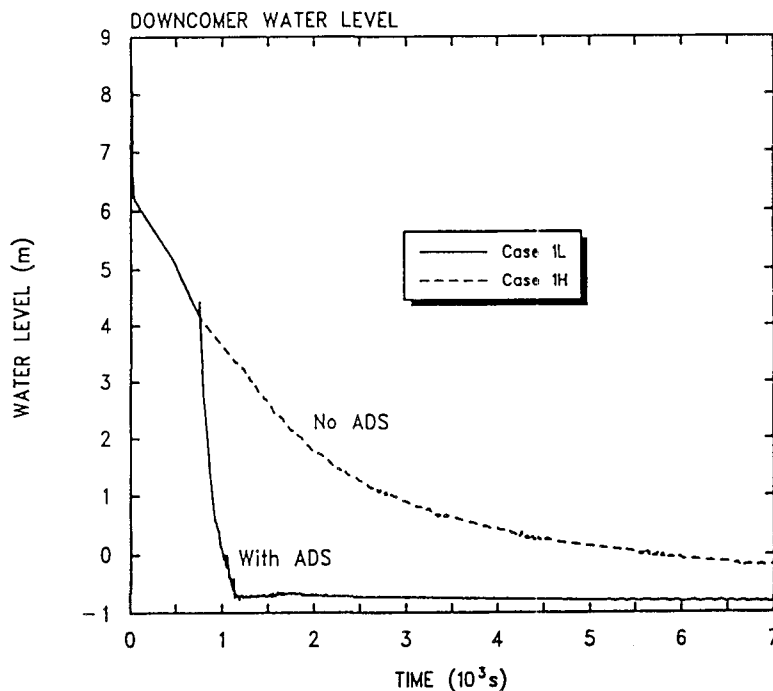


Figure 43. *Decrease in downcomer water level in Forsmark 3 low and high pressure base cases.*

Other results are presented and discussed in the following sections. The SCDAP/ RELAP5 output and plot files contain a huge amount of result parameters of which only a few, crucial parameters were selected here. Time of events and some key results are listed in Table 13 in section 6.2 and in Table 15 in section 6.3.

6.1 BASE CASE CALCULATIONS WITHOUT REFLOODING

6.1.1 Case 1L. Low Pressure Scenario with Normal ADS

The mass loss through ADS led to to early core uncovering and core heat-up from decay power in the fuel. The pressure dropped to saturation pressure of the water in lower plenum within a minute after ADS opened which started flushing and temporarily improved cooling of the core. The low flow rates and low pressure drops along the core made the flow oscillate and redistribute between the parallel channels. However, the fuel rods were all uncovered and started to heat up within a relatively short period of time, from the top of the core at 16.5 min. to the bottom at about 18 min. after TB. The highest temperatures were obtained where the power density and steam superheat were largest, and with the present, rather flat axial power distribution, this was at the uppermost part at axial levels 6-8 in the centre core zone. The water level decreased to a minimum of about 0.7 m below core inlet.

At 1000 K, after about 1600 s, increased oxidation of the Zircaloy cladding began. After being large in the beginning oxidation was later limited and oscillating due to steam starvation, so that hydrogen production increased only slowly with increasing temperatures.

The first damage to take place was the burst of fuel claddings due to overstrain pressure at 1928 s in the central channels. The cladding temperatures had then only reached about 1250 K, which is slightly lower than the level, 1273 K, for beginning of eutectic reaction between Zircaloy and Inconel. This eutectic mixture melts just above 1500 K.

Radiation became the dominant contributor to radial heat transfer from fuel rods to boxes and control rods with increasing temperatures. The ORNL blade/box model gave in this respect a more realistic picture than the original SCDAP control rod model. When the control rod temperature exceeded 1505 K melting began of the eutectic mixture between boron carbide and the surrounding stainless steel cladding, which began at 2220 s at axial level 8. Most of the control rod material had melted and slumped out of the core before the end of calculations at 7200 s, except in the outermost core channel (zone No. 5).

Heat up of the fuel rods continued and led to rupture of the fuel boxes in the core centre at about 3000 s, facilitated through interaction with melted control rods. Control rod material did also solidify at lower regions which temporarily blocked the bypass channels. The fuel rod claddings were heavily oxidised and a U-Zr-O formation was created which melted and made part of the fuel slump into lower core nodes at 4390 s. Melting of the oxidised Zircaloy cladding and water cross material started to slump and form a debris bed in the lower head already at 4100 s and then continued until the end of the simulation to 7200 s. SCDAP/RELAP5 indicated, however no slumping of UO_2 below the core.

Times of events and main results for Case 1L are listed in Table 13. The end state of the Forsmark 3 core in case 1L is shown in Figure 46 of section 6.1.2.

6.1.2 Case 1H. High Pressure Scenario with Failure to Initiate ADS

In Case 1H the pressure remained at 70 bar throughout the simulated transient until 7200 s, and steam generated by the decay heat was blown off through the safety valves. The water level decrease was considerably slower than with depressurization. Total core uncovering was obtained not until about 6400 s into the transient, compared to after 1080s in Case 1L.

The rather slow uncovering of the core from above left more time to heat up the uppermost core cells than in the low pressure case. This resulted in another temperature distribution, with maximum cladding temperatures in cell 9 and 10 although the power density was lower there. The axial temperature distributions in core zone 1 are compared in Figure 44 at the time when the PCT reached 1800 K, which was later in Case 1H than in Case 1L.

The high pressure gave improved heat transfer and slower heat-up than for Case 1L during the first part of the transient until about 4000 s. After that, with temperatures exceeding 1400 K, the steam rich conditions in Case 1H facilitated metal-water reactions and the exothermic power, shown in Figure 45, accelerated heat-up. The total hydrogen production became 518 kg in Case 1H, compared to 313 kg in Case 1L.

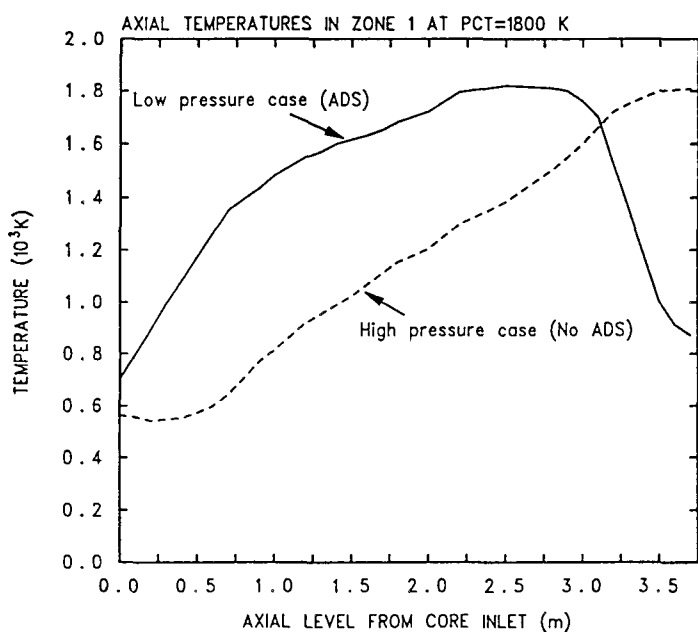


Figure 44. Comparison of axial temperature distributions in zone 1 at time of reflooding at PCT=1800 K. Forsmark 3.

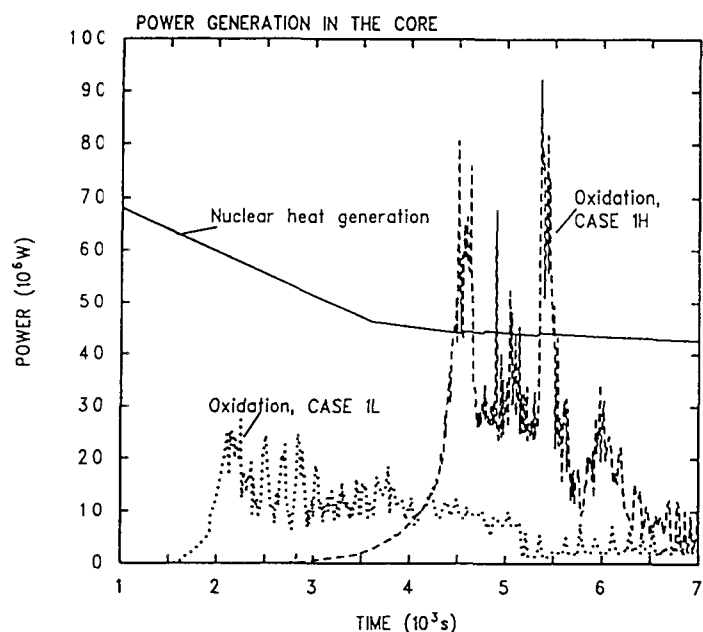


Figure 45. Power generation from nuclear decay and from oxidation. Forsmark 3.

Liquefaction of control rods began at 4150 s at the uppermost levels, and B₄C absorber material in cells 10 to 4 melted away during a period from 4170 to 6650 s. A large fraction of the fuel rod claddings were oxidised but only a small fraction was removed. Local damage to the rod claddings were obtained at the spacer locations due to the eutectic reaction between Inconel and Zircaloy at 4060 s. The results show no removal of UO₂ fuel from the core during the studied 2 hour transient, although there was some liquefaction of a U-Zr-O formation in the upper part of the core at 4800 s.

Times of events and main results for Case 1H are listed in Table 13. The end state of Forsmark 3 core in case 1H is shown in figure 47.

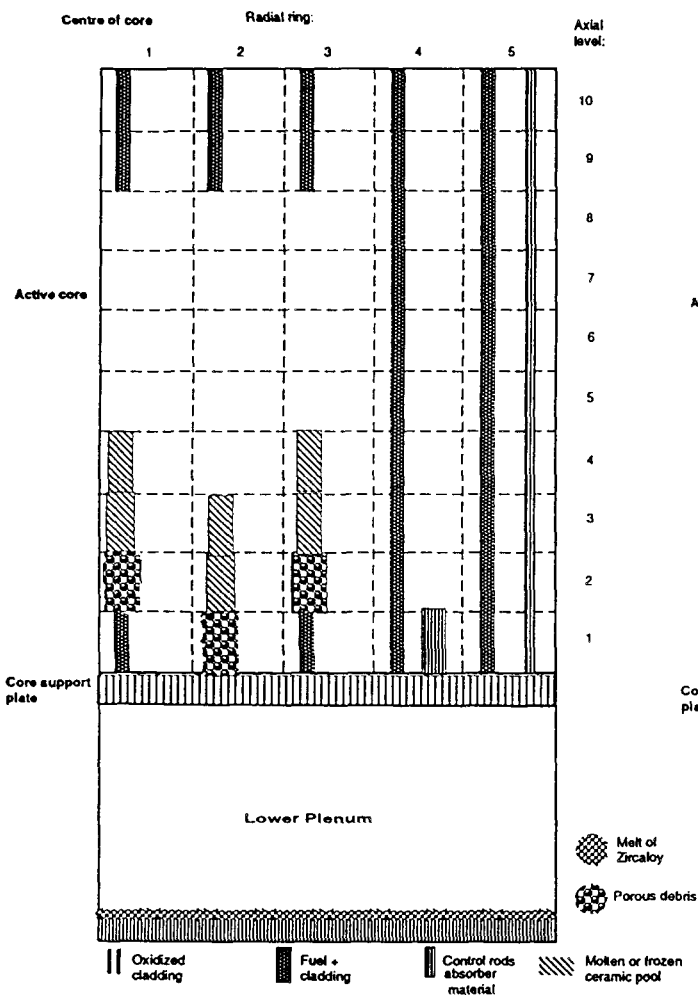


Figure 46. End state of F3 core in case 1L. SCDAP/RELAP5 prediction.

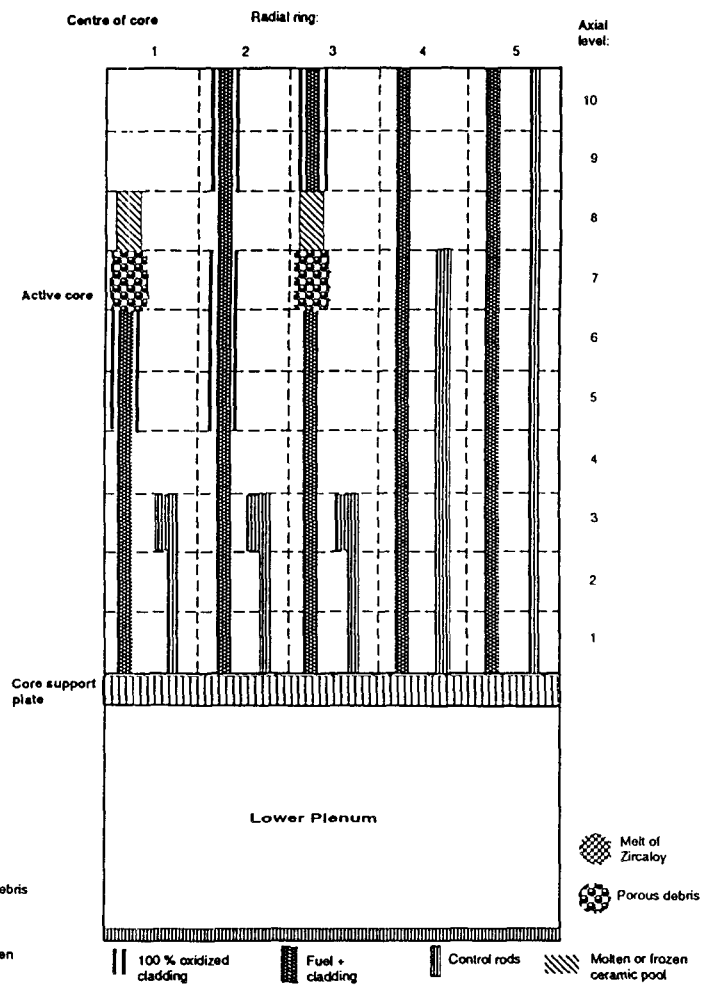


Figure 47. End state of F3 core in case 1H. SCDAP/RELAP5 prediction.

6.2 REFLOODING WITH AUXILIARY FEED WATER AS TOP SPRAY

6.2.1 Low Pressure Cases, Case 2,3,and 4

Reflooding with recovery of the auxiliary feed water system, 327, was simulated for three different core heat-up levels. Injection of top spray with 45 kg/s, corresponding to flow from two loops, was started at a time when the peak cladding temperatures (PCT) had reached the following values:

Table 13: *Low pressure reflooding cases with 45 kg/s top spray*

| Case No. | PCT (K) | Time after TB (s) |
|----------|---------|-------------------|
| 2 | 1400 | 2063 |
| 3 | 1600 | 2261 |
| 4 | 1800 | 2489 |

At start of water injection the collapsed water level had sunk to a rather constant range about 0.7 m below the core. The mass flow was distributed into each of the fuel and bypass RELAP5 channels in proportion to their cross sectional flow area, i. e. 20 % of the total flow was directed into bypass channels.

Since the water was injected above the core it came first into contact with surfaces in the uppermost parts, cell 10, then flowed downwards through the core and thereafter reflooded the core from below. With 45 kg/s it took 550 - 600 s to raise the level to the core inlet level.

Comparisons of maximum surface temperatures and hydrogen generation for all low pressure and high pressure cases are made in Figures 48 and 49.

In Case 2 and 3 the recooling was very effective and the peak cladding temperature turned rapidly downwards. In Case 3 where coolant injection was started at a PCT of 1600 K there was only a 8 K increase in temperature before it turned around. There was a small increase in oxidation due to the additional supply of water, but only for a short period of time (Fig. 48). Complete rewetting was obtained at about 6200 s in Case 3, i. e. after that the spray had been on for about 4000 s.

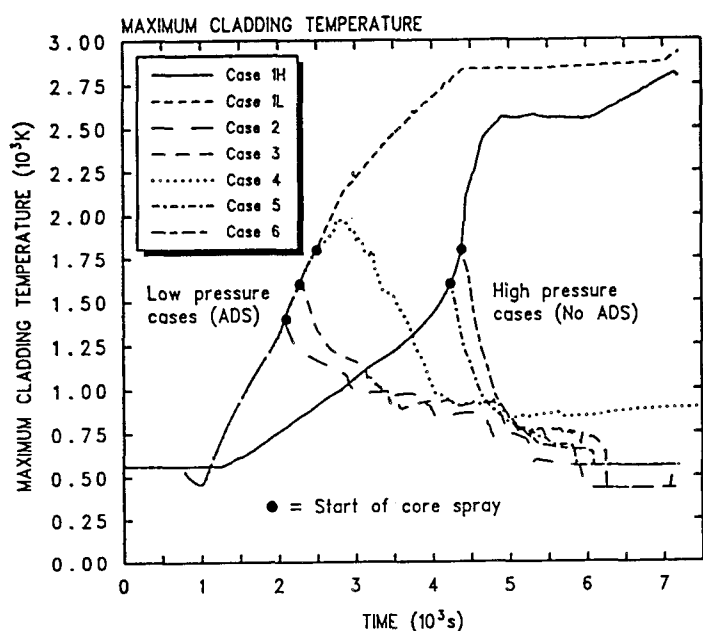


Figure 48. Maximum fuel surface temperatures. Comparison of all cases with 45 kg/s top spray SCDAP/RELAP5 calculations.

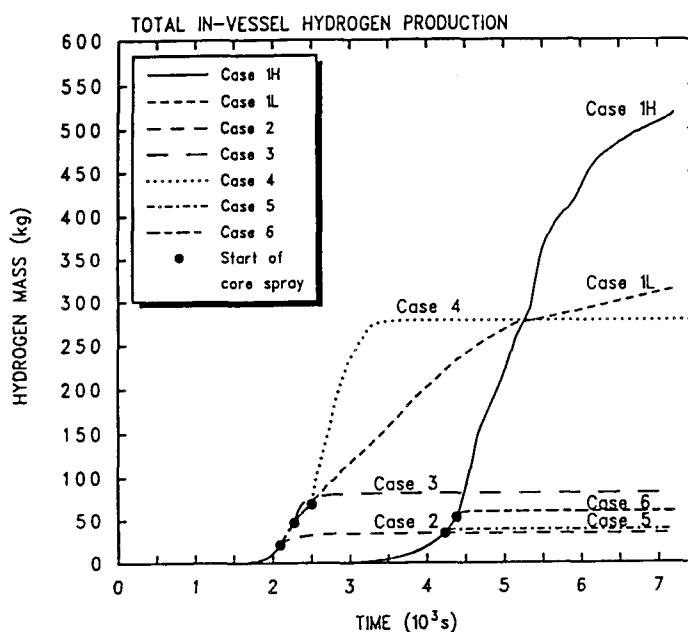


Figure 49. Total in-vessel hydrogen production in Forsmark 3. Comparison of all cases with 45 kg/s top spray. SCDAP/RELAP5 calculation.

With higher cladding temperatures cooling with the low flow rate of 45 kg/s became harder. Supplying water at a PCT of 1800 K as in Case 4 enhanced oxidation and gave a peak in the reaction with additional power generation. This additional heat-up made cladding temperatures increase another 170 K before turn-around. Rewetting was not obtained for all surfaces even when this simulation was extended to 8400 s. In fact, rewetting occurred only in the centre core zone despite of its higher power factor. One reason for this might be the velocity distribution between the parallel channels with the small coolant flow rate. Although there was a larger flow of water downwards in the outer channels the calculations show an almost stagnant steam flow there. In core zone 1, however, there was a considerable upwards flow of steam, not enough to totally counteract the liquid coolant flow downwards, but giving improved cooling. The reflooding gave a rather slow increase of the water level in Case 4, to 1.7 - 2 m above the core inlet at the end of the simulation. In Case 3 and 2 the final water level was higher.

The core damage was reduced by the reflooding in all cases compared to Case 1L without reflooding. Cooling recovery at a PCT of 1400 K resulted in an almost intact core with only minor increase in oxidation compared to the state before water injection. All control rods stayed in place. Also in Case 3 with PCT of 1600 K melting had only occurred locally of control rods in core zone 1 at axial levels 7 and 8. In Case 4 melting of control rods had

already removed most of the absorber material in the upper part of the three central core zones at start of core spray. Melting continued downwards until temperatures had decreased below 1500 K. There was no relocation fuel even if there was an increase in cladding oxidation and also some shattering of zirconium oxide in the very centre of the core. No rupture or melting of box walls was indicated. Porous debris was obtained at axial level 6 in zones 1 and 2.

The end states of the core in cases 2,3 and 4 are shown in Figs 50, 51 and 52 respectively.

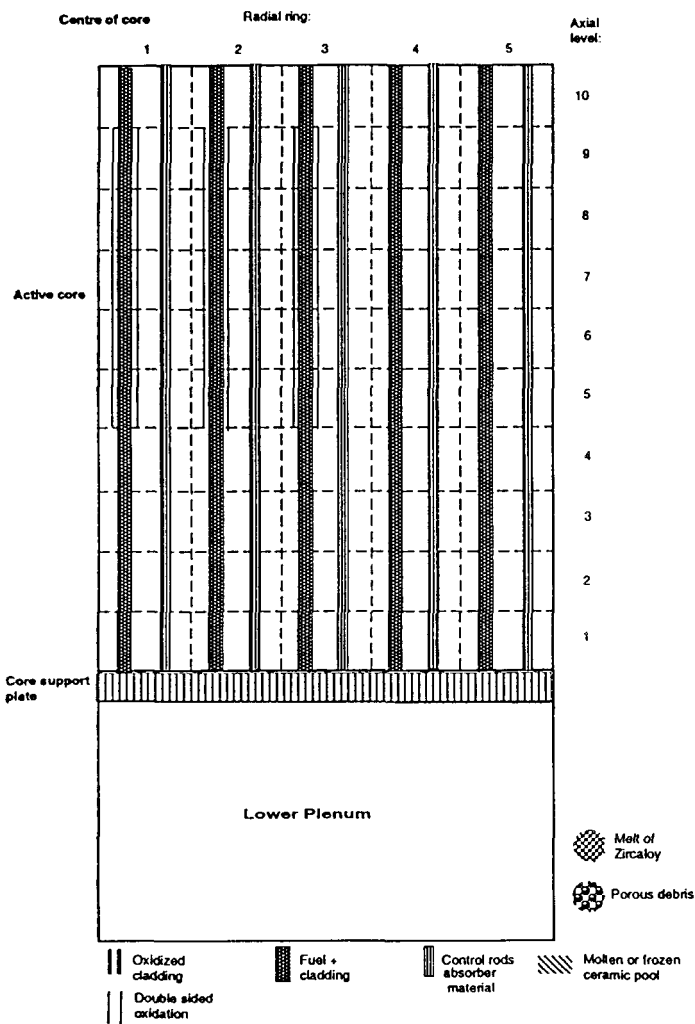


Figure 50. End state of F3 core in case 2.

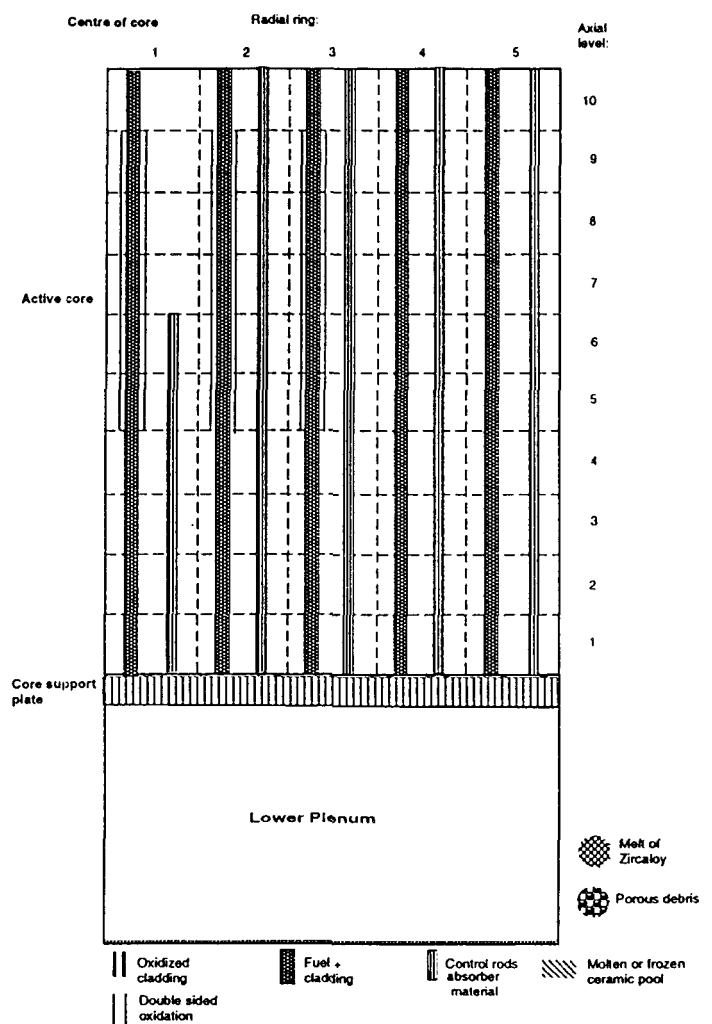


Figure 51. End state of F3 core in case 3.

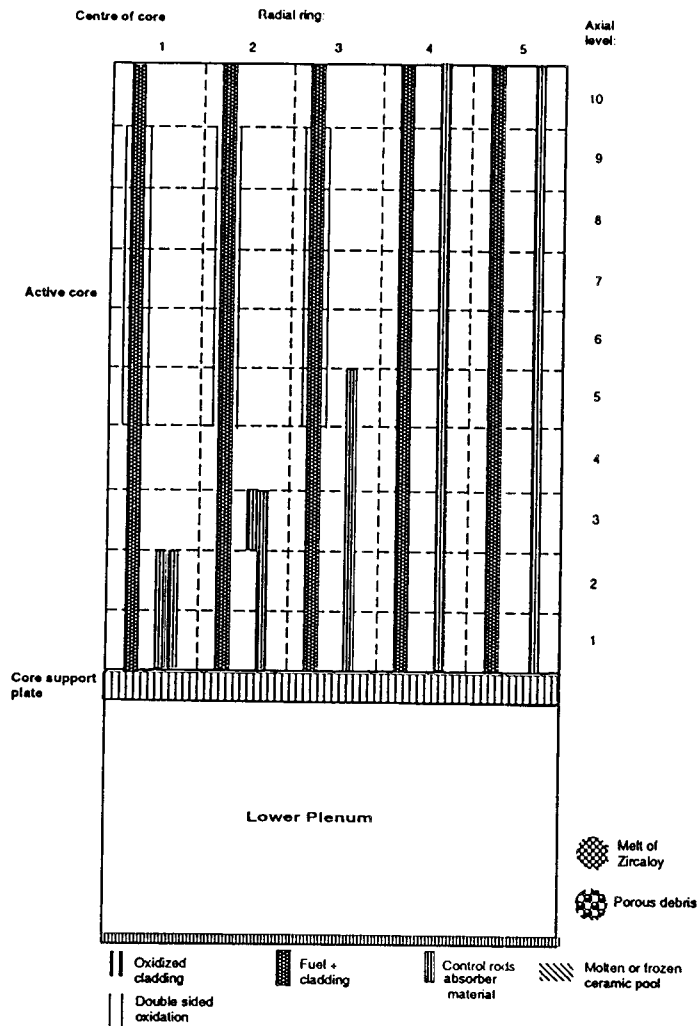


Figure 52. End state of F3 core in case 4.

6.2.2 High Pressure Cases, Case 5 and 6

The two reflooding cases without depressurization had the following conditions at start of 327 top spray injection with 45 kg/s :

Table 14: High pressure reflooding cases with 45 kg/s top spray

| Case No. | PCT (K) | Time after TB (s) |
|----------|---------|-------------------|
| 5 | 1600 | 4228 |
| 6 | 1800 | 4370 |

Table 15: Times of events in seconds (after TB) and results summary for 327 reflooding cases compared with base cases without reflood.

| Event/Result | Low pressure cases | | | | High pressure cases | | |
|--|--------------------|------|-------|-------|---------------------|-------|-------|
| | 1L | 2 | 3 | 4 | 1H | 5 | 6 |
| Loss of AC power | 0 | 0 | 0 | 0 | 0 | 0 | 0 |
| Low level L2, scram signal | 9 | 9 | 9 | 9 | 9 | 9 | 9 |
| Scram | 10 | 10 | 10 | 10 | 10 | 10 | 10 |
| Steam line isolation | 11 | 11 | 11 | 11 | 11 | 11 | 11 |
| Low level L4, ADS valves open | 747 | 747 | 747 | 747 | - | - | - |
| Dryout of top of core (Core heat-up starts) | 1020 | 1020 | 1020 | 1020 | 1340 | 1340 | 1340 |
| Total core uncover | 1140 | 1140 | 1140 | 1140 | 6310 | - | - |
| H ₂ production starts | 1550 | 1550 | 1550 | 1550 | 2710 | 2710 | 2710 |
| Rupture of fuel cladding due to spacer interaction, zone 1 | 1928 | 1928 | 1928 | 1928 | 4054 | 4054 | 4054 |
| First grid spacer slumping | 2170 | 2170 | 2170 | 2170 | 4086 | 4086 | 4086 |
| Melting of B ₄ C starts | 2220 | 2220 | 2220 | 2220 | 4150 | 4150 | 4150 |
| Start of water injection | - | 2063 | 2261 | 2489 | - | 4228 | 4370 |
| Max. temp. turn around | 7190 | 2064 | 2272 | 2790 | 7130 | 4229 | 4371 |
| Total rewetting of core | - | 5930 | 6250 | - | - | 5855 | 6075 |
| Molten fuel starts to slump | 4391 | - | - | 4231* | 7164 | - | - |
| End of simulation | 7190 | 7094 | 8390 | 7190 | 7190 | 7190 | 7190 |
| CPU/real time | 65 | 28 | 55 | 214 | 22 | 12 | 20 |
| In-vessel H ₂ production (kg) | 313 | 34 | 81 | 278 | 518 | 39 | 60 |
| Max. surface temperature (K) | 2926 | 1400 | 1608 | 1971 | 2805 | 1600 | 1800 |
| Fraction of fuel slumped to lower core levels | 0.468 | 0 | 0 | 0 | 0.074 | 0 | 0 |
| Fraction of B ₄ C slumped | 0.812 | 0 | 0.052 | 0.417 | 0.556 | 0.026 | 0.104 |

* Rubble formation (Porous debris)

Because of the relatively good cooling conditions at full pressure, 70 bar, it took about twice as long time after loss of power to reach the targeted PCTs as in the low pressure cases. During this extra period the core power had decayed about 21 %, which contributed to the fast recooling in the high pressure cases as shown in Figure 48. The loss of coolant caused by steam blow off through the safety valves was relatively small compared to the cases with ADS. At start of water injection in Case 5 and 6 the core was therefore not totally uncovered, so the water level stayed at about 0.5 m above core inlet. The highest temperatures were encountered in the uppermost part of the core which had experienced dryout conditions for the longest period of time. The temperature distribution at start of reflooding, shown in Figure 44, led to lower stored energy in the middle and lower part of the core than in the low pressure cases. This is probably the main reason for the faster recooling in the high pressure cases.

Immediate recooling was now obtained after coolant recovery also for the 1800 K case 6. Complete rewetting took place at 6070 s, i. e. less than half an hour after start of water injection. The rewetting was followed by additional condensation of steam by the cold 327 water, which caused a temporary drop in pressure, in Case 6 down to about 67 bar.

Recooling at full pressure at a maximum PCT of 1800 K caused almost no additional core

damage in excess of that already present at start of water injection. There was only a minor increase in cladding oxidation in the top of the core, but no oxide shattering took place. Control rods had melted in the two uppermost cells in the core centre and melting advanced one cell downwards before recooling. No damage to the fuel rods was experienced except for cladding rupture at interaction and melting of spacers in two upper positions in the centre of the core.

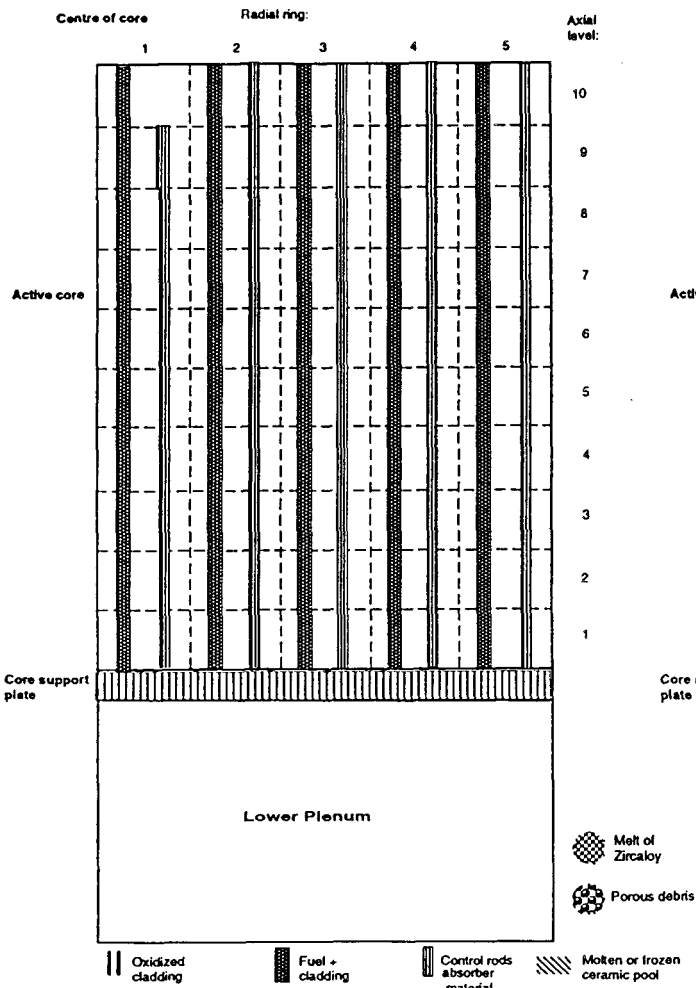


Figure 53. End state of F3 core in case 5.

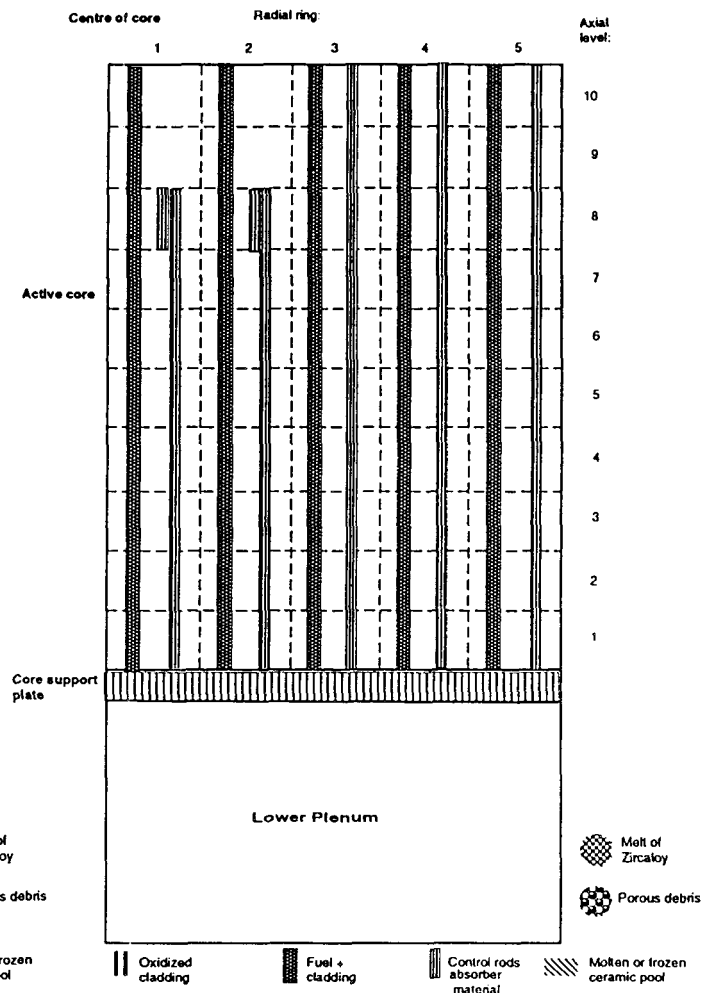


Figure 54. End state of F3 core in case 6.

6.3 REFLOODING WITH HIGH FLOW RATES FROM THE ECCS

Two cases were calculated in which reflooding was made by means of the low pressure ECCS, system 323, instead of system 327. Also here it was assumed that only half the capacity was available, i. e. two of four loops were engaged. In both cases reflooding was to be started at a PCT of 1800 K, the difference being that in Case 7 water was injected through the core spray nozzles and in Case 8 into the downcomer.

The 323 flow, which is driven by centrifugal pumps, is nominally large, but depends on the pressure difference between vessel and containment. Since the containment pressure was not determined in the SCDAP/RELAP5 calculations, a back pressure of 4 bar was assumed initially, which corresponds to 290 kg/s per loop. It was further assumed that the flow went to zero at a vessel pressure of 16 bar. The 323 flow will cease also when the downcomer level is restored, and is then tripped on high level, 5 m above core exit.

The intention was that the reflooding water should reach the core at a PCT of 1800 K in both Case 7 and 8. In Case 7, where the water was fed into the core from the top, it arrived into the core instantly. In Case 8, with downcomer injection and water reflooding from bottom of the core, the level had firstly to be raised 0.7 m up to the core inlet level. This implicated that 323 injection had to be started earlier in Case 8 than in Case 7 at times shown in Table 8 below. The fresh supply of water speeded up the temperature increase so that 1800 K was reached earlier than without reflooding.

Table 16: *Low pressure reflooding cases with 580 kg/s with top spray and DC injection*

| Case No. | Location of water injection | Time after TB at start of 323 (s) | PCT at start of 323 (K) | Time after TB when water reaches core (s) | PCT when water reached core (K) |
|----------|-----------------------------|-----------------------------------|-------------------------|---|---------------------------------|
| 7 | Above core | 2490 | 1800 | 2490 | 1800 |
| 8 | Downcomer | 2453 | 1775 | 2476 | 1800 |

The large amount of water forced into the hot core caused a prompt increase in steam production which raised the pressure considerably, although the ADS valves stayed open. The increased pressure counteracted the ECCS flow, which began to oscillate in opposition with pressure. The water level increased faster with top spray than with downcomer injection.

Top spray injection gave also faster recooling since the water reached all of the hot surfaces from above within a short period of time, as shown in Figure 55. Despite of temporarily high upstream vapour velocities which blew out some incoming water through CCFL¹ effects and caused the flow oscillate strongly between the parallel channels, there was a large net reflooding rate until the time of rewetting. With DC injection the level was not raised as fast which gave more time to heat up the upper levels before rewetting. Not only the maximum temperature was higher in Case 8 than in Case 7 (Fig. 55) but also the oxidation and hydrogen production as shown in Figure 56. Rewetting was obtained after 400 s of ECCS injection in Case 7 and after 500 s in Case 8.

¹CCFL=Counter Current Flow Limitation

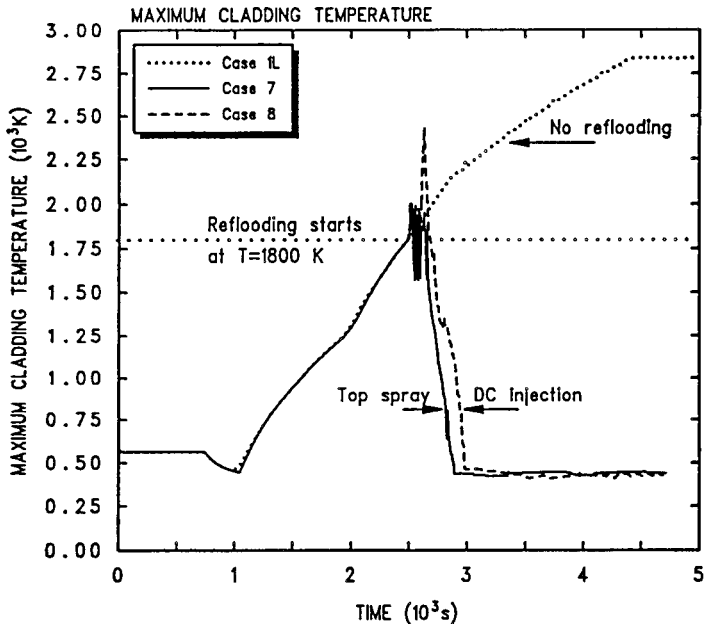


Figure 55. Maximum fuel surface temperature in Forsmark 3 in cases 7 and 8. SCDAP/RELAP5 prediction.

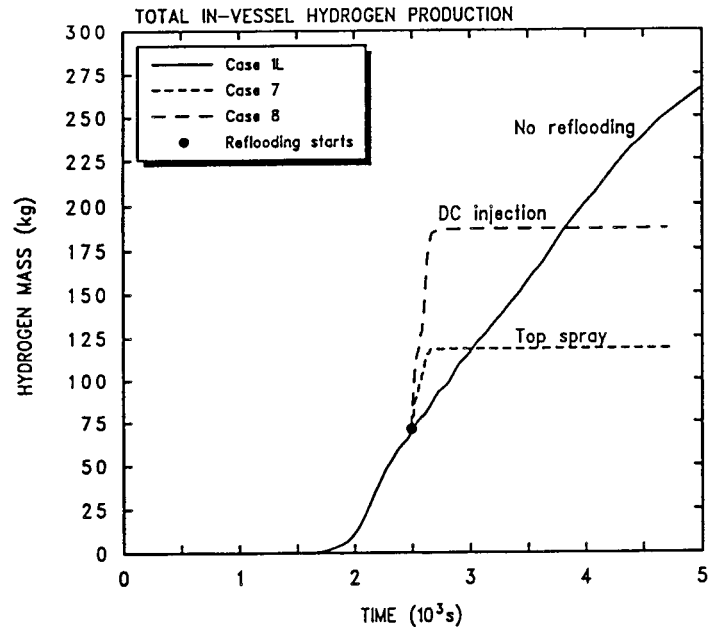


Figure 56. Total in-vessel hydrogen production in Forsmark 3 in cases 7 and 8. SCDAP/RELAP5 prediction.

Injecting water from above the core seemed to depress the water levels in the core channels which lifted the downcomer level so that the ECCS water flow was stopped on high DC level earlier in Case 7 than in Case 8. In Case 7 the redistribution of water between core and downcomer caused several restarts of the ECCS injection.

Because of the quick recooling with the large ECCS reflooding rates there was only limited increase in core damage compared to the state of the core at start of ECCS injection. The supply of water caused, however, increased zirconium oxidation and hence some local shattering of fuel rod claddings, more in Case 8 than in Case 7. In Case 7, with top spray, the quenching caused local embrittlement and fragmentation at the hottest location of fuel rods. In Case 8 the interstitial side of the fuel boxes in the centre, at axial node 7 were lost due to interaction between control rod and box material. Neither of the cases experienced any fuel relocation, according to SCDAP/RELAP5.

Table 16: Times of events in seconds (after TB) and results summary for 323 reflooding cases compared with no-reflooding Case 1L. (Times < 1020 s are same as in Table 13).

| Event/Result | 1L | 7 | 8 |
|--|-------|-------|-------|
| Dryout of top of core | 1020 | 1020 | 1020 |
| Total core uncover | 1140 | 1140 | 1140 |
| H ₂ production starts | 1550 | 1550 | 1550 |
| Rupture of fuel cladding due to spacer interaction, zone 1 | 1928 | 1928 | 1928 |
| First grid spacer relocation | 2170 | 2170 | 2170 |
| Melting of B ₄ C starts | 2220 | 2220 | 2220 |
| Start of water injection | - | 2490 | 2453 |
| Water reaches core | - | 2490 | 2476 |
| Max. temp. turn around | 7190 | 2500 | 2620 |
| Oxide shattering, fuel cladding, (zone 1, level 7) | - | 2539 | 2546 |
| Embrittled cladding quenched and fragmented | - | 2819 | - |
| Total rewetting of core | - | 2895 | 2990 |
| Molten fuel starts to slump | 4391 | - | - |
| End of simulation | 7190 | 4680 | 4690 |
| CPU/real time | 65 | 8.4 | 133 |
| In-vessel H ₂ production (kg) | 313 | 118 | 186 |
| Max. surface temperature (K) | 2926 | 2000 | 2432 |
| Fraction of fuel slumped to lower core levels | 0.468 | 0 | 0 |
| Fraction of B ₄ C slumped | 0.812 | 0.286 | 0.286 |

The end states of F3 core in cases 7 and 8 are shown in Figures 57 and 58 respectively.

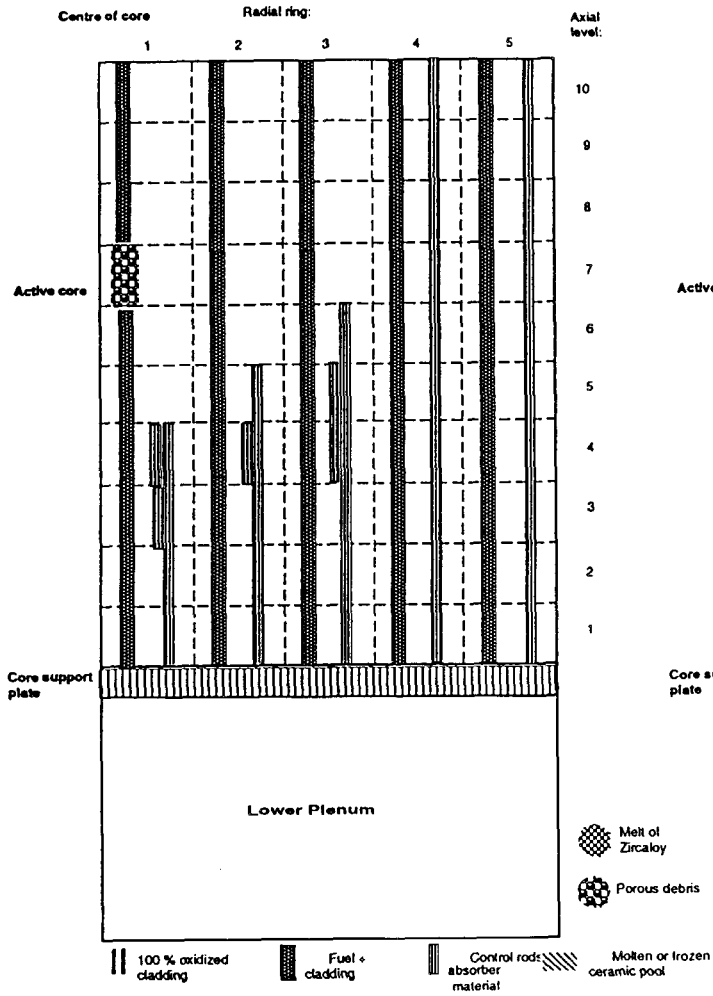


Figure 57. End state of F3 core in case 7.

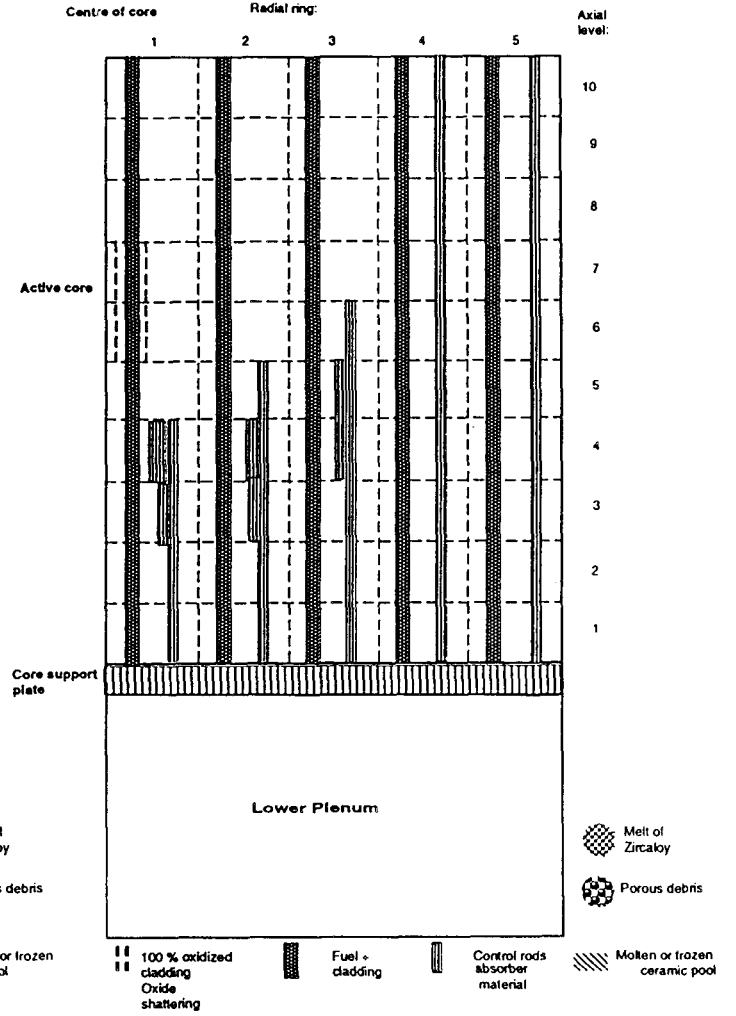


Figure 58. End state of F3 core in case 8.

7. DISCUSSION OF UNCERTAINTIES

Presently there has been only one plant scale example of a situation with reflooding of a badly damaged reactor core, namely TMI-2. As is well known, none of the earlier code versions were able to properly simulate the later stages of the progression of TMI-2 accident. Furthermore, TMI-2 is a PWR plant, and the well-known accident represents only one point in the space of severe accidents. Similar plant data for BWRs does not exist.

However, at least MAAP4 and MELCOR seem to produce core end states resembling that of the TMI-2 core (Fig. 59) (melt pool formation in MAAP4 and unquenched rubble bed in MELCOR). The SCDAP/RELAP5 calculations for TVO did not run long enough in low pressure scenarios to allow proper comparison with the TMI-2 core end state.

SCDAP/RELAP5 calculations for Forsmark 3 seemed to result generally in less damaged end states of the core than MAAP4 and MELCOR predictions in low pressure cases. This difference might be explained, in addition to possible modelling differences of various codes, by the fact that according to calculations the core top spray is more efficient in recooling of the core than the downcomer injection.

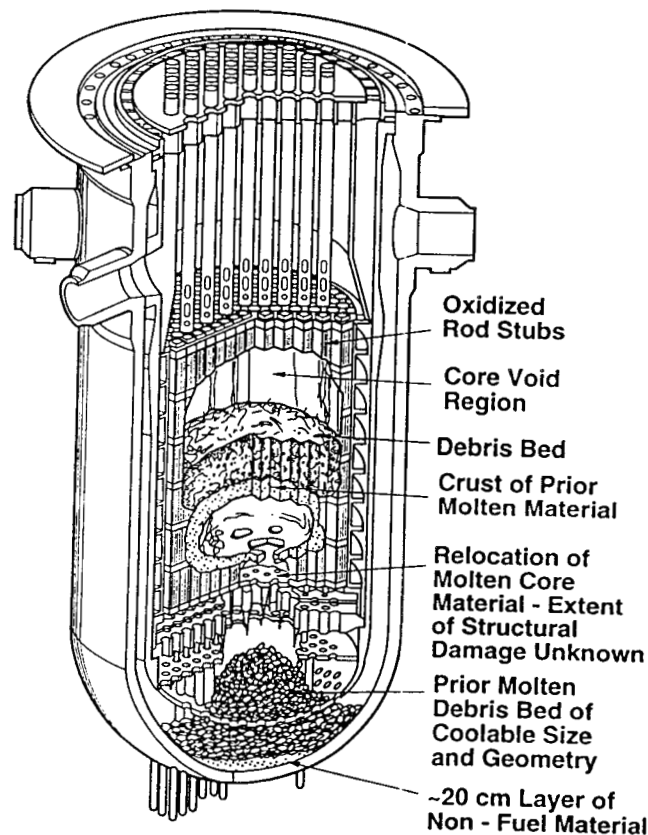


Figure 59. The end state of the core in TMI-2 accident. [Ref. 16].

In order to predict reliably the hydrogen production during the reflood of the degraded core it is important to know the real mechanisms that contribute to the end result (total amount of hydrogen produced during the quenching). However, the relationship between the oxidation percentage and the possible mechanisms that can break the covering oxide layer in different temperature levels, exposing unoxidized material to steam, are still open questions. The trend in the calculations seem to be right but the coded correlations and the knowledge of the physical background that eventually produce the calculated result may still be inadequate. More experimental results is needed to obtain good quality data for reliable correlations.

Formation of a melt pool in the core is also still an open question in the BWR core geometry. This issue is being addressed with XR experiments at Sandia National Laboratories.

The core degradation models of MELCOR have been extensively exercised against experimental data [Ref. 11, Ref. 12]. Tautges in Sandia National Laboratories has calculated DF-4 and MP-1 and MP-2 experiments with MELCOR 1.8.2 including an extensive parameter study of the core model.

The DF-4 BWR Damaged Fuel Experiment investigated the behaviour of BWR-type fuel materials and configurations in a high-temperature oxidizing environment typical of the conditions during a Loss-Of-Coolant Accident.

Tautges used in the base case input the MATPRO value of 2200 K for Zr melting point and an elevated B₄C/stainless steel eutectic reaction temperature: 1570 K. These values have been seen to be superior to the default values in the former MELCOR validation tasks.

The results [Ref. 12] showed that the base case model under-predicted control blade temperatures in the lower temperature regions, but in later stages of the experiment, when all the core damage was taking place, calculated control blade temperatures corresponded almost exactly to measured values. Control rod failure times in most of the test bundle were predicted almost exactly compared to experimental data.

Cladding temperatures were predicted almost exactly compared to experimental data at all times and at all levels except for the uppermost part of the test bundle. MELCOR over-predicted temperatures in the upper-most axial level by about 10 % in the middle of the experiment. Fuel failure times calculated by MELCOR corresponded almost exactly to experimental data.

The hydrogen production during DF-4 test was predicted by MELCOR to be 36.4 g which is well within the uncertainty boundaries of the experimental value of 38.0 ± 4.0 g. MELCOR, however, predicted the autocatalytic oxidation to begin sooner than was measured.

The calculations showed that candling/refreezing heat transfer coefficients may affect significantly on the material relocations within core. The default candling heat transfer coefficients resulted in the control rod material refreezing quite close to the axial location from which it melted. All the core materials relocated downward at the same time, rather than relocations would have taken place by melting temperatures of different components. In the DF-4 test the control blade material candled to the bottom of the test bundle leaving fuel pellets in stack. If the candling heat transfer coefficients were reduced, the relocation pattern became closer to that observed in the experiment, but the calculated temperature prediction

became worse.

However, even if DF-4 test showed fuel stacking in the debris configuration, it is not clear that this configuration represents the behaviour in full scale reactor cores during postulated severe accidents. In particular the shattering effects of cold water injection during reflooding on bare fuel pellet stacks were not investigated in DF-4 experiment. Tautges concludes in his report that sensitivity studies are recommended in plant applications of MELCOR.

The MP-1 and MP-2 experiments were carried out in atmosphere without steam. These experiments tested the behaviour of a degraded core after the postulated formation of a metallic blockage upon which a rubblized debris bed rested. The MELCOR predictions for temperatures in MP-1 and MP-2 tests were within 20 % from the measured values in all calculational nodes and within 10 % in many regions. The MELCOR prediction of melting and relocations agreed well with experimental data [Ref. 11].

It seems that MELCOR is reasonably well capable of predicting core melt progression under conditions without reflooding. One could expect that these models form a sound basis for further refining the core model to accurately cover also the reflooding effects. According to the code developers this would involve the ability to predict quenching rates in geometries of interest, spallation of oxide from the fuel rod cladding with accelerated oxidation, shattering of the fuel rods during quench, the occurrence and effects of ballooning and the possibility of forming a molten pool [Ref. 14].

The core collapse criteria in MAAP4 is given as a user-input parameter as a fraction of clad oxidized. This causes the core to collapse on reflood resulting in smaller values of Kutateladze number for heat transfer than intact geometry. The value used in these calculations was 10 %. No peeling off of zirconia layer was taken into account to enhance oxidation.

In MAAP4 the lowest core node, which contains core plate, is well cooled in the calculations. The side crust failure causes melt to flow into the lower plenum without core plate failure. However, the flow is so slow that the debris is quenched and no vessel failure results. Conditions for crust failure are given as user-input, which suggests that sensitivity studies are needed. In the MAAP calculations the large differences in the end states depend on changes in geometry. Parameters which control changes in core geometry are mostly given in the user-input. The coolability of the core plate is essential for keeping the melt in the original core volume. However, the validation of the core plate model in MAAP4 is not complete and it thus constitutes an uncertainty in the calculations.

The development of SCDAP/RELAP5/MOD3 models has been accompanied by an extensive validation and assessment against available severe accident tests, reported in Volume 5 of the manual [Ref.4]. These tests comprise among others various CORA tests, ACCR experiment DF-4, PBF tests SFD 1-4, SFD1-3, SFD 1-1-, the Phebus B9+ experiment and LOFT test LP-FP-2. The grid spacer model has successfully been validated against CORA 13 results. The ORNL BWR blade/box model is based on CORA-16, -28, -31, -33 and other separate effects tests. Large efforts have also been spent on modelling of the TMI-2 and assessment based on post accident investigation results.

Most of the assessments have led to model improvements giving variations between calculated and measured parameters typically within ± 20 % including modelling and

experimental uncertainties. Hydrogen generation during reflood is probably more underpredicted, especially if there is a large fraction of debris bed below the core. The latter problem is being addressed by the new model for shattering and debris bed thermal-hydraulics.

Nodalization studies on full plant calculations have shown that a minimum of 5 radial times ten axial core nodes should be used in order to avoid effects of nodalization on core damage results. This number of nodes was here employed both for TVO I/II and Forsmark 3.

As a general comment to all calculations presented in this paper it can be concluded that the correlations applied in the codes for calculating the phenomena that occur during the extreme conditions of quenching are still under discussion. The embrittlement mechanisms and the possible fragmentation induced by thermal shock are understood only in qualitative manner. The most interesting and latest single rod tests (QUENCH facility) were performed in KfK in Germany [Ref.15]. These experiments 100-150 mm long fuel rod specimens were heated to 800-1600 C (at onset of quenching). Pre-oxidation (single and double-sided) could be varied. Flooding rate was 0.3-3 cm/s (water temperature 20-100 C). The observations after the tests showed that the upper parts of the rods were oxidized almost completely but surprisingly most hydrogen was produced using pre-oxidized specimens. One possible explanation may be spalling of oxide layers during quenching that brings more Zr available for steam oxidation. Although these experimental results are preliminary, it is clear that the calculational results presented in this report, even if they show some similar trends, may partly be based on inadequate knowledge about the nature of the phenomena concerned.

8. CONCLUSIONS

All three computer codes predicted the progression of core damage slightly differently. In the performed calculations MELCOR predicted the fragmentation of the fuel and formation of a rubble bed with no fuel or cladding slumping into the lower head in the majority of the cases. Some of the code sensitivity parameters are anticipated to have effect on the results. MAAP4 in turn favors formation of a melt pool in the core, with no material relocations to the lower plenum, when core is reflooded. Also MAAP4 results are sensitive to user-input parameters. A SCDAP/RELAP5 calculation resulted in melt pool formation and rapid slumping of material into the lower head (in case, where the code was able to calculate far enough). The material relocation to the lower head was, however, controlled by user-specified input parameters in SCDAP/RELAP5.

All codes predict an increase in hydrogen production at the time water level reached the bottom of the active fuel. In the scenarios with failure to depressurize the reactor coolant system, all calculated cases with the three codes resulted in quenched end state of the core.

In the cases with reflooding and successful depressurization the core damages were larger than in the respective high pressure variations.

The final state of the core according to MAAP4 calculations for TVO is the same if the reflooding is started at 1h 15 min independently whether the reactor is depressurized or not. The intact core geometry is lost and a melt pool has formed in the original core volume.

According to the EOP for severe accidents at TVO, the reactor coolant system will be depressurized at latest 1 h into the accident. This seems to be close to optimum predicted by the calculations of this report. An earlier depressurization would lead to more rapid core degradation due to early loss of reactor coolant inventory. Delaying the depressurization does not add time to maintain intact fuel geometry after reflooding. By delaying the depressurization beyond 1 h there is a risk that debris relocates into the lower head at high reactor pressure and eventually causes high pressure melt ejection to the containment.

All codes predicted a relatively small time window between the relocation of the control rods and the fuel in the core. According to MELCOR the time gap was only 1-2 min, MAAP4 predicted the time gap to vary between 3 min - 15 min. However, the rubble bed in MELCOR results consists of fuel and cladding particles with no absorber material present. The calculated results suggest that recriticality may not be possible or the related power level will be low.

SCDAP/RELAP5 analyses for TVO suggest similar trend in the core behaviour as the two other codes. The lack of blade/box model in the applied code version for TVO was a deficiency.

Totally nine SCDAP/RELAP5 calculations of anticipated station blackout (TB) sequences in Forsmark 3 BWR were carried out. The simulated time was 2 hours for cases with reflooding from system 327 core spray and 1 hour, 20 minutes for cases with system 323 injection. The used, newer code version SCDAP/RELAP5/MOD3. /Release C included the BWR specific blade/box models.

The results for Forsmark 3 show, that the maximum temperature for which the core can be recooled might be slightly above 1800 K at normal ADS. The following main results and conclusions from the analysis can be mentioned:

- * For maximum cladding temperatures < 1600 K fast recooling was obtained even with such a low coolant flow rate as 45 kg/s. Core damage was then limited to slight increase in oxidation. Removal of absorber material in control rods was indicated at only few locations. All of the UO_2 fuel remained intact.
- * At maximum temperatures of 1800 K, and above, injection of water increased core damage considerably. With the low coolant flow rate, 45 kg/s, recooling was obtained only after a long period with increased oxidation and temperature increase due to exothermic steam-metal reactions. With higher water injection flow rates recooling was faster, but caused oxide shattering and embrittlement of the oxide layer on fuel rods.
- * Start of water injection at 1800 K led to more melt down of control rod B_4C with low reflooding flow rates than with high flow rates. Although large oxidation and removal of fuel rod claddings, no removal of UO_2 fuel was indicated.
- * Water injection above the core gave a more efficient recooling than with downcomer injection with large flow rates from the low pressure ECCS .
- * The fast recooling with the low pressure ECCS caused pressure increase which reduced the coolant mass flow rate and on occasions even stopped the flow. This has to be considered at the assessment of the efficiency of system 323.

For nextcoming recriticality studies extended analysis of the core configuration especially with respect to the state of control rods should be done. The reactivity balance of the core and the reactivity worths of remaining absorber material in the damaged core has to be evaluated for the reflooding period. Additional calculations might be needed in order to find cases with larger risks for recriticality. At that time next version of the SCDAP/RELAP5 code will be installed in which the ORNL blade/box model is fully operable, including interactions with lower plenum COUPLE models. Hopefully that version will also have implemented the new lower plenum debris oxidation models.

In general, when discussing about reflooding of severely damaged core, further information about the pertinent physical phenomena occurring during the quenching process is needed. This is particularly important in order to evaluate the adequacy of the present calculational tools for applications in the context of accident management.

REFERENCES

- 1 Dahlerup, L., et al; *Project plan proposal for the Nordic research programme in the research area RAK-2: Säkerhet mot utsläpp vid reaktorhaverier. 1994 - 1997. August 29, 1994.*
- 2 Frid, W; NKS/SIK-2. *Severe accidents in LWR. Studies of computer codes, selected aspects of phenomenology and accident management, Final Report.*
- 3 Lindholm, I, et al; *Core reflooding studies for Olkiluoto and Forsmark nuclear power plants in NKS/RAK-2 project. Summary report (in progress)*
- 4 Allison, C. M., et al; *SCDAP/RELAP5/MOD3.1 Code Manual. Vols. 1 - V. NUREG/CR-6150, EGG-2720. Idaho National Laboratory, Idaho Falls, 1994.*
- 5 Griffin, F. P.; *BWR control blade/channel box interaction and melt relocation models for SCDAP. Rev. 2. ORNL/NRC/LTR-92/12/R2. December 30, 1993.*
- 6 Nilsson, L.; *Implementation and testing of SCDAP/RELAP5/MOD3.1. STUDSVIK/ES-95/2. Studsvik Eco & Safety AB, January 1995.*
- 7 Nilsson, L.; *Analysis with SCDAP/RELAP5 of reflooding of an overheated core in Forsmark 3 BWR after loss of electric power. STUDSVIK/ES-93/55. Studsvik Eco & Safety AB, 1993.*
- 8 Griffin, P.; *Private communication, Fax letter from ORNL, December 22, 1994.*
- 9 Jung, G.; *Private communication, Results of POLCA4 calculation for Forsmark 3. Vattenfall, February 2, 1995.*
- 10 R. M. Summers, R. K. Cole Jr., E. A. Boucheron, M. K. Carmel, S. E. Dingman and J. E. Kelly. *MELCOR 1.8.0: A computer code for nuclear reactor severe accident source term and risk assessment analyses. Technical Report SAND90-0364, NUREG/CR-5531, Sandia National Laboratories, January 1991.*
- 11 Tautges T.J., *MELCOR 1.8.2 Assessment: The MP-1 and MP-2 Late Phase Melt Progression Experiments, Sandia report SAND-0133, Sandia National Laboratories, May 1994.*
- 12 Tautges T. J., *MELCOR 1.8.2 Assessment: The DF-4 BWR Damaged Fuel Experiment, Sandia report SAND-1377, Sandia National Laboratories, October 1994.*
- 13 *MAAP4, Modular Accident Analysis Program, User's Manual, Electric Power Research Institute, Palo Alto, USA, May 1994.*

- 14 *MELCOR 1.8.3 Reference Manual*, Sandia National Laboratories, Albuquerque, NM, USA, July 1994.
- 15 Hofmann P., Noack V., *Experiments on the Quench Behaviour of Fuel Rods*, Kernforschungszentrum Karlsruhe, Institut für Materialforschung 1, Presentation handouts at OECD/CSNI PWG-2/TG on In-Vessel Degraded Core Behaviour, Paris, 1-2 December 1994.
- 16 Powers D. A., Kmetyk L. N., Schmidt R. C., *A review of the technical Issues of Air Ingression During Severe Reactor Accidents*. NUREG/CR-6218, SAND94-0731, Sandia National Laboratories, Albuquerque, NM, September 1994.
- 17 Nilsson L., *Core reflooding calculations for Forsmark 3 BWR with SCDAP/RELAP5/Mod3.1*, Studsvik Eco&Safety AB, May 1995 (to appear).

Distribution:

Denmark

Beredskabsstyrelsen (2)
Attn: Björn Thorlaksen
Louise Dahlerup
P.O.Box 189
DK-3460 Birkerød

Forskningscenter Risö (4)
Attn: Povl Ölgaard
Frank Höjerup
Peter Fynbo
Knud Ladekarl Thomsen
P.O.Box 49
DK-4000 Roskilde

Finland

Finnish Center of Radiation & Nucl.
Safety (STUK) (6)
Attn: Lasse Reiman (3)
Kalevi Haule
Timo Karjunen
Juhani Hyvärinen
P.O.Box 14
FIN-00881 Helsinki

Teollisuuden Voima Oy (5)
Attn: Markku Friberg
Heikki Sjövall (2)
Seppo Koski
Risto Himanen
FIN-27160 Olkiluoto

IVO International Ltd (3)
Attn: Petra Lundström
FIN-01019 IVO

Klaus Sjöblom
Loviisan Voimalaitos
P.O.Box 23
FIN-07901 Loviisa

Björn Wahlström
VTT Automation
P.O.Box 13002
FIN-02044 VTT

VTT Energy (10)
Attn: Lasse Mattila
Esko Pekkarinen
Eija Puska
Ari Silde
Ilona Lindholm (6)

Iceland

Tord Walderhaug
Geislavarnir ríkisins
Laugavegur 118 D
IS-150 Reykjavik

Norway

Institutt för Energiteknikk (4)
Attn: Egil Stokke
Oivind Berg (3)
P.O.Box 175
N-1750 Halden

Sverre Hornkjöl
Statens Strålevern
P.O.Box 55
N-1345 Österås

Sweden

Swedish Nuclear Power Inspectorate
(SKI) (10)
Attn: Lennart Hammar
Wiktor Frid (8)
Oddbjörn Sandervåg
S-10658 Stockholm

Vattenfall AB (5)
Attn: Veine Gustavsson (4)
Klas Hedberg
P.O.Box 528
S-16216 Stockholm

Forsmarks Kraftgrupp AB (4)
Attn: Gustaf Löwenhielm (3)
Henning Danielsson
S-74203 Östhammar

Kenneth Persson (3)
Vattenfall AB
Ringhalsverket
S-43022 Väröbacka

Emil Bachofner (3)
OKG AB
S-57093 Figeholm

Lars Nilsson (6)
Studsvik EcoSafe AB
S-61182 Nyköping

Peter Moritz (3)
Barsebäck Kraft AB
P.O.Box 524
S-24625 Löddeköpinge

ABB Atom AB (2)
Attn: Yngve Waaranperä
Nils-Olov Jonsson
S-72163 Västerås

Erik Söderman
ES-Konsult AB
P.O.Box 3096
S-16103 Bromma

Kjell Andersson
Karinta Konsult HB
P.O.Box 6048
S-18306 Täby

Raj Sehgal
Royal Institute of Technology
Nuclear Power Safety
S-10044 Stockholm

Torkel Bennerstedt (5)
NKS
PL 2336
S-76010 Bergshamra

Science and Engineering International (2)
Attn: Kazimierz Salwa
Tomasz Jackowski
Konwaliowa 7
03-194 Warszawa
POLAND

Alan Debenham
Risley
Warrington
Cheshire WA3 6AT
UNITED KINGDOM

Remond R. Pahladsingh
Joint Nuclear Power Station of the
Netherlands
P.O.Box 40
6669 ZG Dodewaard
THE NETHERLANDS

U.S. Nuclear Regulatory Commission (2)
Attn: John Ridgely
Charles Tinkler
Washington, DC 20555
U.S.A

Brent Boyack
Los Alamos National Laboratory
P.O.Box 1663
Los Alamos, NM 87545
U.S.A

Sandia National Laboratories (2)
Attn: Arnold Elsbernd
Lubomyra Kmetyk
Dept. 6418
Albuquerque
NM 87185-5800
U.S.A

Chris Allison
Idaho National Engineering Laboratory
P.O.Box 1625
Idaho Falls, ID 83404
U.S.A

Jason Chao
Electric Power Reserach Institute
P.O.Box 10412
Palo Alto, CA 94303
U.S.A

Forschungszentrum Karlsruhe GmbH (2)
Attn: Peter Hofmann
Wolfgang Breitung
P.O.Box 3640
D-76021 Karlsruhe